

Analysis of Autogenous and Drying Shrinkage of Concrete

ANALYSIS OF AUTOGENOUS AND DRYING SHRINKAGE OF CONCRETE

By

RABIH S. KHAIRALLAH, B.ENG.

A Thesis

Submitted to the School of Graduate Studies

In Partial Fulfilment of the Requirements

For the Degree

Master of Applied Sciences

McMaster University

© Copyright by Rabih Khairallah, September 2009

MASTER OF APPLIED SCIENCES

(Civil Engineering)

McMASTER UNIVERSITY
Hamilton, Ontario

TITLE: Analysis of Autogenous and Drying Shrinkage of Concrete

AUTHOR: Rabih S. Khairallah,

B.Eng. (Lebanese University - Branch II,
2000)

SUPERVISOR: Professor Samir E. Chidiac, Ph.D, P.Eng.

NUMBER OF PAGES: xv, 154

Abstract

Concrete undergoes volume change as it changes phases from plastic to solid. Volume change due to water movement and losses within the concrete are referred to as chemical and autogenous shrinkage and drying and plastic shrinkage are due to water exchange with the surrounding environment. Shrinkage strains need to be investigated as they can have detrimental effects on the serviceability and durability of concrete.

For this study, an experimental program was developed using fractional factorial principles to investigate the effects of curing regime and concrete mixture namely, water to cement ratio (w/c), water content (w), maximum aggregate size (size), silica fume replacement percent (SF), ground granulated furnace slag replacement percent (GGBFS), and volume of coarse aggregate (CA), on the magnitude of autogenous and drying shrinkage. A new test setup was developed to measure autogenous shrinkage, capillary pressure and temperature. The results were found to concur with those reported in the literature, i.e., moist cured samples exhibit chemical shrinkage and that air cured samples exhibit both chemical and drying shrinkage and that the magnitude of the latter is much greater than the former. Values of drying shrinkage are found to range from 450 to 800 $\mu\text{m/m}$. The results also revealed that all the parameters studied do contribute to shrinkage but not to the same degree. An increase in the volume and size of coarse aggregate is found to produce concrete that exhibits less drying shrinkage strains. The addition of SF as cement replacement is found in general to increase shrinkage strains. The statistical investigation has revealed that the following parameters, CA volume, w/c^2 , CA^2 , $w/c \cdot SF$, $w/c \cdot GGBFS$, $size \cdot SF$, $size \cdot CA$, $w/c \cdot w \cdot size$, $w/c \cdot SF \cdot GGBFS$, and $w/c \cdot SF \cdot CA$ are statically significant to a 90% confidence level.

For autogenous shrinkage, w/c is found to be a significant parameter. The results also revealed that increasing the amount of chemical admixtures, WRA and VEA, has led to a significant increase in strains. Autogenous strains were found to occur when there is a rise in capillary suction pressure, occurring due to self-desiccation.

Seven models proposed in the literature to estimate strains due to shrinkage were evaluated using the experimental data. The majority of these models have been adopted by North American, European or Japanese concrete standards. The assessment has revealed that only two models, namely B3 and ACI – 209 are somewhat adequate in their predictions of strains in concrete that is 28 days or older. Regression models developed in this study are found to provide a better estimation of the concrete shrinkage strains at 3 days, 7 days, 14 days, 28 days and 119 days.

Acknowledgements

I would like to express my deep and honest appreciation to my supervisor Professor Samir E. Chidiac for his encouragements and advices before and during the course of my studies. His efforts and constructive criticism as well as his close follow up and valuable suggestions and directions have pushed me ahead in my work and contributed substantially to the development of this thesis.

I would like also to extend my gratitude for the support offered by the staff of the civil engineering department and the technicians of the Applied Dynamics Laboratory in particular, Kent Wheeler, Dave Perrett and Peter Koudys. I would like also to extend my thanks to my fellow graduate students and best friends, Omar Daoud, Fayez Moutassem and Hanif Mahmoodzada, who were involved in this experimental program. Their immeasurable help inside and outside the laboratory was invaluable.

The financial support provided by the NSERC, the department of Civil Engineering and the Centre for Effective Design of Structures are greatly appreciated. My appreciation is also extended to LAFARGE – North America for donating the cement, aggregates, and mineral admixtures and for BASF for donating the chemical admixtures.

I dedicated this thesis to my four kids, Romy-Maria, Ralf, Rowy, and Rona and my wife Rana who were always by my side, encouraging, supporting and helping me.

TABLE OF CONTENTS

CHAPTER 1 INTRODUCTION	1
1.0 Preliminaries.....	1
1.1 Statement of Purpose.....	2
1.2 Overview	2
CHAPTER 2 LITERATURE REVIEW	4
2.0 Introduction	4
2.1 Shrinkage.....	7
2.1.1 Chemical Shrinkage.....	7
2.1.2 Autogenous Shrinkage.....	11
2.1.3 Plastic Shrinkage	23
2.1.4 Drying Shrinkage.....	26
2.1.5 Carbonation Shrinkage	30
2.1.6 Thermal Shrinkage	31
2.2 Shrinkage Strain Predictive Models	32
2.2.1 ACI – 209	32
2.2.2 B3	34
2.2.3 GL 2000.....	36
2.2.4 CEB – FIP 1990.....	37
2.2.5 EHE	39
2.2.6 Eurocode 2	40
2.2.7 JSCE Specification 2002	41
2.2.8 Model Parameters	43
2.3 Concluding Remarks	46

CHAPTER 3 EXPERIMENTAL PROGRAM	47
3.0 Introduction	47
3.1 Concrete Mixture Design	48
3.2 Material	51
3.2.1 Coarse Aggregates.....	51
3.2.2 Fine Aggregates.....	52
3.2.3 Cementitious Material	54
3.2.4 Air Entraining Agent	55
3.2.5 Water Reducer or Super-plasticizer.....	55
3.2.6 Viscosity Enhancing Agent	55
3.3 Experimental Procedure	55
3.4 Testing Methods	59
3.4.1 Shrinkage	59
3.4.2 Concrete Compressive Strength	59
3.5 Experimental Results.....	59
CHAPTER 4 ANALYSIS OF EXPERIMENTAL DATA.....	75
4.0 Introduction	75
4.1 Effect of Curing Regime on Shrinkage	75
4.2 Effect of Concrete Mixture on Drying Shrinkage	84
4.3 Autogenous Shrinkage	89
4.4 Effect of Curing Conditions and Shrinkage Strain on Compressive Strength of Concrete	103
4.5 Statistical Analysis	104
4.5.1 Complete shrinkage regression models	104
4.5.2 Shrinkage regression models excluding variables interaction	106
4.5.3 Complete shrinkage regression including chemical admixtures	107

CHAPTER 5 EVALUATION OF CONCRETE SHRINKAGE STRAIN PREDICTION MODELS	108
5.0 Introduction	108
5.1 Shrinkage Strain Prediction Models	109
5.2 Statistical Indicators	135
5.2.1 Residual Squared, R^2	135
5.2.2 Error Percentage	135
5.2.3 Coefficient of Variation	135
5.3 Model Predicted Values	136
CHAPTER 6 CONCLUSIONS AND RECOMMENDATIONS	140
6.0 Summary	140
6.1 Conclusions	141
6.2 Recommendations	143
REFERENCES	144

LIST OF TABLES

Table 2.1:	Chemical shrinkage of cement paste (Power, 1935)	8
Table 2.2:	Values of a and b as a function of w/c	42
Table 2.3:	Parameters used in shrinkage prediction models	44
Table 2.4:	Ranking of shrinkage models	45
Table 3.1:	Upper and lower limit values for concrete mixtures.....	48
Table 3.2:	Design of concrete mixtures – Mixtures with Chemical Admixtures	49
Table 3.3:	Design of concrete mixtures – Main Points.....	50
Table 3.4:	Design of concrete mixtures – Star Points	51
Table 3.5:	Chemical and physical properties of hydraulic cement GU-type 10, GUb-SF cement type IP 8, and GGBFS	54
Table 3.6a:	Shrinkage strain from age 2 days to 14 days for air cured cylinders for mix #5 to mix #35	60
Table 3.6b:	Shrinkage strain from age 21 days to 49 days for air cured cylinders for mix #5 to mix #35	61
Table 3.6c:	Shrinkage strain from age 56 days to 119 days for air cured cylinders for mix #5 to mix #35	62
Table 3.6d:	Shrinkage strain from age 2 days to 14 days for air cured cylinders for mix #36 to mix #66	63
Table 3.6e:	Shrinkage strain from age 21 days to 49 days for air cured cylinders for mix #36 to mix #66	64
Table 3.6f:	Shrinkage strain from age 56 days to 119 days for air cured cylinders for mix #36 to mix #66	65
Table 3.7a:	Shrinkage strain from age 2 days to 14 days for moist cured cylinders for mix #5 to mix #35	66
Table 3.7b:	Shrinkage strain from age 21 days to 49 days for moist cured cylinders for mix #5 to mix #35	67
Table 3.7c:	Shrinkage strain from age 56 days to 119 days for moist cured cylinders for mix #5 to mix #35	68
Table 3.7d:	Shrinkage strain from age 2 days to 14 days for moist cured cylinders for mix #36 to mix #66	69

Table 3.7e: Shrinkage strain from age 21 days to 49 days for moist cured cylinders for mix #36 to mix #66	70
Table 3.7f: Shrinkage strain from age 56 days to 119 days for moist cured cylinders for mix #36 to mix #66	71
Table 3.8: Average and standard deviation values for concrete compressive strength at the age of 119 days for air cured and moist cured samples	72
Table 4.1: Covariance values for drying and chemical shrinkage strains for mix #5 to mix #36	78
Table 4.2: Covariance values for drying and chemical shrinkage strains for mix #37 to mix #66	79
Table 4.3a: Covariance values for chemical shrinkage strains from age 2 days to 28 days for mix #5 to mix #35	80
Table 4.3b: Covariance values for chemical shrinkage strains from age 35 days to 119 days for mix #5 to mix #35	81
Table 4.4a: Covariance values for chemical shrinkage strains from age 2 days to 28 days for mix #36 to mix #66	82
Table 4.4b: Covariance values for chemical shrinkage strains from age 35 days to 119 days for mix #36 to mix #66	83
Table 4.5: Group I – Concrete mixes with w/c = 0.3.....	89
Table 4.6: Group II – Concrete mixes with w/c = 0.4	89
Table 4.7: Group III – Concrete mixes with w/c = 0.5 and w/c = 0.6	89
Table 4.8: Regression models for total shrinkage strain.....	105
Table 4.9a: Statistical indicators for total shrinkage strain with 90% confidence level	106
Table 4.9b: Statistical indicators for total shrinkage strain with 95% confidence level.....	106
Table 5.1: Models assessment according to the residuals squared method	136
Table 5.2: Models assessment according to the error percentage method.....	137
Table 5.3: Models assessment according to the coefficient of variation method	138
Table 5.4: Models assessment summary.....	139
Table 5.5: Ranking of shrinkage models	139

LIST OF FIGURES

Figure 2.1: Chemical shrinkage (Paulini, 1996)	8
Figure 2.2: Dilatometry test arrangement (Holt, 2001)	10
Figure 2.3: Reduced buoyancy test arrangement. (Holt, 2001)	10
Figure 2.4: Chemical shrinkage measurements versus time (Tazawa et al., 1999)	11
Figure 2.5: Chemical and autogenous shrinkage interaction in the horizontal direction (Tazawa et al., 1999).....	12
Figure 2.6: Autogenous shrinkage and chemical shrinkage versus time (Hammer, 1999)	13
Figure 2.7: Relative humidity versus pore pressure based on Laplace and Kelvin relations (Holt, 2001)	14
Figure 2.8: Effect of cement type on autogenous shrinkage strain of cement paste with water to cement ratio equals to 0.3 (Lura et al., 2003)	15
Figure 2.9: Effect of super-plasticizer on autogenous shrinkage strain of cement paste (Lura et al., 2003).....	15
Figure 2.10: Effect of fly ash on autogenous shrinkage of mortar with water to binder ratio equals to 1.0 by volume (Lura et al., 2003).	16
Figure 2.11: Effect of granulated blast furnace slag on autogenous shrinkage of mortar with water to binder ratio equals to 1.0 by volume (Lura et al., 2003).....	17
Figure 2.12: Effect of w/c on autogenous shrinkage strain (Lura et al., 2003).....	17
Figure 2.13: Embedded gauges test setup (Tazawa et al., 1999).....	19
Figure 2.14: Suspended gauges test setup (Holt, 2001).....	20
Figure 2.15: Gauges through walls test setup (Tazawa et al., 1999)	20
Figure 2.16: Non-contact test setup (Tazawa et al., 1999)	21
Figure 2.17: Lasers on surface test setup (Tazawa et al., 1999)	21
Figure 2.18: Method proposed for measuring vertical strain of autogenous shrinkage (Nawa and Horita, 2004).....	22
Figure 2.19: Autogenous shrinkage and capillary pressure of concrete during the first 24 hours (Holt, 2001).....	23

Figure 2.20: Cracks induced by plastic shrinkage at the surface of a fresh concrete (Mehta and Meterio, 2006)	24
Figure 2.21: Cracks mechanisms due to plastic shrinkage (Newman and Choo, 2003)..	25
Figure 2.22: Drying shrinkage mechanism according to Power's theory – Stresses pushing water meniscus down between two cement particles (Radocea, 1992)	27
Figure 2.23: Effect of aggregate on drying shrinkage (CCAA, 2002).....	28
Figure 2.24: Effect of aggregate volume concentration on drying shrinkage (CCAA, 2002)	28
Figure 2.25: Drying Shrinkage cracks in a wall – The vertical lines show the position of the reinforcement (Newman and Choo, 2003).....	30
Figure 3.1: 14 mm coarse aggregate gradation curve	52
Figure 3.2: 20 mm coarse aggregate gradation curve	53
Figure 3.3: Fine aggregate gradation curve	53
Figure 3.4: Autogenous shrinkage test setup (drawn not to scale)	57
Figure 3.5: Strain versus time	73
Figure 3.6: Temperature versus time	73
Figure 3.7: Capillary pressure versus time	74
Figure 4.1: Effect of GGBFS addition on shrinkage at the age of 119 days	84
Figure 4.2: Effect of GGBFS and SF addition on shrinkage at the age of 119 days	86
Figure 4.3: Effect of coarse aggregate volume on shrinkage at the age of 119 days	87
Figure 4.4: Effect of water reducing agent on shrinkage at the age of 119 days	87
Figure 4.5: Temperature versus time for mixes #44 and #55	90
Figure 4.6: Autogenous shrinkage strain versus time for mixes #44 and #55	91
Figure 4.7: Capillary pressure versus time for mixes #44 and #55	91
Figure 4.8: Temperature versus time for mixes #61 and #66	92
Figure 4.9: Autogenous shrinkage strain versus time for mixes #61 and #66	93
Figure 4.10: Capillary pressure versus time for mixes #61 and #66	93
Figure 4.11: Temperature versus time for mixes #50 and #61	94

Figure 4.12: Autogenous shrinkage strain versus time for mixes #50 and #61	95
Figure 4.13: Capillary pressure versus time for mixes #50 and #61	95
Figure 4.14: Temperature versus time for mixes #53 and #61	96
Figure 4.15: Autogenous shrinkage strain versus time for mixes #53 and #61	97
Figure 4.16: Capillary pressure versus time for mixes #53 and #61	97
Figure 4.17: Temperature versus time for mixes #39 and #44	98
Figure 4.18: Autogenous shrinkage strain versus time for mixes #39 and #44	99
Figure 4.19: Capillary pressure versus time for mixes #39 and #44	99
Figure 4.20: Temperature versus time for mixes #64 and #66	100
Figure 4.21: Autogenous shrinkage strain versus time for mixes #64 and #66	101
Figure 4.22: Capillary pressure versus time for mixes #64 and #66	101
Figure 4.23: Concrete compressive strength of moist cured versus air cured cylinders	103
Figure 5.1a: ACI - 209 Model – Predictions of shrinkage strains versus measured values for 3 days concrete	109
Figure 5.1b: JSCE 2002 Model – Predictions of shrinkage strains versus measured values for 3 days concrete	110
Figure 5.1c: B3 Model – Predictions of shrinkage strains versus measured values for 3 days concrete	110
Figure 5.1d: CEB – FIP 1990 Model – Predictions of shrinkage strains versus measured values for 3 days concrete	111
Figure 5.1e: EHE Model – Predictions of shrinkage strains versus measured values for 3 days concrete	111
Figure 5.1f: GL 2000 Model – Predictions of shrinkage strains versus measured values for 3 days concrete	112
Figure 5.1g: Eurocode 2 Model – Predictions of shrinkage strains versus measured values for 3 days concrete	112
Figure 5.1h: Regression Model (90% Confidence level) – Predictions of shrinkage strains versus measured values for 3 days concrete	113

Figure 5.1i: Regression Model (95% Confidence level) – Predictions of shrinkage strains versus measured values for 3 days concrete	113
Figure 5.2a: ACI - 209 Model – Predictions of shrinkage strains versus measured values for 14 days concrete	114
Figure 5.2b: JSCE 2002 Model – Predictions of shrinkage strains versus measured values for 14 days concrete	115
Figure 5.2c: B3 Model – Predictions of shrinkage strains versus measured values for 14 days concrete	115
Figure 5.2d: CEB – FIP 1990 Model – Predictions of shrinkage strains versus measured values for 14 days concrete	116
Figure 5.2e: EHE Model – Predictions of shrinkage strains versus measured values for 14 days concrete	116
Figure 5.2f: GL 2000 Model – Predictions of shrinkage strains versus measured values for 14 days concrete	117
Figure 5.2g: Eurocode 2 Model – Predictions of shrinkage strains versus measured values for 14 days concrete	117
Figure 5.2h: Regression Model (90% Confidence level) – Predictions of shrinkage strains versus measured values for 14 days concrete	118
Figure 5.2i: Regression Model (95% Confidence level) – Predictions of shrinkage strains versus measured values for 14 days concrete	118
Figure 5.3a: ACI - 209 Model – Predictions of shrinkage strains versus measured values for 28 days concrete	119
Figure 5.3b: JSCE 2002 Model – Predictions of shrinkage strains versus measured values for 28 days concrete	120
Figure 5.3c: B3 Model – Predictions of shrinkage strains versus measured values for 28 days concrete	120
Figure 5.3d: CEB – FIP 1990 Model – Predictions of shrinkage strains versus measured values for 28 days concrete	121

Figure 5.3e: EHE Model – Predictions of shrinkage strains versus measured values for 28 days concrete	121
Figure 5.3f: GL 2000 Model – Predictions of shrinkage strains versus measured values for 28 days concrete	122
Figure 5.3g: Eurocode 2 Model – Predictions of shrinkage strains versus measured values for 28 days concrete	122
Figure 5.3h: Regression Model (90% Confidence level) – Predictions of shrinkage strains versus measured values for 28 days concrete	123
Figure 5.3i: Regression Model (95% Confidence level) – Predictions of shrinkage strains versus measured values for 28 days concrete	123
Figure 5.3j: Regression model (95% Confidence level – without interaction parameters) – Predictions of shrinkage strains versus measured values for 28 days concrete	124
Figure 5.4a: ACI - 209 Model – Predictions of shrinkage strains versus measured values for 56 days concrete	125
Figure 5.4b: JSCE 2002 Model – Predictions of shrinkage strains versus measured values for 56 days concrete	125
Figure 5.4c: B3 Model – Predictions of shrinkage strains versus measured values for 56 days concrete	126
Figure 5.4d: CEB – FIP 1990 Model – Predictions of shrinkage strains versus measured values for 56 days concrete	126
Figure 5.4e: EHE Model – Predictions of shrinkage strains versus measured values for 56 days concrete	127
Figure 5.4f: GL 2000 Model – Predictions of shrinkage strains versus measured values for 56 days concrete	127
Figure 5.4g: Eurocode 2 Model – Predictions of shrinkage strains versus measured values for 56 days concrete	128
Figure 5.4h: Regression Model (90% Confidence level) – Predictions of shrinkage strains versus measured values for 56 days concrete.....	128

Figure 5.4i: Regression Model (95% Confidence level) – Predictions of shrinkage strains versus measured values for 56 days concrete	129
Figure 5.5a: ACI - 209 Model – Predictions of shrinkage strains versus measured values for 119 days concrete	130
Figure 5.5b: JSCE 2002 Model – Predictions of shrinkage strains versus measured values for 119 days concrete	130
Figure 5.5c: B3 Model – Predictions of shrinkage strains versus measured values for 119 days concrete	131
Figure 5.5d: CEB – FIP 1990 Model – Predictions of shrinkage strains versus measured values for 119 days concrete	131
Figure 5.5e: EHE Model – Predictions of shrinkage strains versus measured values for 119 days concrete	132
Figure 5.5f: GL 2000 Model – Predictions of shrinkage strains versus measured values for 119 days concrete	132
Figure 5.5g: Eurocode 2 Model – Predictions of shrinkage strains versus measured values for 119 days concrete	133
Figure 5.5h: Regression Model (90% Confidence level) – Predictions of shrinkage strains versus measured values for 119 days concrete	133
Figure 5.5i: Regression Model (95% Confidence level) – Predictions of shrinkage strains versus measured values for 119 days concrete	134

LIST OF PHOTOS

Photo 3.1: Setup for autogenous shrinkage measurements.....	58
Photo 3.2: Experiment in progress.....	58

Chapter 1

Introduction

1.0 Preliminaries

Concrete is the most employed construction material around the globe due to its ease of use, high compressive strength, high stiffness, durability, relatively low cost, and its ability to be formed in any shape and be used even under water. One of the major disadvantages of concrete is its weak resistance to tensile forces; under such forces, cracks may develop and make the concrete prone to many environmental effects that may affect its durability and strength. Researchers and engineers have been focusing during the past decades on enhancing the concrete properties especially its compressive strength, workability, and resistance to cracking. Similar to other porous materials, concrete undergoes volume change known as concrete shrinkage or concrete swelling; concrete shrinkage leads to cracking that undermines the serviceability and durability of the material. There are many types of shrinkage that affect concrete, namely drying shrinkage, autogenous shrinkage, chemical shrinkage, carbonation shrinkage, thermal shrinkage, and plastic shrinkage.

1.1 Statement of purpose

The aim of this study is to investigate experimentally the different parameters that influence concrete's early age and long term shrinkage. Autogenous shrinkage occurs during the early ages of concrete, whereas chemical and drying shrinkage can occur for a much longer period. The experimental program is founded on the factorial design of experiments with six main parameters: water-to-cement ratio, water content, maximum aggregate size, ground granulated blast furnace slag as cement replacement, silica fume as cement replacement, and bulk volume of coarse aggregate. This study also assesses the adequacy of analytical models adopted by international standards for predicting concrete shrinkage strain.

1.2 Overview

This thesis contains six chapters. The first chapter provides a brief description of the research topic and identifies the objectives of this study. Chapter 2 presents a literature review on all types of shrinkage that affect concrete along with their mechanisms, test methods, controlling factors, and mitigation techniques. It also presents a review of the different prediction models for shrinkage that have been proposed in the literature and adopted by European, Japanese and North American standards.

Chapter 3 presents the experimental program developed on the basis of fractional factorial design to study the influence of the different parameters that affect shrinkage strain values. This chapter also deals with the experimental procedure, test methods, and presents the experimental results.

Chapter 4 provides an assessment for chemical, drying and autogenous shrinkage strain, and an evaluation of the concrete compressive strength for air and moist cured cylinders. The shrinkage strains at different ages are mathematically modeled using regression techniques. The statistical significance of the investigated parameters is assessed for the shrinkage strain at different ages. Relations between autogenous shrinkage, capillary pressure, temperature, and the mixture compositions are also discussed in this chapter.

Chapter 5 provides a statistical assessment of the existing prediction models for concrete shrinkage strains. A tabulated comparison for the different models is presented at the end of this chapter. A summary of this study, conclusions and recommendations are presented in Chapter 6.

Chapter 2

Literature Review

2.0 Introduction

Concrete is a mixture of cement, water and aggregate. Cement and water constitute the glue (paste) that covers and binds the fine and coarse aggregates. Portland cement is a hydraulic material since it reacts with water and transforms the heterogeneous mixture to a solid mass. The properties of the formed solid material that are of interest to structural engineers are specifically compressive strength and shrinkage strain. These properties are related to the proportions and properties of concrete mixture.

Concrete shrinkage is defined as a reduction in volume through time, and is mainly due to water movement within a concrete's porous structure and to chemical reactions. The emptying of pores due to water movement generates tensile stresses that pull the cement

paste closer causing shrinkage, while chemical reactions generate products whose volume is less than the volume of the initial ingredients (Tazawa et al., 1999; Holt, 2001).

Shrinkage has been divided into two phases; the early age shrinkage, which occurs in the first 24 hours and the long term shrinkage, which occurs after 24 hours (Holt, 2001). This division was put toward to distinguish between the driving mechanisms for each phase (Holt, 2001). For a concrete mixture with water-to-cement ratio greater than 0.42, the shrinkage at early age is mainly due to the chemical hydration reactions, while the long term shrinkage is attributed to water exchange and evaporation. Traditionally, the early age shrinkage was not a concern since its magnitude was considered to be negligible in comparison to the long term drying shrinkage (Holt, 2001). However, with the development of high strength concrete that possesses low water-to-cement ratio, it was found that the early age shrinkage must be accounted for. Early age shrinkage strain is important because it occurs at a time when concrete is developing stiffness at a faster rate than its strength. As such, the development of cracks becomes inevitable (Nawa and Horita, 2004).

The magnitude of shrinkage strain depends highly on the cementing properties and mixture proportions. Shrinkage occurs due to paste volume change, while the coarse aggregates act to resist it. Therefore, concrete mixtures containing a high content of coarse aggregates with high modulus of elasticity and rough surfaces yield less shrinkage strain (Cement and Concrete Association of Australia – CCAA, 2002). Mineral admixtures such as silica fume, fly ash and ground granulated blast furnace slag, which are added as cementing materials, also influence shrinkage strain because their addition has been shown to enhance the pore refinement of the cement paste, thus yielding a stiffer and stronger material (Mazloom et al., 2004; Khatri and Sirvivatnanon, 1995). It should be noted that the consequence of pore refinement is an increase in capillary tension and hence more autogenous shrinkage (Mazloom et al., 2004; Jensen and Hansen, 2001; Tazawa and Miyazawa, 1995; Zhang et al., 2003). Moreover, a further increase in the amount of mineral admixtures is found to augment shrinkage, both autogenous and drying, because the specific

gravity of these minerals is less than that of ordinary Portland cement (ACI Committee 226, 1994). Water-to-cement ratio is also known to have a major influence on shrinkage. Concrete mixtures containing more water imply less rigidity and more pores, which in turn, will yield higher drying shrinkage and lower autogenous shrinkage (Smadi et al., 1987). Shrinkage strains and corresponding stresses at the early age of concrete can lead to initiation and propagation of cracks, which diminish a concrete's ability to bar the entry of water and other substances. Subsequently, the durability of concrete is compromised (Lura et al., 2003).

From a structural point of view, early and long term shrinkage can lead to undesirable results such as residual stresses, loss of prestress forces, and a reduction in the moment of inertia, which in turn affects serviceability and deflection. If concrete members were free to shrink, then shrinkage would not be an issue. However, concrete elements are always restrained either by other structural elements or supports. Moreover, steel reinforcement introduces restraints to concrete deformation. Restraints imposed on concrete generate tensile stresses that yield cracks when the magnitude of the stresses is greater than the concrete tensile strength. These cracks are time dependent since the shrinkage strain is time dependent (Gilbert, 2001).

This chapter provides a review of the different types of shrinkage strain reported in the literature along with the corresponding driving mechanism, test methods and mitigation techniques. Subsequently, predictive shrinkage strain models reported in the literature that have been adopted by various codes and standards are reviewed.

2.1 Shrinkage

Water movement and moisture losses within the concrete mixtures are the major factors causing shrinkage. Chemical reactions induce water movements within the concrete elements leading to chemical and autogenous shrinkage, however water movement outside the concrete elements, which are water losses, causes drying shrinkage (Chidiac, 2009; Mehta and Monterio, 2006). In the literature, shrinkage has been divided into six types reflecting the different mechanisms. They are chemical shrinkage, autogenous shrinkage, plastic shrinkage, drying shrinkage, carbonation shrinkage and thermal shrinkage.

2.1.1 Chemical Shrinkage

Chemical shrinkage is defined as “the phenomenon in which the absolute volume of hydration products is less than the total volume of unhydrated cement and water before hydration.” (Tazawa et al., 1999). This type of shrinkage is due mainly to chemical reactions in the concrete. At the early stage, when the concrete is still plastic, i.e., in the liquid phase, the chemical shrinkage results in overall reduction of the specimen volume. However, at the stage where the concrete begins to be stiffer, chemical shrinkage tends to create pores within the mix structure (Lura et al., 2003).

Shrinkage of the cement phases, as given in Table 2.1, was studied by Power (1935). The results show that at 28 days tricalcium aluminate, C_3A , shrinks the most and dicalcium silicate, C_2S , shrinks the least. Shrinkage of tricalcium silicate, C_3S , and tetracalcium alumino ferrite, C_4AF , is found to be closer to that of C_2S .

Table 2.1 Chemical shrinkage of cement paste (Power, 1935)

Phase	Shrinkage (cm^3/g)				
	1 day	3 days	7 days	14 days	28 days
C ₃ S	0.0188	0.0300	0.0336	0.0409	0.0481
C ₂ S	0.0110	0.0126	0.0106	0.0140	0.0202
C ₃ A	0.0632	0.0759	0.1133	0.1201	0.1091
C ₄ AF	0.019	0.0202	0.0415	0.0352	0.0247

Paulini also studied the chemical shrinkage of ordinary Portland cement (OPC) phases up to 7 days and the results are shown in Figure 2.1. By comparing the values in Table 2.1 and Figure 2.1, after 7 days one observes that C₃A exhibits the largest shrinkage and C₂S the smallest value. However, the measured chemical shrinkages for the two phases are significantly different. The same observation can be made in regard to the values of the other phases, namely, C₄AF and C₃S. The difference in results can be attributed to improvement in testing techniques and in the ability to extract the pure cement phases from OPC.

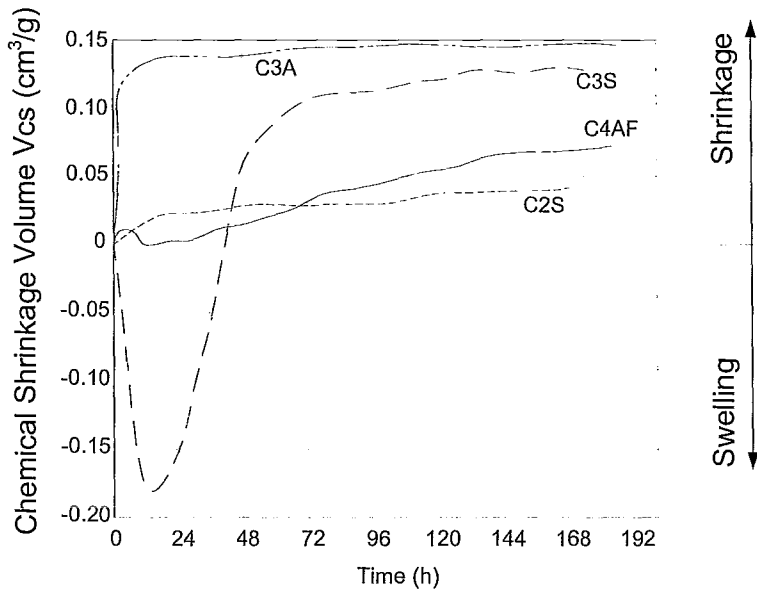


Figure 2.1 Chemical shrinkage (Paulini, 1996)

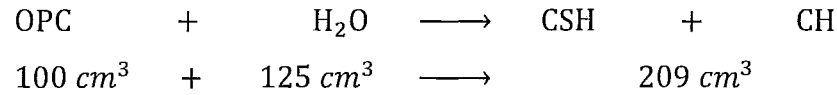
Chemical shrinkage, V_{CS} , is calculated as follows (Tazawa et al., 1999):

$$V_{CS} = \frac{(V_c + V_w) - V_{hy}}{V_{ci} + V_{wi}} \times 100 \quad (2.1)$$

where V_c is the volume of hydrated cement, V_{ci} the volume of cement before mixing, V_{wi} the volume of water before mixing, V_w the volume of reacted water, and V_{hy} the volume of hydrated products. Paulini (1996) proposed to calculate the chemical shrinkage (cm^3/g of cement) from its phases:

$$V_{CS} = 0.0532 [\text{C}_3\text{S}] + 0.0400 [\text{C}_2\text{S}] + 0.1113 [\text{C}_4\text{AF}] + 0.1785 [\text{C}_3\text{A}] \quad (2.2)$$

This indicates that mitigation of chemical shrinkage is possible by reducing the amount of two phases, namely C_3A and C_4AF . When examining the overall reaction of OPC paste, the chemical shrinkage is about 7% (Chidiac, 2009):



where H_2O , CSH and CH represent respectively, water, calcium silica hydrate and calcium hydroxide.

Le Chatelier (1900) and Power (1935) were the first to develop methods for measuring chemical shrinkage. Current technology such as Dilatometry test and Weighing reduced buoyancy allows for a more precise measurement of chemical shrinkage (Holt, 2001). With the Dilatometry method shown in Figure 2.2, a diluted cement paste is placed into a sample vessel and connected to a pipette. The chemical shrinkage is measured by monitoring the water level variation in the pipette. The second method is based on Archimedes principles where the volume reduction of the submerged sample is monitored through an apparent weight increase. This method can be automated as shown in Figure 2.3.

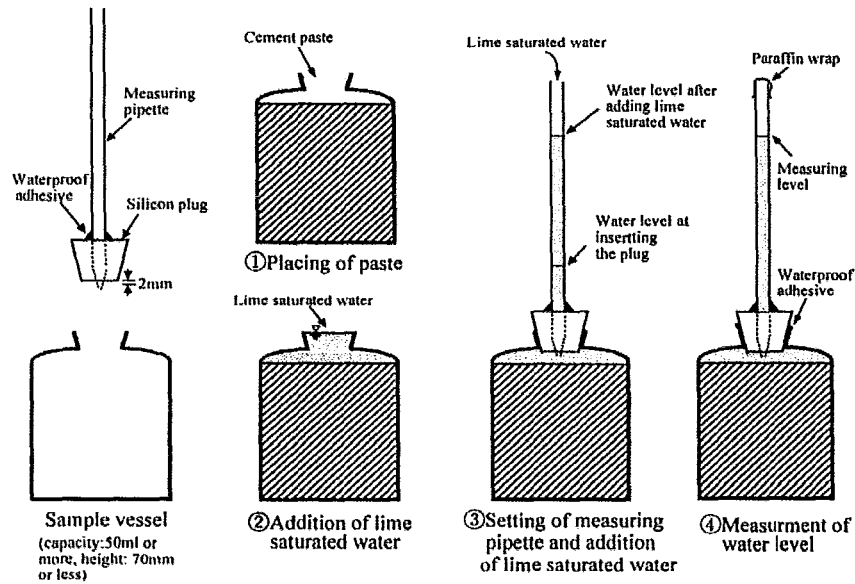


Figure 2.2 Dilatometry test arrangement (Holt, 2001)

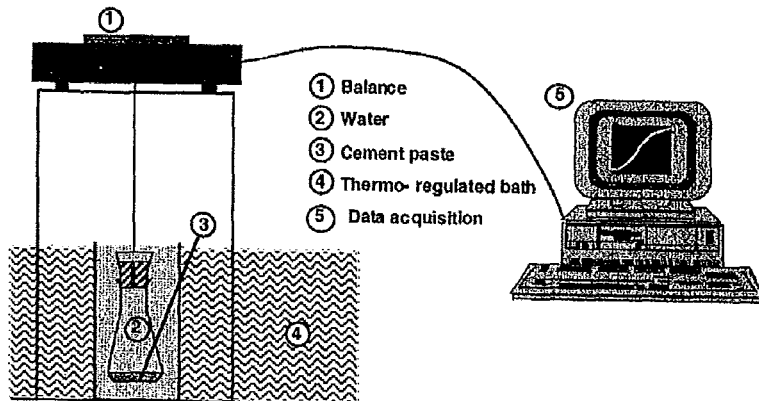


Figure 2.3 Reduced buoyancy test arrangement (Holt, 2001)

Figure 2.4 illustrates chemical shrinkage strain evolution as a function of time for an OPC with a water cement ratio of 0.5. The results indicate that chemical shrinkage passes from 3% at 1 day to 5% after a week then to 7.5% after a month. These results also indicate that the major portion of chemical shrinkage takes place in the first month of concrete age.

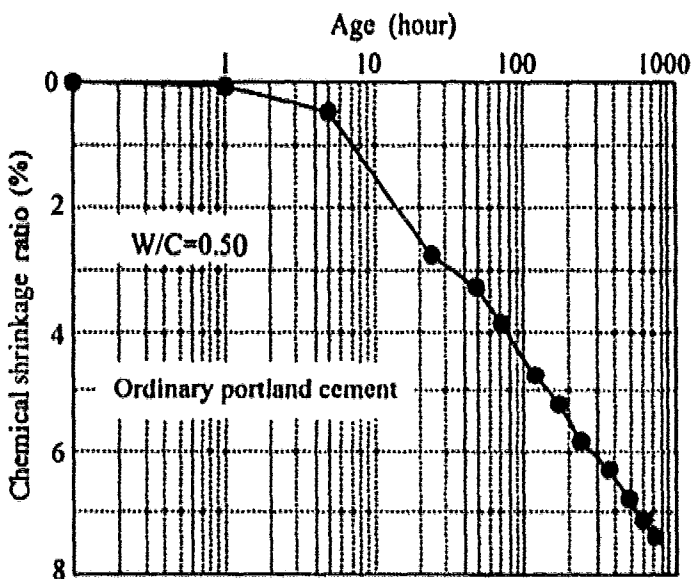


Figure 2.4 Chemical shrinkage measurements versus time (Tazawa et al., 1999)

2.1.2 Autogenous Shrinkage

The Japan Concrete Institute, JCI, (Tazawa et al., 1999) has defined autogenous shrinkage as “the macroscopic volume reduction of cementitious materials when cement hydrates after initial setting. Autogenous shrinkage does not include the volume change due to loss or ingress of substances, temperature variation, application of an external force and restraint”. Therefore, the autogenous shrinkage is a volume reduction of the concrete with no moisture transfer with the outer environment. The autogenous shrinkage is a concern where concrete has a water-to-cement ratio less than 0.42 (Holt, 2001). According to Justnes et al. (1996), autogenous shrinkage has been given many labels such as bulk shrinkage, Le Chatelier shrinkage, indigenous shrinkage, self desiccation shrinkage, and autogenous volume change.

The relation between autogenous and chemical shrinkage is shown in Figure 2.5. The results show that chemical shrinkage induces internal voids and autogenous shrinkage results in element shortening. Autogenous shrinkage’s magnitude and mechanism depend highly on the mixture proportions and not on factors such as casting, pouring and curing methods (Holt,

2001). Autogenous shrinkage needs to be considered for concrete that has low cement to water ratio and for mineral admixtures that have lower specific gravity in comparison to OPC such as high fine granulated blast furnace slag and silica fume (Tazawa et al., 1999).

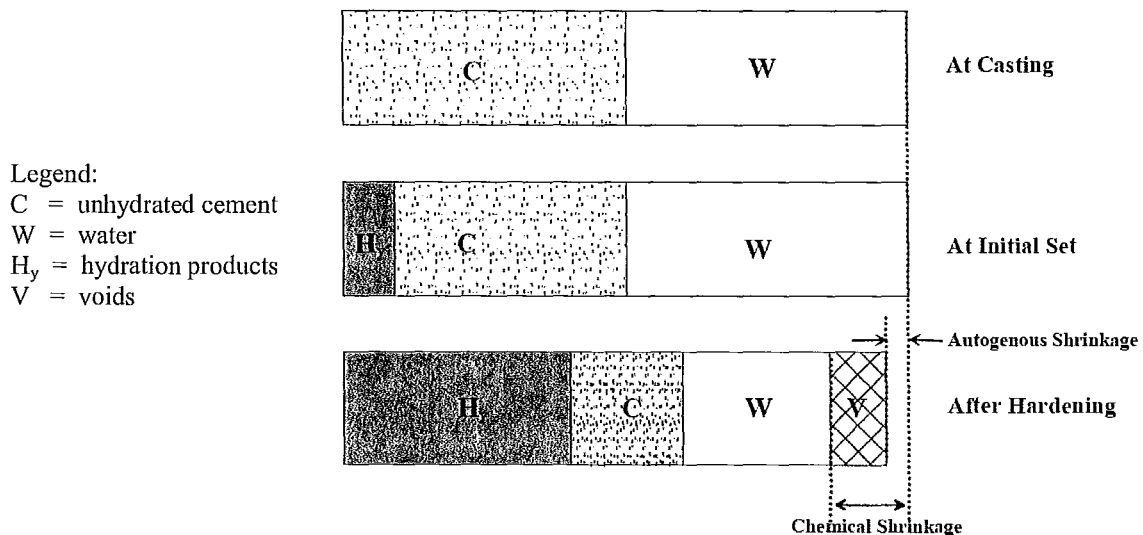


Figure 2.5 Chemical and autogenous shrinkage interaction in the horizontal direction
(Tazawa et al., 1999)

At the very early stage of hydration, when the concrete mixture is still in liquid state, the autogenous shrinkage and chemical shrinkage are the same phenomenon and induce an overall volume reduction as shown in Figure 2.6. However, as the hydration of cement proceeds, the concrete skeleton begins to form and resists the stress induced by the chemical shrinkage. At this stage, the chemical and autogenous shrinkage differ from each other (Lura et al., 2003). The hydration from that point on will create pores in the concrete structures. Autogenous shrinkage is related to the stiffness and strength of the concrete skeleton, which in turn is related to the hydration morphology (Tazawa et al., 1999).

Once the hard skeleton is formed, autogenous shrinkage becomes due to self desiccation. As the hydration of cement proceeds, the free water is gradually consumed and fine pores are formed. Therefore, for concrete with low water-to-cement ratio, there is a lack of free water

for the hydration. The cement, in search of the extra water will attract it first from the capillary pores and then from the gel water for the hydration of cement to progress. The consumption of capillary water and gel water decreases the relative humidity in the pores. This phenomenon is called “self desiccation” because of the decrease in the internal humidity without any mass transfer to the exterior (Tazawa et al., 1999).

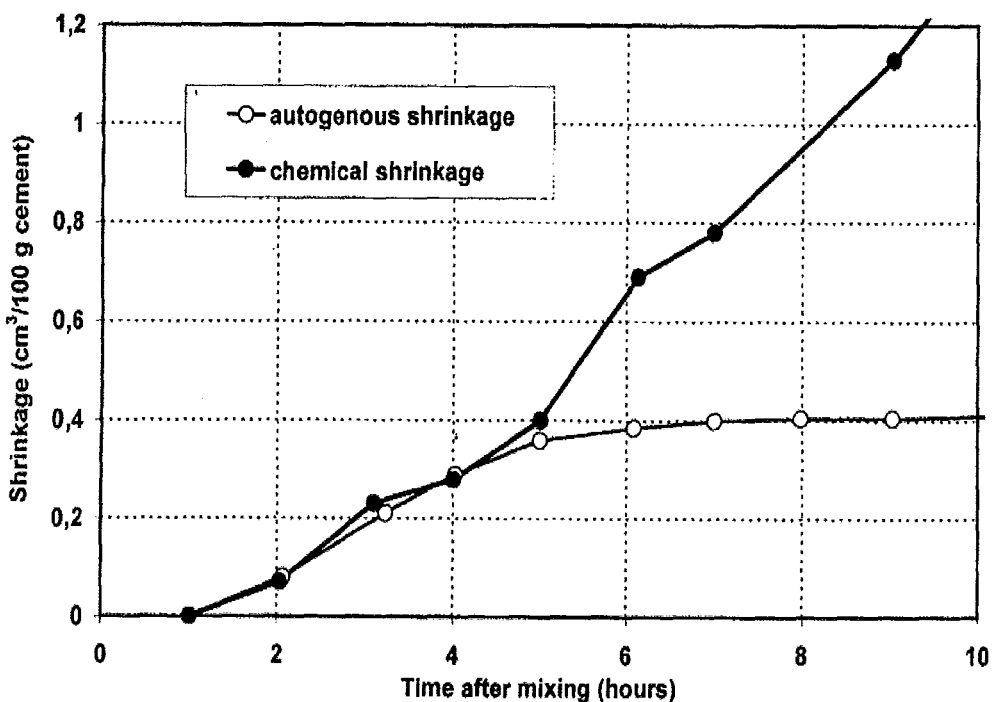


Figure 2.6 Autogenous shrinkage and chemical shrinkage versus time (Hammer, 1999)

The self desiccation induces negative pressure in the meniscus formed, leading to the shrinkage of concrete. The relation between self-desiccation phenomenon and shrinkage or the negative pressure can be explained using Kelvin relation (Chidiac, 2009):

$$\ln \varphi = -\frac{2 \sigma M}{\rho R T r} \quad (2.3)$$

where φ is the relative humidity, M the molecular weight of water (18 kg/kmol), ρ the density of water (998 kg/m³), R the gas constant (8,214 J/(kmol°K)), T the temperature (°K), r the

pore radius (m), and σ the surface tension of air-water interface (~ 0.074 N/m). The suction pressure or pore pressure, s (Pa), is then obtained by using Laplace Relation (Janz, 2000), where r' is the meniscus radius (m).

$$s = \frac{2\sigma}{r'} \quad (2.4)$$

By substituting Eq. 2.3 into Eq. 2.4 and assuming that the pore radius is equal to the meniscus radius, an expression that relates relative humidity and suction pressure is obtained:

$$\ln\varphi = -\frac{s M}{\rho RT} \quad (2.5)$$

Graphical plot of Eq. 2.5 is shown in Figure 2.7.

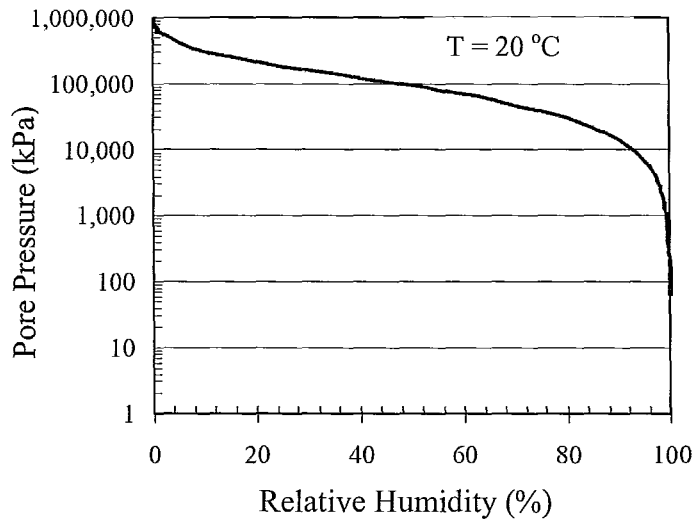


Figure 2.7 Relative humidity versus pore pressure based on Laplace and Kelvin relations
(Holt, 2001)

Autogenous shrinkage is found to be more affected by the hydration of C_3A and C_4AF in comparison to the hydration of C_2S and C_3S , and is also a function of cementing type as shown in Figure 2.8 (Tazawa et al., 1999; Lura et al., 2003). The addition of chemical

admixtures such as super-plasticizer or expansive additive has an influence on the autogenous shrinkage strain as shown in Figure 2.9 (Tazawa et al., 1999). Autogenous shrinkage is also affected by other factors such as the setting time or any mixture parameters that can delay the development of stiffness and strength since in such circumstances the modulus of elasticity will be lower than normal and the deformation therefore will be higher (Lura et al., 2003).

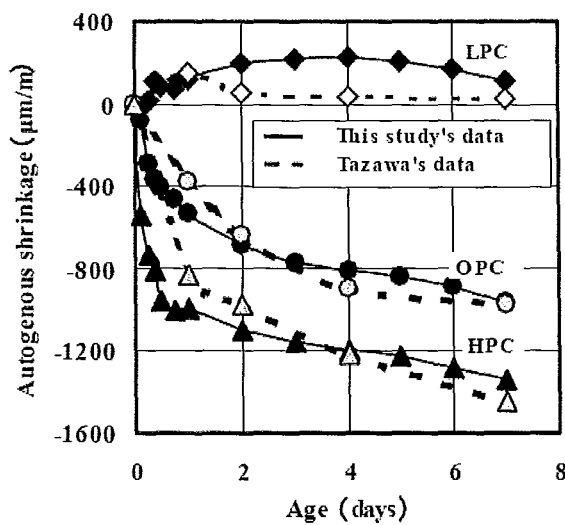


Figure 2.8 Effect of cement type on autogenous shrinkage strain of cement paste with water-to-cement ratio equals to 0.3 (Lura et al., 2003)

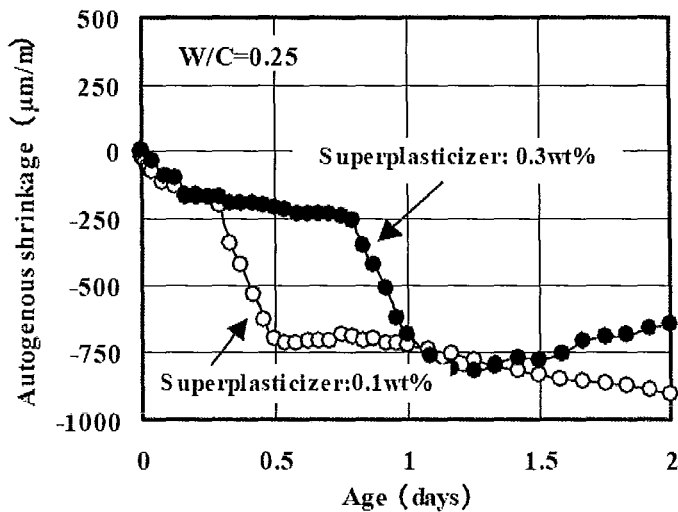


Figure 2.9 Effect of super-plasticizer on autogenous shrinkage strain of cement paste (Lura et al., 2003)

The effects of mineral admixtures on autogenous shrinkage vary depending on the type and amount of admixture added to the mixture. The addition of fly ash is found to reduce the autogenous shrinkage since its presence causes the chemical expansion of the cement paste (Tangtermsirikul, 1995). The results of a series of tests taking different percentage of fly ash content are shown in Figure 2.10. However, the addition of silica fume or ground granulated blast furnace slag (GGBFS) augments the pores refinement leading to an increase in capillary tension and more contraction stress, which increase the autogenous shrinkage (Omar et al., 2008). In addition, and since the specific gravity of GGBFS is less than that of OPC paste, high replacement percentage yields higher paste volume that augments further the autogenous shrinkage as shown in Figure 2.11 (ACI Committee 226, 1994).

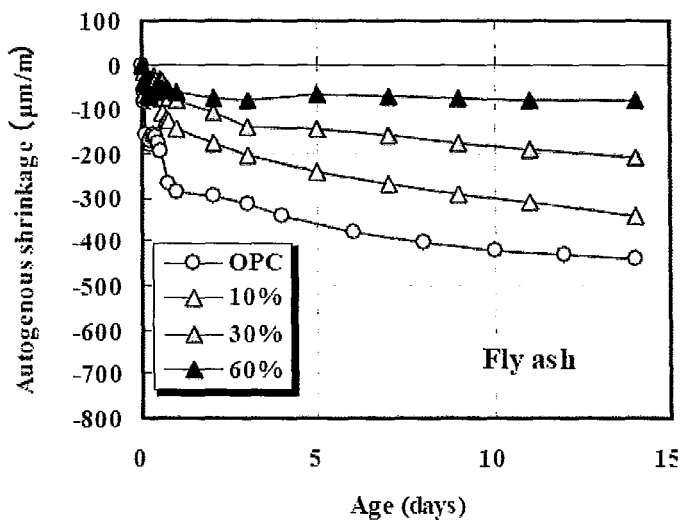


Figure 2.10 Effect of fly ash on autogenous shrinkage of mortar with water to binder ratio equals to 1.0 by volume (Lura et al., 2003)

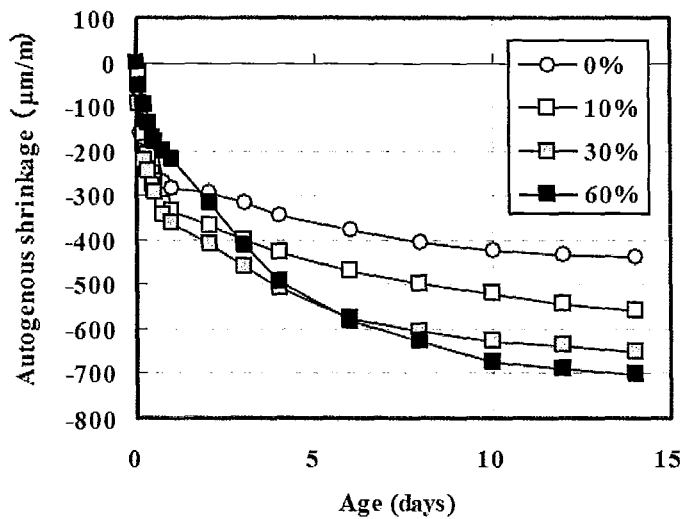


Figure 2.11 Effect of granulated blast furnace slag on autogenous shrinkage of mortar with water to binder ratio equals to 1.0 by volume (Lura et al., 2003)

The effect of water-to-cement ratio, w/c, on autogenous shrinkage is the most important since the capillary stresses are function of the size of the pores being emptied. Autogenous deformation, which has a strong dependence on w/c, is found to increase drastically once the w/c value goes below 0.4 as shown in Figure 2.12.

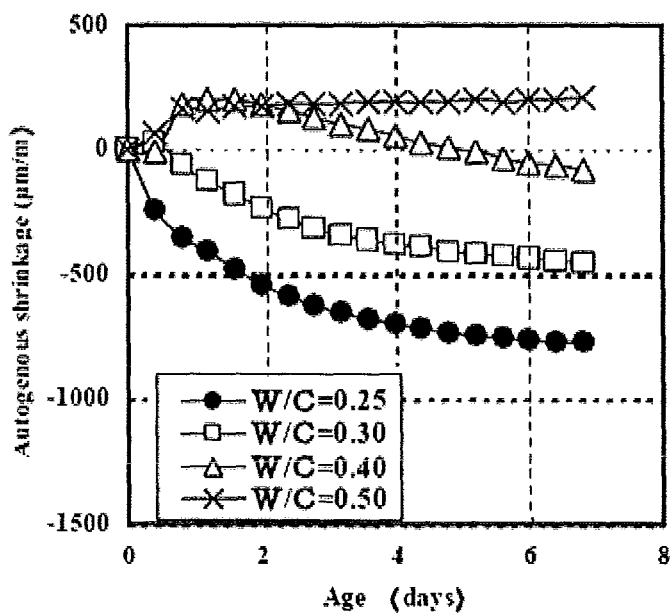


Figure 2.12 Effect of w/c on autogenous shrinkage strain (Lura et al., 2003)

Coarse aggregates influence the autogenous shrinkage depending on their volume concentration and their modulus of elasticity. Shrinkage is due to the cement paste, and aggregates contribute to the resistance against the deformation and stresses induced (Tazawa et al., 1999). Ambient temperature has also been found to affect autogenous shrinkage, where higher temperature accelerates the autogenous shrinkage strain evolution (Tazawa et al., 1999).

Since the autogenous stresses are controlled by the size of the pores that are being emptied during self-desiccation, these stresses can be significantly reduced by incorporating a reservoir of water into the large pores, typically larger than the capillary pores, in the hydrating cement. Hence the idea of Internal Curing, IC, was born. This has been accomplished with the use of partially saturated light weight aggregate, LWA, superabsorbent polymer particles, SAP, (Geiker et al., 2008), saturated wood fibre, and pre-wetted crushed aggregates (Bentz and Weiss, 2008). The addition of SAP or LWA keep the relative humidity in the mix up to a certain level by emptying first the large pores within the LWA or the one formed by SAP particles. Another option for reducing autogenous shrinkage is by minimizing the magnitude of the surface tension of the pore solution, which can be achieved through the addition of shrinkage-reducing agent SRA (Bentz and Weiss, 2008, Geiker et al. 2008), or through the addition of fibres that can enhance the modulus of elasticity of concrete mixture (Ambrosia, Lange and Grasley, 2002).

Measuring the autogenous shrinkage at the early age of concrete is a challenging task, since the concrete sample must be isolated thermally and hygrically and it cannot be structurally restrained. Currently, there is no standardized test method for measuring the autogenous shrinkage in the horizontal direction. The measurement of autogenous shrinkage in the vertical direction can be done according to ASTM C827 (Tazawa et al., 1999). However, many researchers at VTT (Kronlöf et al., 1995; Leivo and Holt, 1997; Holt and Leivo, 1996), Europe, and Japan (Radocea, 1992; Mak et al. 1999; Bjøntegaard, 1999; Hammer, 1999; Tazawa and Miyazawa, 1995) have suggested different test arrangements to

measure more accurately autogenous shrinkage. These methods along with a brief description on their advantages and disadvantages are summarized below. It should be noted that for all of these test methods, the fresh concrete sample is isolated similar to the one shown in Figure 2.15.

Embedded Gauges (Tazawa et al., 1999) – The embedded gauges method places two vertical metal strips in the concrete sample and near the bottom of the mould as shown in Figure 2.13. Autogenous shrinkage is captured by the movement of the metal strips by means of linear voltage differential transducer, LVDT. The major disadvantages of this method are the influence of the concrete setting, the vertical forces and friction resistance on the horizontal movement measurements as well as the difficulties in keeping the verticality of the metal strips during the test period.

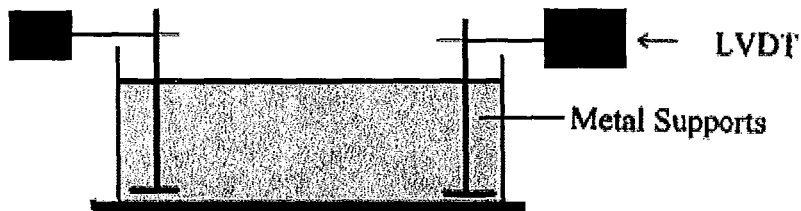


Figure 2.13 Embedded gauges test setup (Tazawa et al., 1999)

Suspended Gauges (Holt, 2001) – This method is a modification of the embedded gauge, in which the metal strips are hanging on a support frame as shown in Figure 2.14. The advantage of this method is the reduction in friction between the metal strips bases and the concrete as well as the forces exerted on the strips. However, the interactions of vertical movement with the horizontal movements still exist with an additional friction between the strips and the metal support.

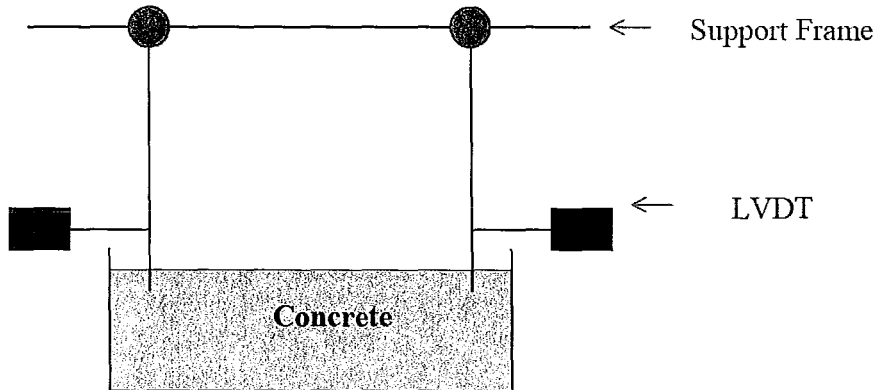


Figure 2.14 Suspended gauges test setup (Holt, 2001)

Gauges through walls (Tazawa et al., 1999) – This method is more common in northern Europe. In this method, two horizontal plates are linked to dial gauge at mid-height of the mould as shown in Figure 2.15. The main advantage of this method is that the friction between the metal strips and the concrete surface is removed. However, the friction at the connection between the links and the dial gauges at the walls' interface is a concern and may alter the values of the early measurements.

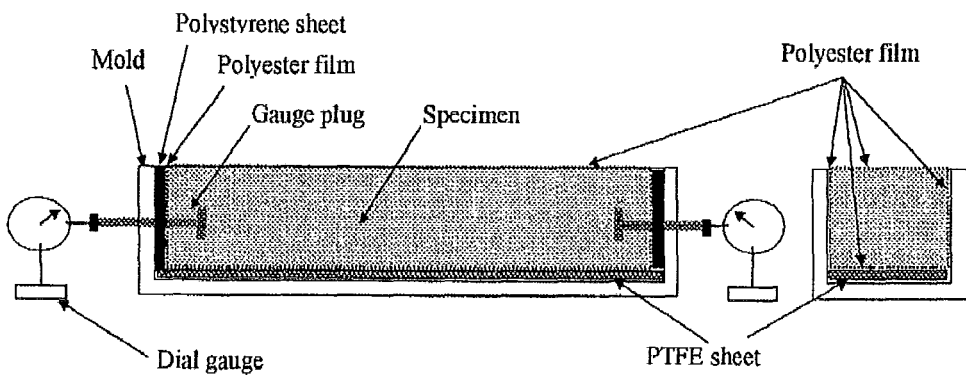


Figure 2.15 Gauges through walls test setup (Tazawa et al., 1999)

Non-Contact Along walls (Tazawa et al., 1999) – This method is a minor modification of gauges through wall set-up, where the friction at the wall interface is removed, Figure 2.16.

The material of the mould must be non-interfering materials. The arrangement in this method is the most advantageous in comparison to the three previous methods. However, many concerns still exist such as the verticality of the vertical strips, which cannot be seen or verified in this method, and the vertical forces exerted by the concrete setting on them.

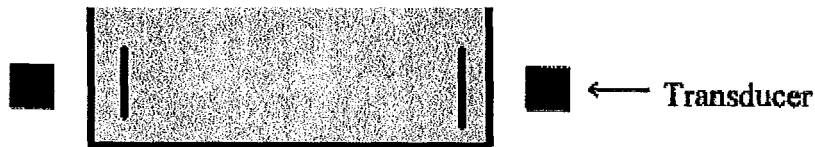


Figure 2.16 Non-contact test setup (Tazawa et al., 1999)

Lasers on surface (Tazawa et al., 1999) – Currently, this method is the most accurate and has been adopted by VTT. With this method, lightweight sensors are placed on the top surface of the concrete sample to detect the movement as shown in Figure 2.17. The friction between the measuring tools and the concrete or mould is removed, and the only concern is keeping the sensors levelled.

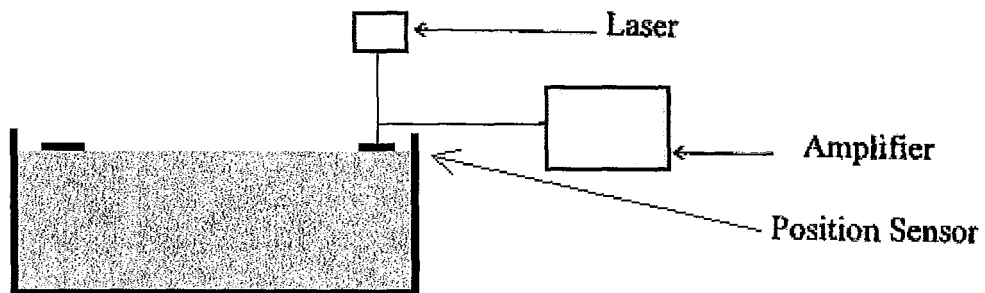


Figure 2.17 Lasers on surface test setup (Tazawa et al., 1999)

Vertical Autogenous Shrinkage – Nawa and Horita (2004) proposed the arrangement shown in Figure 2.18 to measure the vertical strain as well as the temperature of the concrete. The concrete is poured into a cylindrical mould with a vertical gauge and thermometer. The

concrete is isolated through a film and Teflon sheet. The gauge embedment and set up are verified at the end of the test, after cleaving the concrete sample. The measurements of strain must take into account the difference in the thermal expansion coefficients of both the concrete and the strain gauge. The strain gauge should be treated by immersing it in deionised water for 24 hours in order to prevent absorption of moisture from the paste. This method gives results to a high level of accuracy, however the setup needs high level of precision and cautions.

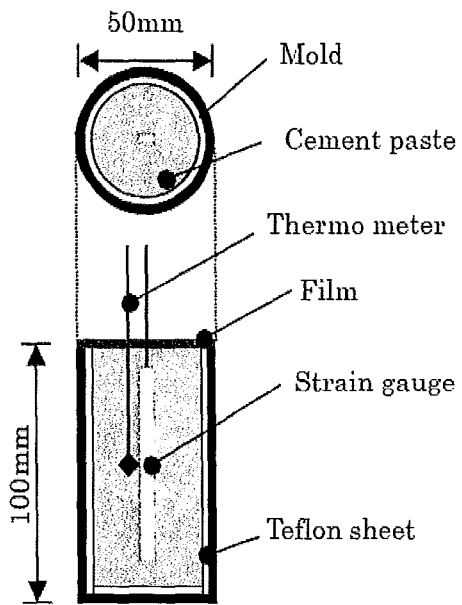


Figure 2.18 Method proposed for measuring vertical strain of autogenous shrinkage (Nawa and Horita, 2004)

Figure 2.19 shows autogenous shrinkage values for an early age concrete along with the capillary pressure. The results indicate that a strong relation exists between the autogenous shrinkage strain and capillary pressure.

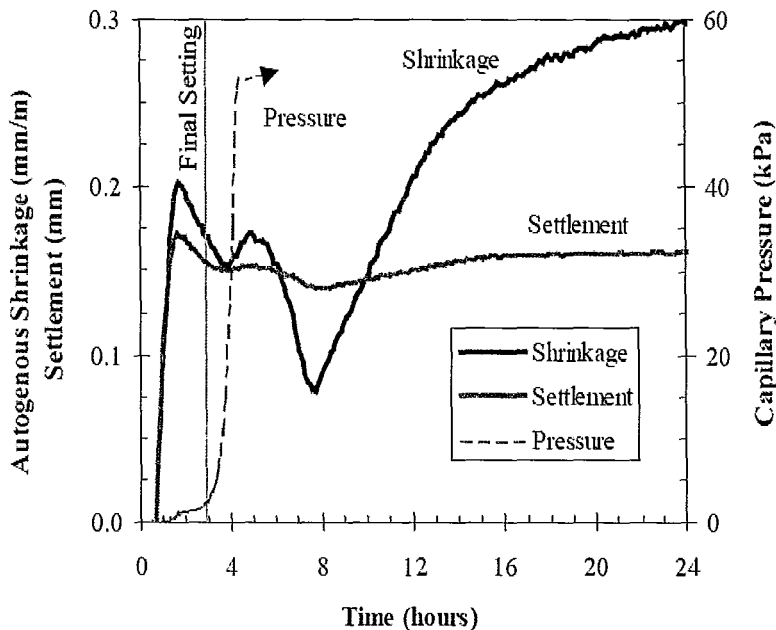


Figure 2.19 Autogenous shrinkage and capillary pressure of concrete during the first 24 hours (Holt, 2001)

2.1.3 Plastic Shrinkage

Plastic shrinkage relates to the strain of the concrete surface when it is in the plastic phase, a short term phenomenon. This type of shrinkage is mainly due to water evaporation and differs from the drying shrinkage, which is a long term process. The generated cracks due to plastic shrinkage form between 1 and 6 hours after casting and are not noticed before 24 hours (Newman and Choo, 2003).

Plastic shrinkage cracks are most critical in thin slabs. They create shallow cracks that range from 50 mm to 3 m in length, 20 mm to 50 mm in depth, and are up to 5 mm in width (Newman and Choo, 2003). An example of plastic shrinkage pattern in a thin slab is shown on Figure 2.20, where one can notice their repeated and frequent locations.

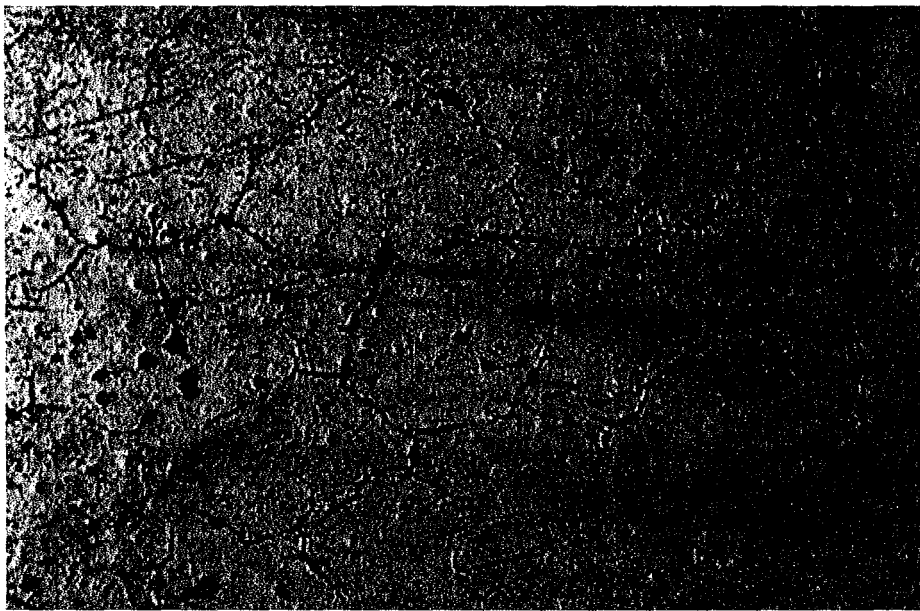


Figure 2.20 Cracks induced by plastic shrinkage at the surface of a fresh concrete
(Mehta and Meterio, 2006)

At the early age, when the concrete is still fluid and fresh, the water is relatively free to move within the mixture. During compaction, the water will move upward and the heaviest materials downward leading to bleeding. If the rate of evaporation at the concrete surface exceeds the rate of bleeding, meniscus will be formed between the solid particles. The meniscuses induce surface tension forces that create tensile stresses. The crack formation due to plastic shrinkage mechanism is illustrated in Figure 2.21. These cracks are generated when the tensile stresses exceed the fresh concrete tensile strength.

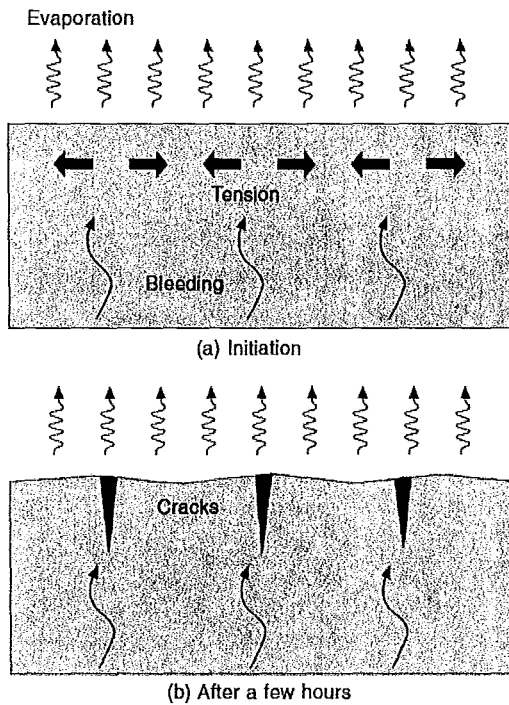


Figure 2.21 Cracks mechanisms due to plastic shrinkage (Newman and Choo, 2003)

The factors that lead to the rapid evaporation of water from the concrete surface are the main controlling factors of plastic shrinkage. These factors are high wind speed, low relative humidity, and high ambient or concrete temperature (Chidiac, 2009).

Proper early curing conditions are vital in mitigating plastic shrinkage. This can be accomplished through different measures such as moistening the subgrade and forms, moistening aggregates that are dry and absorptive, reducing wind speed by means of windbreaks, reducing exposure to sun through sunshades, protecting concrete with temporary coverings such as polyethylene sheeting during any appreciable delay between placing and finishing, minimising the gap between time of placing and time of curing, and cover the concrete surface instantly after finishing by wet burlap or fog spray (Mehta and Meterio, 2006). In addition, the use of polypropylene fibres seems to be very useful in enhancing the concrete tensile strength and reducing bleed water at surface (Newman and Seng Choo, 2003).

2.1.4 Drying Shrinkage

Drying shrinkage is due to the loss of the water from the concrete pores. As the water evaporates to the outside, concrete shrinks. Drying shrinkage is similar to the autogenous shrinkage where both occur due to loss of water. For drying shrinkage, the water is transferred to the outside, whereas for autogenous shrinkage the water is transferred within the pore structure.

When the concrete is in contact with the exterior environment and in conditions of low humidity or high temperature, water begins to evaporate from the exposed surface. During the first stages of drying shrinkage, the free water exits from the concrete mass to the surface as a bleed water (Holt, 2001). When the free water is evaporated, the drying process continues by pulling out gel water from the interior of the concrete mass with the bigger pores being emptied first (Koenders, 1997). The water evaporation causes a relative humidity reduction in the pores which induces tensile stresses. The tensile stresses in the pores are equilibrated by compressive forces in the surrounding concrete. These compressive forces lead to the drying shrinkage (CCAA, 2002). Power explained the drying shrinkage as follow (Holt, 2001):

“The liquid surface becomes converted to myriad curved surfaces (menisci), which are concave between the particles. Since the fluid pressure on the convex side of a meniscus is less than on the concave side, that is, less than the pressure of the atmosphere, the difference constitutes a motive force in addition to gravity driving the topmost particles downward. The curvature of the water surface is limited by the dimensions of the interstitial spaces among the particles at the surface.”

Figure 2.22 shows that as the water evaporation proceeds, the surface tension responsible for the drying shrinkage increases.

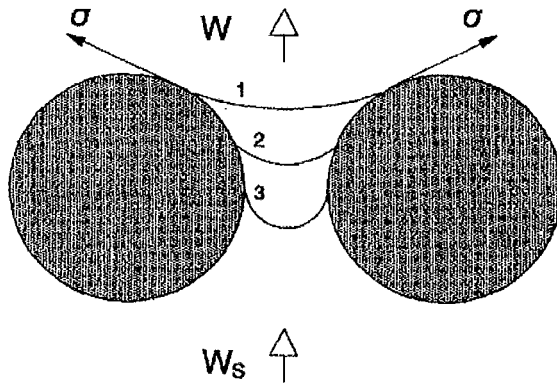


Figure 2.22 Drying shrinkage mechanism according to Power's theory – Stresses pushing water meniscus down between two cement particles (Radocea, 1992)

The tensile stresses responsible for drying shrinkage can be calculated by Kelvin – Laplace Formula (Chidiac, 2009) as follow:

$$\sigma = \frac{2\gamma}{r} = \frac{-\ln(RH) RT}{V_m} \quad (2.6)$$

with V_m being the molar volume of water. Equation 2.6 assumes in its derivation that the pores are cylindrical and a contact angle of zero degrees exists between the pore solution and the pore walls.

The factors that affect the drying shrinkage are divided into two categories: external and internal. The external factor is the curing method (CCAA, 2002). The internal factors include the cement composition such as the proportion of C_3A and SO_3 , the aggregate properties and proportions in the mix design, and water content or w/c ratio (Smadi et al., 1987). Figures 2.23 and 2.24 show the interaction between drying shrinkage, aggregate, and volume concentration of aggregates, respectively.

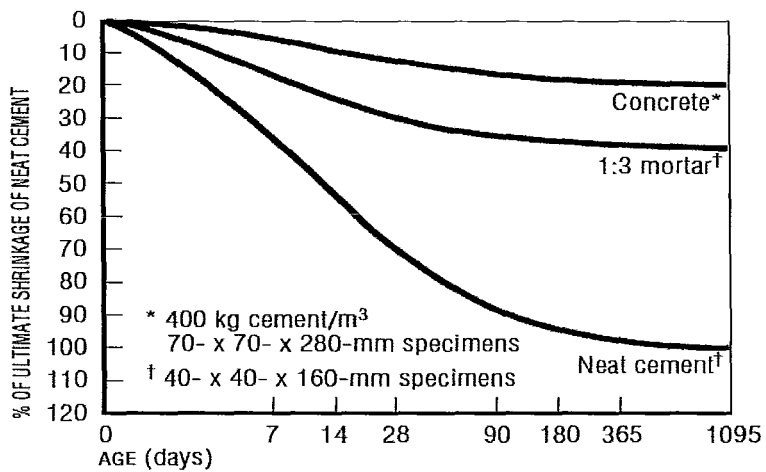


Figure 2.23 Effect of aggregate on drying shrinkage (CCAA, 2002)

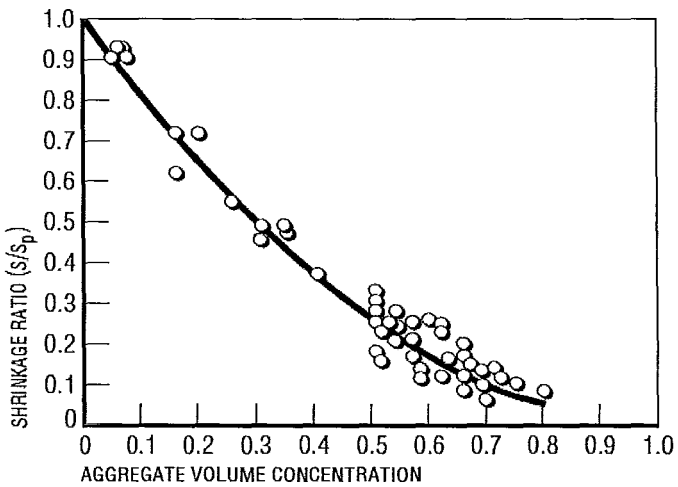


Figure 2.24 Effect of aggregate volume concentration on drying shrinkage (CCAA, 2002)

Among other internal factors affecting the drying shrinkage are mineral admixtures, namely silica fume, ground granulated blast furnace slag, GGBFS, and fly ash (Omar et al. 2008). Silica fume and GGBFS, when added within certain proportion, play a major role in reducing the drying shrinkage due to the additional pozzolanic reactions that lead to stronger concrete pore structure and elevated resistance to deformations (Li and Yao, 2001; Haque,

1996). The use of fly ash in a mixture reduces the water requirement, therefore reduces drying shrinkage (Tangtermsirikul, 1995). However beyond certain proportions the mineral admixture can augment the drying shrinkage strain due to their specific gravity, which is less than that of cement. This composition induces a higher paste volume in the mixture.

The addition of chemical admixtures such as super-plasticizer modifies the internal structure of concrete. Since it breaks the big agglomerates into a smaller one, super-plasticizer tends therefore to increase the rate of shrinkage strain (Omar et al., 2008). The rate of shrinkage is also affected by the volume to surface ratio since greater surface yields more drying operations.

Drying shrinkage can be mitigated by establishing a minimum required water-to-cement ratio in the concrete mix, utilizing the highest possible fraction of aggregate and the maximum possible aggregate size, avoiding the use of admixture that enhances drying shrinkage such as admixtures that contains calcium chloride, ensuring proper curing and placing on site, adopting expansive cement, and using shrinkage reducing admixture that can reduce the surface tension of the pore solution (CCAA, 2002; Bentz and Weiss, 2008; Mehta and Meterio, 2006). Drying shrinkage is measured in accordance with ASTM C157 – Test Method for length change of Hardened Hydraulic Cement Mortar and concrete (Tazawa et al., 1999).

Figure 2.25 shows the distribution of drying shrinkage cracks in a wall. The pattern and distribution are similar to the ones shown in Figure 2.20. This behaviour is expected because the driving mechanism for drying shrinkage and plastic shrinkage is the same.

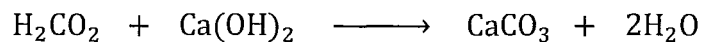


Figure 2.25 Drying shrinkage cracks in a wall – The vertical lines show the position of the reinforcement (Newman and Choo, 2003)

2.1.5 Carbonation Shrinkage

Carbonation shrinkage is the result of the reaction between calcium hydroxide present in the concrete and carbon dioxide present in the atmosphere with the existence of moisture (Chidiac, 2009). The rate of shrinkage carbonation is slow and its effect is limited to the upper layers of concrete, except for thin elements. Its magnitude is usually negligible in comparison to the other types of shrinkage (Newman and Choo, 2003). Carbonation reactions cause the rearrangement of the concrete microstructure, decrease the porosity, and create a differential volume change between the top surface and the bulk concrete, which may cause crazing (Lee and Kim, 2006).

Carbon dioxide, CO_2 , existing in the air reacts with the moisture to form carbonic acid, H_2CO_3 , which in turn reacts with calcium hydroxide, $\text{Ca}(\text{OH})_2$, to form calcium carbonate, CaCO_3 , (Mehta and Monteiro 1993).



This reaction lowers the pH in the concrete which can lead to the corrosion of reinforcement steel (Kosmatka and Panarese, 1988). The major cause of carbonation shrinkage is due to the loss of water equilibrium (Houst, 1997). The major factors that affect the carbonation shrinkage are permeability of concrete, moisture content, relative humidity, high w/c of the mixture, and rate of carbon dioxide in the air (Newman and Seng Choo, 2003).

2.1.6 Thermal Shrinkage

Solid materials such as concrete undergo contraction on cooling and expansion on heating. The rate of strain associated with these temperature changes are related to the rate of temperature changes and to the materials properties such as the coefficient of thermal expansion. These volume changes due to temperature changes are referred to as thermal shrinkage or swelling. Thermal shrinkage is a concern with the concrete at early age when the tensile strength is low and in massive concrete structure where the heat of hydration produced is very high.

2.2 Shrinkage Strain Predictive Models

Models for predicting shrinkage in concrete that have been proposed in the literature are discussed in this section. They include American Concrete Institute method (ACI-209 (1992)), Z. P. Bazant and S. Baweja model (B3 (2000)), Gardner and Lockman's model (GL (2000)), Euro-International Concrete Committee and International Federation for Prestressing model (CEB-FIP (1990)), Spanish Code for Structural Concrete model (EHE), Euro Code (2004) model, and Japanese Society for Civil Engineer model (JSCE (2002)). These models have been incorporated in various codes and standards, with the exception of B3 and GL2000 models. Moreover, these models are empirical and have been developed from experimental data.

2.2.1 ACI - 209

The shrinkage model according to the ACI - 209R – 92 is given as a hyperbolic function of time multiplied by a series of correction factors that take into account relative humidity, curing method, sample size, slump value, type of cement and air content in the mix design (Bhal and Jain, 1996). ACI is the only model that accounts for the slump value and not for the concrete compressive strength. Therefore, the user must be aware of this when using this model, as the slump value can vary with the use of super-plasticiser. This comes from the understanding that w/c affects both slump value and compressive strength, whereas super-plasticizer affects mostly the slump. ACI predictions are found to correlate well with experimental measurements for concrete with compressive strength up to 45 MPa (Omar et al., 2008).

For 100% relative humidity, this model yields no volume change which is in contradiction to what test results have shown. A major advantage of ACI - 209 model is its simplicity and ease of use. However, the lack of accuracy for concrete with high compressive strength limits its application. ACI model is given by:

$$\epsilon_s(t, t_0) = \epsilon_{shu} \cdot F_t \cdot F_H \cdot F_{th} \cdot F_s \cdot F_f \cdot F_a \cdot F_c \quad (2.7)$$

$$\varepsilon_{shu} = \begin{cases} 0.00080 & \text{for moist cured concrete} \\ 0.00073 & \text{for steam cured concrete} \end{cases}$$

$$F_t = \frac{t - t_0}{k + (t - t_0)} \quad (2.8)$$

$$k = \begin{cases} 35 & \text{for } t \geq 7 \text{ days} \\ 55 & \text{for } 3 \leq t \leq 5 \text{ days} \end{cases}$$

$$F_H = \begin{cases} 1.4 - 0.01H & \text{for } 40\% \leq H \leq 80\% \\ 3.0 - 0.03H & \text{for } 80\% \leq H \leq 100\% \end{cases} \quad (2.9)$$

$$F_{th} = 1.2 e^{-0.00472 * (\frac{V}{S})} \quad (2.10)$$

$$F_s = 0.89 + 0.0016s \quad (2.11)$$

$$F_f = \begin{cases} 0.0014\varphi + 0.30 & \text{for } \varphi \leq 50\% \\ 0.0020\varphi + 0.90 & \text{for } \varphi > 50\% \end{cases} \quad (2.12)$$

$$F_a = 0.0082\alpha + 0.9486 \quad (2.13)$$

$$F_c = 0.0007c + 0.719 \quad (2.14)$$

where $\varepsilon_s(t, t_0)$ is the shrinkage strain (m/m), t the time at which the strain is calculated (days), t_0 the time when the shrinkage begins (days), ε_{shu} the ultimate shrinkage strain for infinite time (m/m), F_t the time dependence factor, H the relative humidity in percentage, F_H the relative humidity correction factor, V/S the volume to surface ratio (mm), F_{th} the shape and size correction factor, s the slump value (mm), F_s the slump correction factor, φ the fine aggregate percentage, F_f the fines content correction factor, α the air content percentage, F_a the air content correction factor, c the cement content in kg/m³, and F_c the cement content correction factor.

2.2.2 B3

B3 is a third generation model following the development of BP Model and BP-KX Model at the Northwestern University (Bazant and Baweja, 2000). The improved version is simpler, fits better with the measured shrinkage strain and has improved theoretical justification (Omar et al., 2008). This model is one of the few methods that yields swelling at high relative humidity. For a relative humidity less than 98.45%, the system undergoes shrinkage, for values greater than 98.45%, the sample undergoes swelling. However, this model requires more complex mathematical calculations and more input data as noted below. This model is only applicable to OPC with the following conditions:

- 1) $0.35 \leq w/c \leq 0.85$
- 2) $2.5 \leq a/c \leq 13.5$
- 3) $17 \text{ MPa} \leq \bar{f}_c \leq 70 \text{ MPa}$
- 4) $160 \text{ kg/m}^3 \leq c \leq 720 \text{ kg/m}^3$

The mean shrinkage strain in the concrete cross section is calculated through these equations (Kiang, 2006).

$$\varepsilon_{sh}(t, t_0) = \varepsilon_{sh\infty} \cdot k_h \cdot S(t) \quad (2.15)$$

$$S(t) = \tanh \sqrt{\frac{t - t_0}{\tau_{sh}}} \quad (2.16)$$

$$\tau_{sh} = k_t \cdot (k_s \cdot 2 \cdot v/s)^2 \quad (2.17)$$

$$k_t = 8.50 t_0^{-0.08} f_c^{-1/4} \frac{\text{days}}{\text{cm}^2} \quad (2.18)$$

$$k_h = \begin{cases} (1 - h^3) \text{ for } h \leq 0.98 \\ -0.2 \text{ for } h = 1 \text{ (swelling in water)} \\ \text{linear interpolation for } 0.98 \leq h \leq 1 \end{cases} \quad (2.19)$$

$$k_s = \begin{cases} 1.00 \text{ for an infinite slab} \\ 1.15 \text{ for an infinite cylinder} \\ 1.25 \text{ for an infinite square prism} \\ 1.30 \text{ for a sphere} \\ 1.55 \text{ for a cube} \end{cases} \quad (2.20)$$

$$\varepsilon_{s\infty} = \alpha_1 \cdot \alpha_2 \cdot \left[\frac{1.9}{100} w^{2.1} f_c^{-0.28} + 270 \right] \cdot 10^{-6} \quad (2.21)$$

$$\alpha_1 = \begin{cases} 1.00 \text{ for type I cement} \\ 0.85 \text{ for type II cement} \\ 1.10 \text{ for type III cement} \end{cases}$$

$$\alpha_2 = \begin{cases} 0.75 \text{ for steam curing} \\ 1.20 \text{ for sealed or normal curing in air with initial protection against drying} \\ 1.00 \text{ for curing in water or at 100% relative humidity} \end{cases} \quad (2.22)$$

$$\varepsilon_{sh\infty} = \varepsilon_{s\infty} \frac{E(607)}{E(t_0 + \tau_{sh})} \quad (2.23)$$

$$E(t) = E(28) \left(\frac{t}{4 + 0.85 t} \right)^{1/2} \quad (2.24)$$

By substituting Eqs 2.15 to 2.23, the following expression is obtained:

$$\begin{aligned} & \varepsilon_{sh}(t, t_0) \\ &= \alpha_1 \cdot \alpha_2 \left[\frac{1.9}{100} w^{2.1} f_c^{-0.28} + 270 \right] \frac{\left(\frac{607}{520} \right)^{1/2}}{\left(\frac{t_0 + \tau_{sh}}{4 + 0.85 (t_0 + \tau_{sh})} \right)^{1/2}} (1 \\ & \quad - h^3) \tanh \sqrt{\frac{t - t_0}{0.085 t_0^{-0.08} f_c^{-1/4} \cdot (k_s \cdot 2 \cdot v/s)^2}} \cdot 10^{-6} \end{aligned} \quad (2.24)$$

where $\varepsilon_{sh}(t, t_0)$ is the shrinkage strain (m/m), t the time at which the strain is calculated (days), t_0 the time when the shrinkage begins (days), w the water content (kg/m³), w/c the water-to-cement ratio, a/c the aggregate cement ratio by weight, \bar{f}_c the concrete compressive strength at the age of 28 days (MPa), c the cement content in kg/m³, $S(t)$ the time correction factor, k_h the humidity correction factor, k_s the size correction factor, v/s the volume to surface ration (mm), α_1 the correction factor related to the type of cement, α_2 the correction factor related to curing method, τ_{sh} the shrinkage half-time (days), $\varepsilon_{sh\infty}$ the factor related to compressive strength, type of cement and curing method, and $\varepsilon_{sh\infty}$ the time dependence of ultimate shrinkage.

2.2.3 GL2000

GL 2000 (Gardner and Lockman, 2001) is a modified model of GZ that was proposed by Gardner and Zhao (1993). This model takes into account the mean compressive strength, relative humidity, volume to surface ratio, and type of cement as parameters to evaluate the shrinkage strain. For 100% relative humidity, this model yields no volume change, opposite to what tests results show. This model is not very common due to its complicated calculations and low accuracy in comparison with other models.

According to Gardner and Lockman (2001), the mean shrinkage strain in the concrete cross section is given by:

$$\varepsilon_s(t) = \varepsilon_{shu} \cdot \beta_h \cdot \beta(t) \quad (2.25)$$

$$\beta(t) = \left(\frac{t - t_c}{t - t_c + 0.12(\frac{V}{S})^2} \right)^{1/2} \quad (2.26)$$

$$\beta(h) = [1 - 1.18 h^4] \quad (2.27)$$

$$\varepsilon_{shu} = \frac{1000}{10^6} \cdot k \cdot \left[\frac{30}{f_{cm28}} \right]^{1/2} \quad (2.28)$$

$$k = \begin{cases} 1.00 & \text{for type I cement} \\ 0.75 & \text{for type II cement} \\ 1.15 & \text{for type III cement} \end{cases}$$

By substituting Eqs. 2.25 to 2.28, the following expression is obtained:

$$\varepsilon_s(t) = \frac{1000}{10^6} \cdot k \cdot \left[\frac{30}{f_{cm28}} \right]^{\frac{1}{2}} \cdot [1 - 1.18 h^4] \cdot \beta(t) \left(\frac{t - t_c}{t - t_c + 0.12 \left(\frac{V}{S} \right)^2} \right)^{\frac{1}{2}} \quad (2.29)$$

where $\varepsilon_s(t)$ is the shrinkage strain (m/m), ε_{shu} the ultimate shrinkage strain (m/m), t the time at which the strain is calculated (days), t_c the time when the drying begins (days), h the relative humidity in decimal, $\beta(t)$ the time correction factor, $\beta(h)$ the humidity correction factor, k the cement type factor, V/S the volume to surface ration (mm), and f_{cm28} the concrete mean compressive strength at 28 days (MPa).

2.2.4 CEB-FIP 1990

This model was developed by the Comite Euro-International Du Beton and International Federation for Prestressing. It is a refinement of the CEB-FIP 1970 and CEB-FIP 1978 models. It takes into account relative humidity, notional dimension, concrete compressive strength, and type of cement as parameters for predicting the shrinkage strain. The model is limited to concrete mixes having a compressive strength varying from 12 MPa to 80 MPa, mean relative humidity 40% to 100% and mean temperature 5°C to 30 °C (Omar et al., 2008). For relative humidity less than 99%, the system undergoes shrinkage, for values equal to or greater than 99% the sample undergoes swelling. The predictive equation for mean shrinkage strain in the concrete cross section is given by (Omar et al., 2008):

$$\varepsilon_{cs} = \varepsilon_{cs0} \beta_s \quad (2.30)$$

$$\varepsilon_{cs0} = \varepsilon_s \beta_{RH} \quad (2.31)$$

$$\beta_s = \sqrt{\frac{t - t_s}{350(\frac{h}{100})^2 + (t - t_s)}} \quad (2.32)$$

$$\beta_{RH} = \begin{cases} 1.55 \left(1 - \left(\frac{RH}{100}\right)^3\right) & \text{for } 40\% \leq RH \leq 99\% \\ 0.5 & \text{for } RH \geq 99\% \end{cases} \quad (2.33)$$

$$\varepsilon_s = \left[160 + 10 \beta_{sc} \left(9 - \frac{f_{cm}}{10}\right) \right] \cdot 10^{-6} \quad (2.34)$$

$$\beta_{sc} = \begin{cases} 8 & \text{Rapid Hardening high strength} \\ 5 & \text{Normal and rapid hardening} \\ 4 & \text{Slowly hardening} \end{cases}$$

By substituting Eqs. 2.30 to 2.34, the following expression is obtained for RH values greater than 40% and less than 99%:

$$\varepsilon_{cs} = \left[160 + 10 \beta_{sc} \left(9 - \frac{f_{cm}}{10}\right) \right] \cdot 10^{-6} 1.55 \left(1 - \left(\frac{RH}{100}\right)^3\right) \sqrt{\frac{t - t_s}{350(\frac{h}{100})^2 + (t - t_s)}} \quad (2.35)$$

where $\varepsilon_{cs}(t)$ is the shrinkage strain (m/m), ε_{cs0} the basic shrinkage strain (m/m), β_s the time correction factor, β_{RH} the relative humidity correction factor, h the notional dimensions which equal $2*V/S$ (mm), t the age of concrete (days), t_c the age at which drying begins (days), RH the relative humidity in percent, f_{cm} the concrete compressive strength at the age of 28 days (MPa), and β_{sc} the type of cement correction factor.

2.2.5 EHE

EHE model was developed and adopted for the Spanish Code for Structural Concrete (EHE) (Gómez and Landsberger, 2007). It is based on the CEB – FIP 1990 model with the exception of the coefficient that accounts for the cement factor, β_{sc} . EHE does not include β_{sc} . It characterizes concrete through its compressive strength, and all the other parameters are identical to CEB – FIP 1990 model. The model is given by (Omar et al., 2008):

$$\varepsilon_{cs} = \varepsilon_{cs0} \beta_s \quad (2.36)$$

$$\varepsilon_{cs0} = \varepsilon_s \beta_{RH} \quad (2.37)$$

$$\beta_s = \sqrt{\frac{t - t_s}{350 \left(\frac{h}{100}\right)^2 + (t - t_s)}} \quad (2.38)$$

$$\beta_{RH} = \begin{cases} 1.55 \left(1 - \left(\frac{RH}{100}\right)^3\right) & \text{for } 40\% \leq RH \leq 99\% \\ 0.5 & \text{for } RH \geq 99\% \end{cases} \quad (2.39)$$

$$\varepsilon_s = [570 - 5 f_{ck}] \cdot 10^{-6} \quad (2.40)$$

By substituting Eqs. 2.36 to 2.40, the following expression is obtained for RH values greater than 40% and less than 99%:

$$\varepsilon_{cs} = [570 - 5 f_{ck}] \cdot 10^{-6} 1.55 \left(1 - \left(\frac{RH}{100}\right)^3\right) \sqrt{\frac{t - t_s}{350 \left(\frac{h}{100}\right)^2 + (t - t_s)}} \quad (2.41)$$

2.2.6 Eurocode 2

Eurocode 2 (EC2) model is proposed by the European Code (Omar et al., 2008). Parameters involved in calculating the total shrinkage are: relative humidity, specimen shape and size, and concrete compressive strength. This model is widely adopted in Europe and is expected to replace BS8110 as well as other local European standards (Omar et al., 2008). The equation for calculating mean shrinkage strain in the concrete cross section is (Omar et al., 2008):

$$\varepsilon_{cd(t)} = (t - t_s) \cdot \varepsilon_{cd0} \cdot k_s \quad (2.42)$$

$$\varepsilon_{cd0} = \frac{k(f_{ck})[72 \exp(-0.046 \cdot f_{ck}) + 75 - RH]10^{-6}}{(t - t_s) + 0.007h_0^2} \quad (2.43)$$

$$k(f_{ck}) = \begin{cases} 18 & \text{if } f_{ck} \leq 55 \text{ MPa} \\ 30 - 0.21f_{ck} & \text{if } f_{ck} \geq 55 \text{ MPa} \end{cases} \quad (2.44)$$

By substituting Eqs. 2.42 to 2.44, the following expression is obtained:

$$\varepsilon_{cd(t)} = (t - t_s) \cdot k_s \cdot \frac{k(f_{ck})[72 \exp(-0.046 \cdot f_{ck}) + 75 - RH]10^{-6}}{(t - t_s) + 0.007h_0^2} \quad (2.45)$$

where $\varepsilon_{cd}(t)$ is the shrinkage strain (m/m), ε_{cd0} the basic shrinkage strain (m/m), h_0 the notional dimensions which equal $2 \cdot V/S$ (mm), t the age of concrete (days), t_s the age at which drying begins (days), RH the relative humidity in percent, f_{ck} the concrete compressive strength at the age of 28 days (MPa), k_s the factor accounting for the element geometry, and $k(f_{ck})$ the factor related to the compressive strength of concrete.

2.2.7 JSCE Specification 2002

JSCE model was developed by the Japanese Society for Civil Engineers in 2002 and constituted a major modification for the 1996 model (Sakata and Shimomura, 2004). This model is the only model that takes into account autogenous shrinkage. The main parameters considered in this model are the water content, volume to surface ratio of the specimen or concrete element, relative humidity, type of concrete, and concrete compressive strength. The total shrinkage according to the JSCE Specification 2003 is the sum of the drying and autogenous shrinkage.

$$\varepsilon'_{cs}(t, t_0) = \varepsilon'_{ds}(t, t_0) + \varepsilon'_{as}(t, t_0) \quad (2.46)$$

The mean drying shrinkage strain in the concrete cross section is calculated according to JSCE 2002 model through the following equation (Sakata and Shimomura, 2004):

$$\varepsilon'_{ds}(t, t_0) = \frac{\varepsilon'_{ds\infty} \cdot (t - t_0)}{\beta + (t - t_0)} \quad (2.47)$$

$$\beta = \frac{4 W \sqrt{V/S}}{100 + 0.7 t_0} \quad (2.48)$$

$$\varepsilon'_{ds\infty} = \frac{\varepsilon_{dsp}}{1 + \eta \cdot t_0} \quad (2.49)$$

$$\varepsilon_{dsp} = \frac{\alpha \left(1 - \frac{RH}{100}\right) W}{1 + 150 \exp\left(-\frac{500}{f_c'(28)}\right)} \quad (2.50)$$

$$\eta = 10^{-4} \{15 \exp(0.007 f_c'(28)) + 0.25 W\} \quad (2.51)$$

$$\alpha = \begin{cases} 11 & \text{for ordinary or low - heat cement} \\ 15 & \text{for high early strength concrete} \end{cases} \quad (2.52)$$

By substituting Eqs. 2.47 to 2.52, the following expression is obtained:

$$\varepsilon'_{ds}(t, t_0) = \frac{\frac{\alpha \left(1 - \frac{RH}{100}\right) W}{1 + 150 \exp\left(-\frac{500}{f_c'(28)}\right)}}{\frac{1 + 10^{-4}\{15 \exp(0.007 f_c'(28)) + 0.25 W\} \cdot t_0}{\frac{4 W \sqrt{V/S}}{100 + 0.7 t_0} + (t - t_0)}} \cdot (t - t_0) \quad (2.53)$$

The mean autogenous shrinkage strain in the concrete cross section is calculated according to JSCE 2002 model through the following equations (Sakata and Shimomura, 2004):

$$\varepsilon'_{as}(t, t_0) = \varepsilon'_{as}(t) - \varepsilon'_{as}(t_0) \quad (2.54)$$

$$\varepsilon'_{as}(t) = \gamma \varepsilon'_{as\infty} [1 - \exp\{-a(t - t_s)^b\}] \quad (2.55)$$

$$\varepsilon'_{as\infty} = 3070 e^{-7.2(\frac{W}{C})} \quad (2.56)$$

Table 2.2 Values of a and b as a function of w/c

w/c	a	b
0.20	1.20	0.40
0.23	1.50	0.40
0.30	0.60	0.50
0.40	0.10	0.70
0.50	0.03	0.80
1.00	0.03	0.80

By substituting Eqs. 2.54 to 2.56, the following expression is obtained:

$$\varepsilon'_{as}(t, t_0) = \gamma 3070 e^{-7.2(\frac{W}{C})} [1 - \exp\{-a(t - t_s)^b\}] - \varepsilon'_{as}(t_0) \quad (2.57)$$

where $\varepsilon'_{cs}(t, t_0)$ is the total shrinkage strain from age t_0 to t ($\times 10^{-6}$), $\varepsilon'_{ds}(t, t_0)$ the drying shrinkage strain from age t_0 to t ($\times 10^{-6}$) (m/m), $\varepsilon'_{ds\infty}$ the drying shrinkage strain from infinite time ($\times 10^{-6}$) (m/m), $\varepsilon'_{as}(t, t_0)$ the autogenous shrinkage strain from age t_0 to t ($\times 10^{-6}$) (m/m), β the time correction factor, W the water content (kg/m^3) for values ranging from $130 \text{ kg}/\text{m}^3$ to $230 \text{ kg}/\text{m}^3$, V/S the volume to surface ratio (mm), RH the relative humidity in percent for values ranging from 40% to 90%, $f_c(28)$ the concrete compressive strength at the age of 28 days (MPa), α the cement type correction factor, w/c the water-to-cement ratio, $\varepsilon'_{as\infty}$ the autogenous shrinkage strain for infinite time ($\times 10^{-6}$) (m/m), t_s the beginning of setting time for autogenous shrinkage, γ the cement type factor for autogenous shrinkage, a and b the coefficients representing the characteristic of progress of autogenous shrinkage.

2.2.8 Model Parameters

Table 2.3 summarizes the parameters needed for the various models to predict shrinkage strain values. All seven models include the following parameters: specimen volume-to-surface ratio, RH, and time drying begins. With exception of ACI – 209, they include compressive strength for predicting strain. Further, these six models account for type of cement, whereas ACI – 209 considers cement content, air content, and fine aggregate content. The curing condition is also accounted for in ACI – 209 and B3. JSCE 2002 is the only model that accounts for w/c. These observations suggest that predictions of shrinkage strain obtained using these models will not be the same.

Table 2.3 Parameters used in shrinkage prediction models

	ACI – 209	B3	GL 2000	CEB – FIP 1990	EHE Model	EC2	JSCE 2002
Specimen Volume to Surface ratio	✓	✓	✓	✓	✓	✓	✓
Specimen Shape/Dimensions		✓					
Relative Humidity	✓	✓	✓	✓	✓	✓	✓
Concrete Compressive Strength at 28 days		✓	✓	✓	✓	✓	✓
Time Drying Begins	✓	✓	✓	✓	✓	✓	✓
Curing Conditions (steam cured, moist cured)	✓	✓					
Cement Type		✓	✓	✓		✓	✓
Cement Content		✓					
Water Content			✓				✓
W/C Ratio							✓
Slump Value		✓					
Air Content		✓					
Fine Aggregate Content		✓					

Various authors have assessed the predictive capabilities of the shrinkage strain models and ranked them as shown in Table 2.4. These assessments are based on experimental data. The results indicate that the ranking is somewhat inconsistent as expected based on the information presented in Table 2.3. Nevertheless, B3 model shows an overall superiority. The inconsistency can be traced to be fact that all of the models were developed based on set of experimental data and not on concrete theoretical foundations, except for model B3, which combines both theoretical and experimental basis. The results demonstrate that concrete shrinkage is a very complex phenomenon involving many parameters and that it is difficult to represent using a simple mathematical relation.

Table 2.4 Ranking of shrinkage models

	Shrinkage Models					
	ACI - 209R	B3	CEB-FIP	EHE Model	EC 2	GL 2000
Bazant and Baweja (2000)	3	1	2			
Al-Manaseer and Lam (2005)	3	2	4			1
Gardner (2005)	3	2	4			1
McDonald and Roper (1993)	1	2	3			
Gómez and Landsberger (2007)	1	2	3	5		4
Kiang (2006)	5	1	2		4	3

2.3 Concluding Remarks

Recent improvement in concrete properties put autogenous shrinkage among the critical phenomenon affecting the concrete durability and serviceability. Even that the driving mechanism, which is water movement, is the same for drying and autogenous shrinkage; autogenous shrinkage is more crucial since it arises at early age and evolves faster than concrete strength. Ensuring proper curing, controlling the casting operation, using of admixtures and internal curing techniques are among measures that can contribute to mitigate the shrinkage. Shrinkage is a complex phenomenon that is very difficult to represent in one mathematical equation.

Chapter 3

Experimental Program

3.0 Introduction

An experimental program was developed to study the effects of varying concrete mixtures and curing conditions on shrinkage of concrete. In this regard, six parameters were selected: water-to-cement ratio (w/c), water content (w), maximum aggregate size (size), silica fume (SF) as cement replacement, ground granulated blast furnace slag (GGBFS) as cement replacement, and bulk volume of coarse aggregate (CA). This chapter provides a description of the material properties, concrete mixture design method, curing regime, and testing methods. The corresponding experimental results are then presented.

3.1 Concrete Mixture Design

This study forms a part of on-going research to study the relation between concrete mixture and properties of fresh and hardened concrete at McMaster University. This study focuses on the relation between concrete mixture and shrinkage, particularly, chemical shrinkage, autogenous shrinkage, and drying shrinkage. The variables that are investigated include: w/c, water content, maximum aggregate size, silica fume, GGBFS, and bulk volume of coarse aggregate. According to the literature review, these variables are known to affect concrete shrinkage strain.

The design of the McMaster study is based on partial factorial design principle (Montgomery and Rung, 2003), in which the control mixture design was an air entrained concrete with compressive strength greater than 20 MPa and a slump value greater than 75 mm. The design of mixture proportions was based on the method proposed by Cement Association of Canada (CAC, 2002).

In order to employ the factorial design principle, upper and lower values for each variable must be defined. The limits for w/c, water content, maximum aggregate size, coarse aggregate volume, and percent replacements of silica fume and GGBFS are summarized in Table 3.1.

Table 3.1 Upper and lower limit values for concrete mixtures

w/c	size (mm)	w (kg/m ³)	SF (%)	GGBFS (%)	CA
0.4	14	193	0	0	0.50
		205			0.62
0.6	20	184	8	30	0.57
		197			0.69

The factorial design adopted in the data analysis is 2^{6-1} . The effects on the response of each single variable as well as the interaction of second and third order were investigated. Therefore, 32 concrete mixtures were required and are referred to as main points. The designs corresponding to the 32 concrete mixtures are summarized in Table 3.3. Recognizing that the response for shrinkage as well as for other concrete properties are not linear, 13 concrete mixtures referred to as star points were added in order to investigate the parameters' interaction of third and fourth levels. These mixes are given in Table 3.4. Details of the fractional factorial design can be found in Chidiac et al. (2009). In order to study the effects of air entraining agent (AEA) as well as the effects of water reducing agent (WRA) and viscosity enhancing agent (VEA) on the concrete shrinkage, 15 more mixes were added and given in Table 3.2.

Table 3.2 Design of concrete mixtures – Mixtures with Chemical Admixtures

No.	w/c	w (kg/m ³)	size (mm)	SF (%)	GGBFS (%)	CA (ml)	WRA (ml)	VEA (ml)	AEA (ml)
7	0.4	216	14	0.0	0	0.50	0	0	0
5	0.6	216	14	0.0	0	0.62	0	0	0
12	0.4	228	14	0.0	0	0.62	0	0	0
10	0.6	228	14	0.0	0	0.50	0	0	0
11	0.4	205	20	0.0	0	0.69	0	0	0
8	0.6	205	20	0.0	0	0.57	0	0	0
13	0.4	216	20	0.0	0	0.57	0	0	0
9	0.6	216	20	0.0	0	0.69	0	500	0
64	0.3	180	14	0.0	0	0.50	600	300	0
59	0.4	180	14	0.0	0	0.50	500	300	0
50	0.3	185	14	0.0	0	0.50	800	400	0
66	0.3	185	14	0.0	0	0.50	600	300	0
61	0.3	185	14	0.0	0	0.50	700	300	0
53	0.4	185	14	0.0	0	0.50	700	400	0
56	0.4	185	14	0.0	0	0.50	500	300	0

Table 3.3 Design of concrete mixtures - Main points

No.	w/c	w (kg/m ³)	size (mm)	SF (%)	GGBFS (%)	CA
44	0.4	193	14	0.0	0	0.50
42	0.6	193	14	0.0	0	0.62
38	0.4	205	14	0.0	0	0.62
43	0.6	205	14	0.0	0	0.50
40	0.4	184	20	0.0	0	0.69
45	0.6	184	20	0.0	0	0.57
39	0.4	197	20	0.0	0	0.57
41	0.6	197	20	0.0	0	0.69
19	0.4	193	14	8.0	0	0.62
14	0.6	193	14	8.0	0	0.50
20	0.4	205	14	8.0	0	0.50
15	0.6	205	14	8.0	0	0.62
18	0.4	184	20	8.0	0	0.57
16	0.6	184	20	8.0	0	0.69
21	0.4	197	20	8.0	0	0.69
17	0.6	197	20	8.0	0	0.57
23	0.4	193	14	0.0	30	0.62
22	0.6	193	14	0.0	30	0.50
26	0.4	205	14	0.0	30	0.50
24	0.6	205	14	0.0	30	0.62
27	0.4	184	20	0.0	30	0.57
25	0.6	184	20	0.0	30	0.69
28	0.4	197	20	0.0	30	0.69
29	0.6	197	20	0.0	30	0.57
35	0.4	193	14	5.6	30	0.50
31	0.6	193	14	5.6	30	0.62
32	0.4	205	14	5.6	30	0.62
34	0.6	205	14	5.6	30	0.50
30	0.4	184	20	5.6	30	0.69
37	0.6	184	20	5.6	30	0.57
33	0.4	197	20	5.6	30	0.57
36	0.6	197	20	5.6	30	0.69

Table 3.4 Design of concrete mixtures - Star points

No.	w/c	w (kg/m ³)	size (mm)	SF (%)	GGBFS (%)	CA
55	0.5	193	14	0.0	0	0.50
52	0.7	175	14	0.0	0	0.50
54	0.5	205	14	0.0	0	0.50
57	0.7	193	14	0.0	0	0.50
51	0.5	193	14	0.0	0	0.62
60	0.7	175	14	0.0	0	0.62
49	0.5	205	14	0.0	0	0.62
58	0.7	193	14	0.0	0	0.62
47	0.5	199	14	0.0	20	0.56
48	0.5	199	14	0.0	40	0.56
62	0.5	199	14	0.0	0	0.45
63	0.5	199	14	0.0	0	0.67
65	0.5	199	14	0.0	0	0.56

3.2 Material

The concrete was prepared using a mixture of crushed limestone, siliceous sand, OPC, silica fume, GGBFS, air entraining agent, super-plasticizer, viscosity enhancing agent, and water.

3.2.1 Coarse Aggregates

The coarse aggregates used in this study were crushed limestone with a maximum size of 14 mm and 20 mm. They were obtained from Lafarge North America's Dundas quarry located in Dundas, Ontario - Canada. The gradation curves for the coarse aggregate with maximum size of 14 mm and 20 mm are shown in Figure 3.1 and Figure 3.2, respectively, and were obtained in accordance with CSA A23.2-2A (2000). Both 14 mm and 20 mm aggregate conform to CSA limits. The specific gravity CSA A23.2-12A (2000), saturated surface dry moisture contents CSA A23.2-12A (2000), and oven dry bulk densities CSA A23.2-10A (2000) were determined and found to be 2.74, 0.88%, and 1576 kg/m³ for the 14 mm aggregates and 2.75, 0.92% and 1636 kg/m³ for the 20 mm aggregate, respectively.

3.2.2 Fine Aggregates

The fine aggregates were siliceous sand, obtained from Lafarge North America's west Paris plant. The particle size distribution test was done in accordance with CSA A23.2-2A (2000), with the results shown in Figure 3.3 along with the CSA requirements for fine aggregates. The specific gravity, saturated surface dry moisture content, and dry packing density of the sand were 2.71, 1.58% and 1812 kg/m^3 respectively. The fineses modulus, FM, for sand was found equal to 2.72.

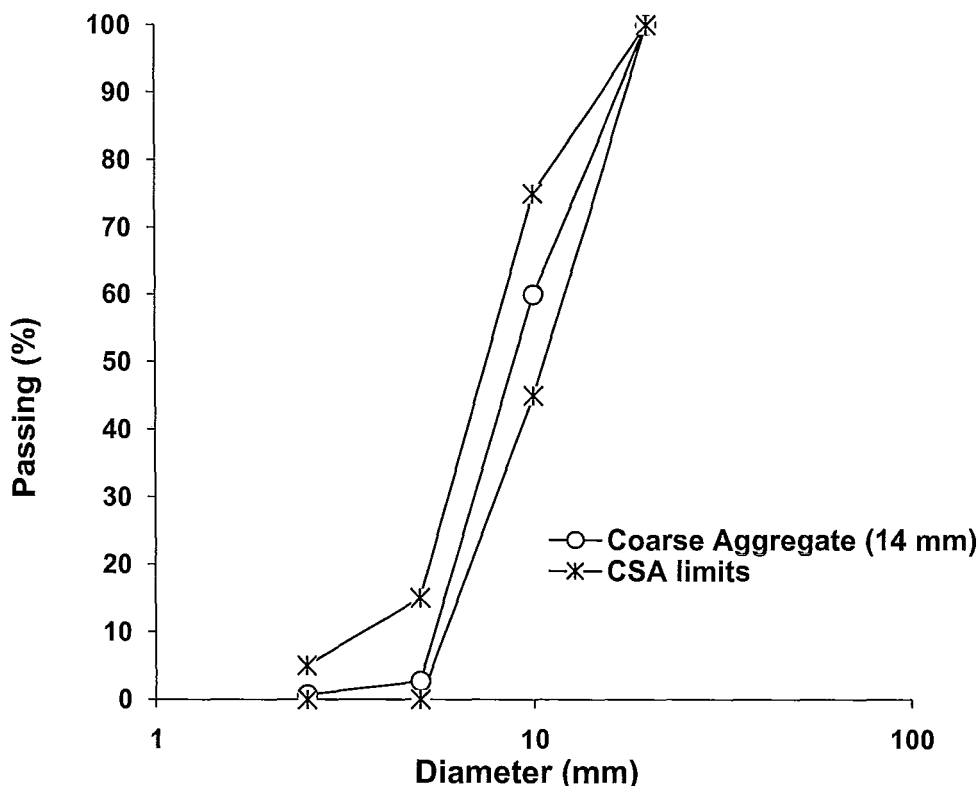


Figure 3.1 14 mm coarse aggregate gradation curve

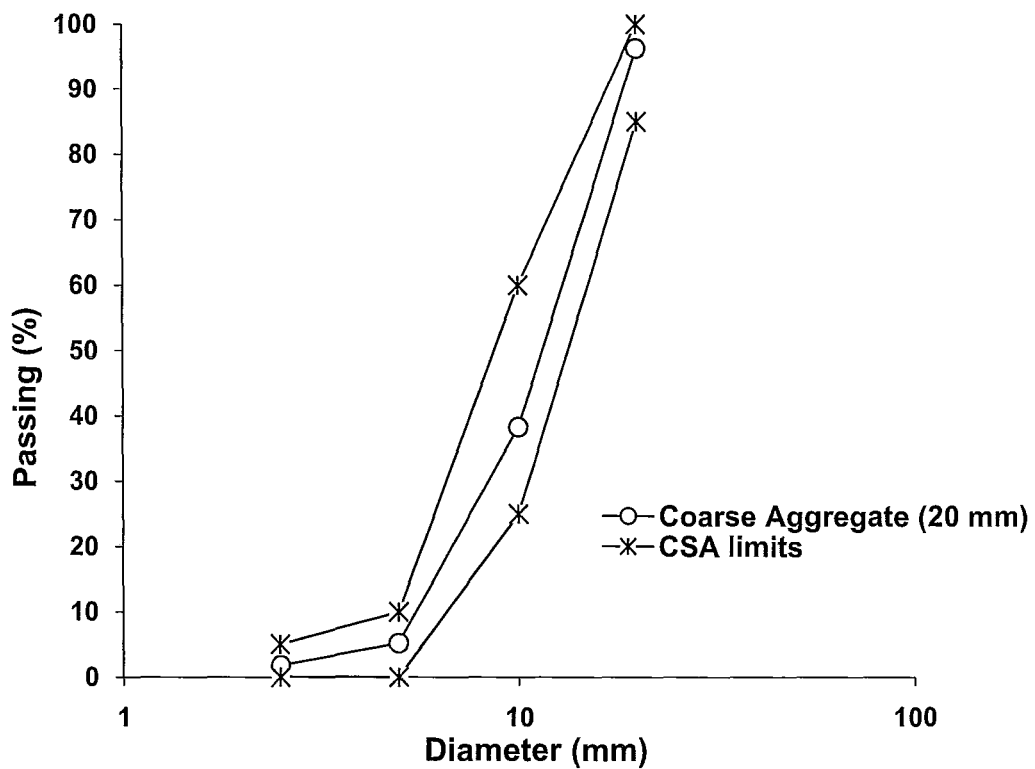


Figure 3.2 20 mm coarse aggregate gradation curve

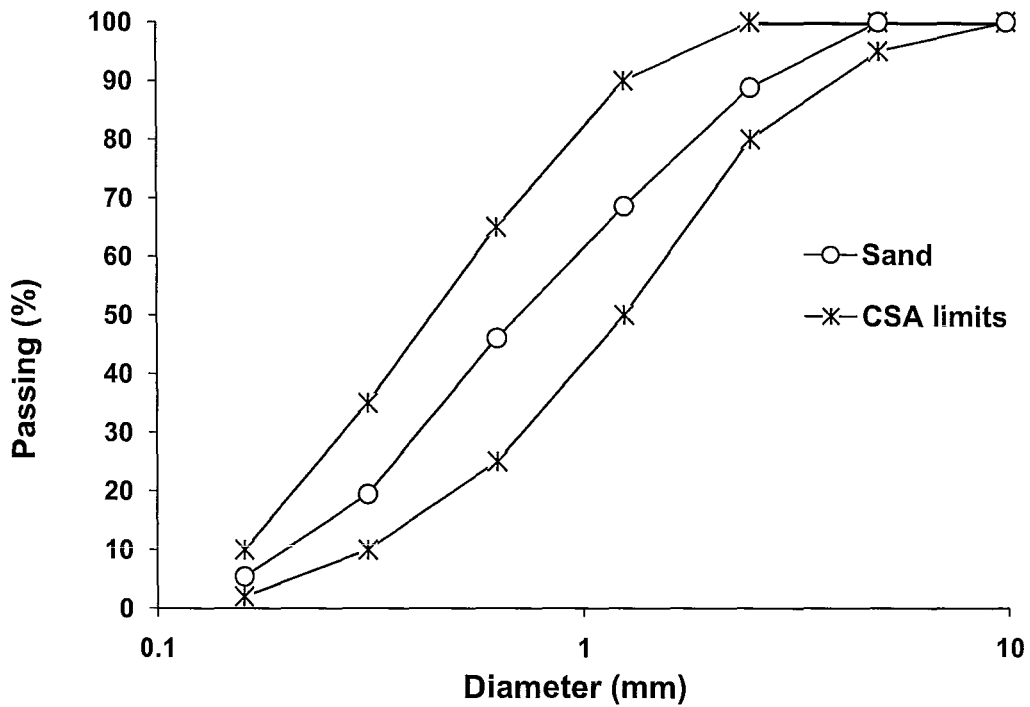


Figure 3.3 Fine aggregate gradation curve

3.2.3 Cementitious Material

Three different types of cementitious material were used in this study, namely, OPC – Hydraulic cement type GU – Type 10, OPC blended with 8% silica fume – GUb-SF Cement type IP 8, and GGBFS – Grade 80. The materials were obtained from Lafarge North America. The chemical and physical properties of the cementitious material are summarized in Table 3.5.

Table 3.5 Chemical and physical properties of hydraulic cement GU-type 10, GUb-SF cement type IP 8, and GGBFS

	Portland Cement	OPC blended with SF	GGBFS
SiO ₂ (%)	19.7	25.4	34.5
Al ₂ O ₃ (%)	4.9	5.1	9.9
Fe ₂ O ₃ (%)	2.4	2.6	0.7
CaO (%)	62.2	57.6	36.5
MgO (%)	3.1	2.7	12.3
SO ₃ (%)	3.4	2.6	3.5
FCaO (%)	1.3	1.7	
K ₂ O (%)			0.4
Na ₂ O (%)			0.3
TiO ₂ (%)			0.7
Mn ₂ O ₃ (%)			0.7
Naeq (%)			0.6
Loss on Ignition (%)	2.9	2.5	
Specific gravity			2.92
Equivalent Alkalies (%)	0.75	0.76	
Silica Fume Addition (%)		8	
Specific Surface Area (Blaine) (cm ² /g)	4280	5890	
% Passing 325 (45um) Mesh (%)	90.7	88.8	98
Time of Setting-Initial (min)	115	110	
Compressive Strength - 3 Day (MPa)	282	242	
Compressive Strength - 7 Day (MPa)	351	343	22

3.2.4 Air Entraining Agent

Micro Air manufactured by BASF Construction Chemicals was used to entrain air (BASF, 2007a). Micro air meets the requirements of ASTM C260-06 (2006a).

3.2.5 Water Reducer or Super-plasticizer

Water reducing agent, WRA, GLENIUM 7500 manufactured by BASF was used in the mixtures (BASF, 2007b). GLENIUM 7500 meets ASTM C 494/C 494M-08a (2008) requirements.

3.2.6 Viscosity Enhancing Agent

Viscosity enhancing agent, VEA, Rheomac VMA 358 manufactured by BASF was used in the mixtures (BASF, 2007c). Rheomac VMA 358 meets AS 1478.1 (2000) requirements.

3.3 Experimental Procedure

The experimental procedure implemented for this study was the same for all of the concrete mixes. This included mixing procedure, placing, consolidating, curing, and test methods. The concrete was mixed in a pan mixer according to these steps:

- Mix water and air entraining agent, AEA, for 30 seconds.
- Pour the coarse aggregate, fine aggregate, cement, and 1/3 of the mixed water and AEA into the pan mixer.
- Mix the content for two minutes.
- Pour the remaining quantity of mixed water and AEA while the mixer is still running.
- Continue mixing for two minutes.
- Stop the mixer for one minute.
- Mix for one minute.

For every mixture, six cylinders, 100 mm in diameter and 200 mm high, were prepared for the purpose of shrinkage and compressive strength measurements. The concrete was placed in accordance with the requirements for compressive strength, i.e., placed in three

layers and each layer was rodded 25 times. The cylinders were sealed for 24 hours. Following demolding and labelling, two sets of dmacs gauges were attached on opposite sides. The gauge length is 10 cm. These gauges are used to monitor shrinkage. After recording the initial measurements, three cylinders from each mix were placed on a shelf in an air curing room, where the relative humidity ranged from 40% to 50% and temperature was 24°C. The remaining three cylinders from each mix were placed for the first seven days in a saturated lime water bath, then on a shelf in a moist curing room, where the relative humidity ranges from 95% to 100%, and the temperature was 24°C.

The experimental procedure and test set-up used to measure autogenous shrinkage was adapted from the work of Holt (2001) and Tazawa et al. (1999), and consisted of a steel mould that is rectangular in shape, 400 mm long, 100 mm wide, and 80 mm high. The interior surface of the mould was covered with 10 mm thick extruded polystyrene insulation to thermally isolate the mould from the fresh concrete. The extruded polystyrene was then covered with Teflon sheets in order to minimize the friction resistance between the concrete movement and the polystyrene. A 3 mm thick polyethylene sheet was placed on top of the Teflon to isolate hygrically the concrete mixture from its surroundings. The same polyethylene sheet was used to seal the concrete top surface from the environment.

Directly after the mixing operation was completed, the fresh concrete was poured into the mould. The concrete was placed in three horizontal layers in order to install the various transducers and plates. The first layer was 25 mm thick. Then two vertical steel plates, 2 cm wide and 10 cm high with a 2 cm by 2 cm base, were placed and levelled 40 mm from the end of the mould. Thereafter, the concrete pouring continued till it reached a thickness of 40 mm; at this stage a thermocouple type T and miniature pressure sensor were introduced. When the concrete height reached the final level, an aluminum plate that was 2 cm by 2 cm and 0.5 mm thick was placed horizontally on top of the sample. The top of concrete sample was then sealed using the polyethylene sheet. The set-up is represented in Figure 3.4 and shown in Photos 3.1 and 3.2.

The miniature pressure gauge PDA – PA by Tokyo Sokki Kenkyujo was used to monitor the capillary pressure inside the concrete. The gauge, which was waterproofed, was 6.5 mm in diameter and 1 mm in thickness, and weighted 0.1 g. It had a capacity of 200 kPa and rated output of 0.8mV/V with a recommended excitation of 2V. The pressure gauge was protected from the concrete by embedding it in a plastic tube and only exposing the sensing area for measurements. Prior to their use, the pressure transducers were calibrated.

Non contact transducers, namely Wenglor Laser Reflex sensors, were used to measure shrinkage by monitoring the movements of the vertical plates and horizontal plate. The sensors' working range is 30 to 80 mm and has a resolution that is less than 8 μm . The laser sensors were calibrated using a vertical milling machine MATSUURA FX – 5G. The latter had a resolution of up to 1 μm . It should be noted that the gauge length adopted to measure autogenous shrinkage ranged from 290 mm to 310 mm.

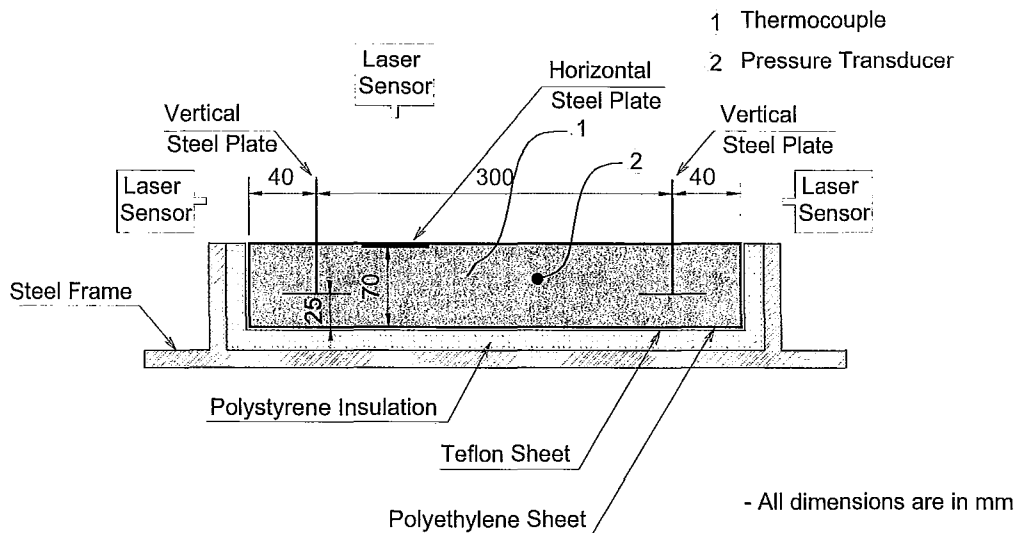


Figure 3.4 Autogenous shrinkage test setup (drawn not to scale)

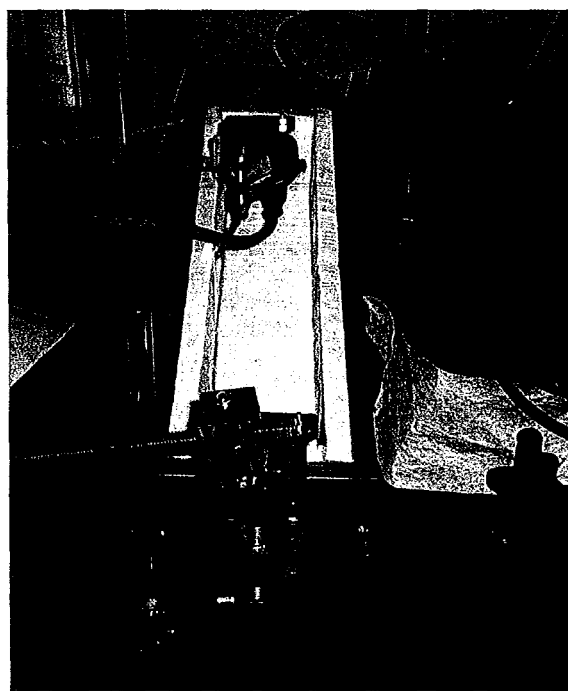


Photo 3.1 Setup for autogenous shrinkage measurements

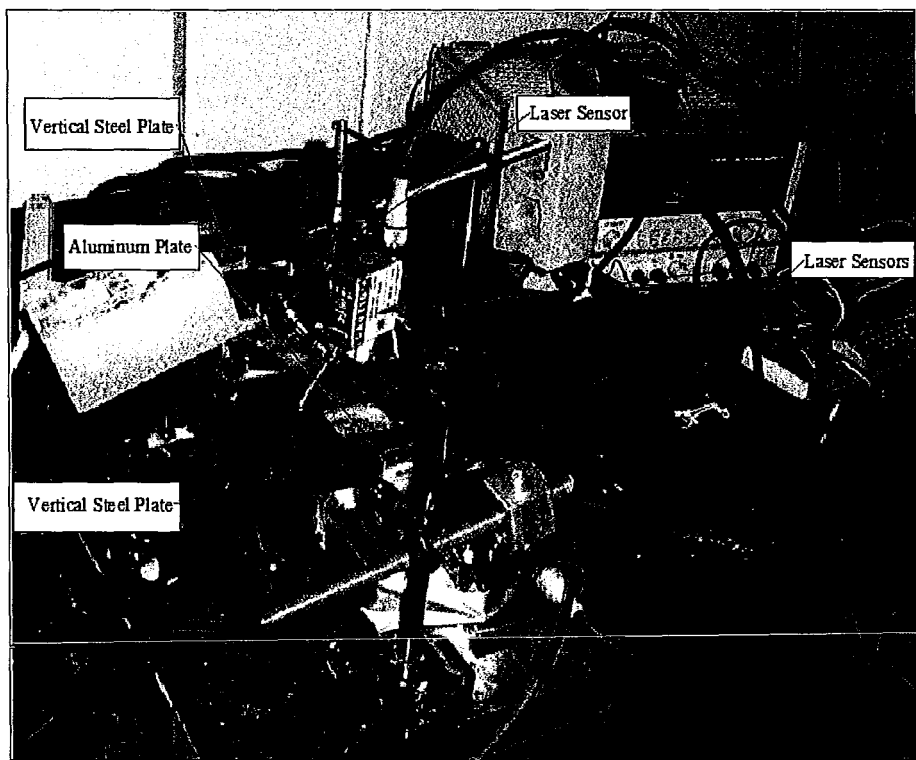


Photo 3.2 Experiment in progress

3.4 Testing Methods

3.4.1 Shrinkage

The shrinkage strain measurements for the air cured and moist cured cylinders were obtained in accordance with the requirements of ASTM – C 341/C 341M-06 (2006b). For each cylinder, the distance between the two opposite dmacs was measured at the time of demoulding and subsequently on the following days: 2, 3, 5, 7, 14, 21, 28, 35, 42, 49, 56, 77, 98, and 119.

The autogenous shrinkage was measured for 24 hours at 3 minutes interval by monitoring the movements of the two vertical plates and the horizontal plate. The corresponding temperature and pressure inside the concrete were also recorded. The measurements of autogenous shrinkage strain were adjusted to account for the thermal strain. The value of concrete thermal coefficient is taken equal to $21 \mu\text{e}/^\circ\text{C}$ and is based on the works of Hedlund (1996) and Byfors (1980). The autogenous shrinkage strain measurements are considered once the capillary pressure begins to vary, i.e. beginning of set time (Holt, 2001).

3.4.2 Concrete Compressive Strength

At the age of 119 days, the concrete compressive strength for all of the cylinders used in the shrinkage measurements was tested according to CSA A23.2-9C (2000). The test was conducted using the Tinius Olsen Universal testing machine 600-kN.

3.5 Experimental Results

The average shrinkage strain measurements and corresponding standard deviation are summarized in Tables 3.6 and 3.7 and those for autogenous shrinkage are displayed in Figure 3.5. The corresponding temperature and pressure are shown in Figures 3.6 and 3.7, respectively. The concrete compressive strength at the age of 119 days for air and moist cured cylinders are given in Table 3.8.

Table 3.6a Shrinkage strain from age 2 days to 14 days for air cured cylinders for mix #5 to mix #35

Time (Days)	Shrinkage Strain ($\mu\text{m/m}$)									
	2		3		5		7		14	
Mix #	ϵ	σ	ϵ	σ	ϵ	σ	ϵ	σ	ϵ	σ
5							73	12	140	10
6							140	62	197	55
7							170	36	273	23
8	-35	22	-12	33	40	64	62	48	160	60
9	-23	3	10	22	73	25	80	9	208	30
10	-43	40	25	13	7	84	130	130	248	159
11	-30	14	50	14	85	49	140	28	270	
12	-60	57	-10	71	80	85	190	85	310	14
13	-5	7	100		170		220	14	355	35
14	27	29	53	16	93	8	132	19	285	22
15	57	85	27	14	82	35	107	35	277	99
16	-47	49	-17	55	50	62	65	65	215	87
17	-18	23	20	80	23	25	72	21	143	56
18	50	26	103	26	152	23	200	26	320	40
19	30	61	82	73	187	16	235	26	372	24
20	102	28	123	40	180	72	238	77	360	69
21	58	6	113	10	187	3	255	5	343	42
22	37	23	35	23	30	31	95	35	210	50
23	65		102	12	148	24	188	32	270	28
24	35	5	37	13	82	16	118	20	190	9
25	37	31	28	40	80	35	127	30	190	26
26	70	40	135	54	200	40	228	34	313	48
27	62	31	115	35	175	26	227	38	282	53
28	82	15	93	23	145	46	213	45	268	46
29	25	30	32	24	52	23	97	20	155	9
30	40	17	47	33	95	40	172	24	237	40
31	45	30	50	10	65	28	107	38	210	17
32	73	50	65	74	135	26	193	45	250	43
33	43	8	52	26	87	6	160	30	218	26
34	47	68	82	107	87	116	115	104	235	91
35	23	13	68	8	138	24	192	12	255	38

Table 3.6b Shrinkage strain from age 21 days to 49 days for air cured cylinders for mix #5 to mix #35

Time (Days)	Shrinkage Strain ($\mu\text{m}/\text{m}$)									
	21		28		35		42		49	
Mix #	ε	σ	ε	σ	ε	σ	ε	σ	ε	σ
5	227	25	280	20	297	25	287	23	327	15
6	307	57	323	49	347	57	340	53	363	59
7	367	12	377	15	413	21	400	53	450	46
8	208	57	248	59	257	40	298	33	290	28
9	250	30	247	24	242	41	283	33	273	6
10	302	135	325	158	358	167	412	182	385	135
11	270		280	28	295	35	315	35	325	7
12	330		385	21	355	35	400	85	380	42
13	395	21	420	57	400	71	480	57	495	78
14	357	16	375	18	433	8	462	6	477	6
15	323	75	345	79	448	115	440	87	430	67
16	257	80	235	79	285	148	303	154	298	113
17	200	76	272	19	288	20	295	30	312	25
18	347	55	343	50	403	37	390	50	403	46
19	398	50	390	53	413	35	437	38	443	50
20	378	55	335	28	413	69	400	70	427	61
21	395	74	368	68	397	62	400	56	412	67
22	278	35	285	41	328	28	332	12	348	13
23	302	33	298	28	348	40	362	47	378	51
24	242	8	260	43	325	18	317	37	353	39
25	257	33	255	35	293	28	290	46	320	44
26	303	28	332	25	363	15	382	25	392	14
27	320	44	332	30	365	46	388	46	410	35
28	280	52	312	32	327	45	335	56	340	56
29	185	26	222	33	263	40	263	32	280	33
30	277	13	270	33	312	46	310	48	338	46
31	250	26	290	30	298	33	298	18	330	36
32	248	36	278	24	305	33	313	24	333	23
33	217	15	255	13	272	19	280	28	290	
34	282	75	352	81	383	67	395	84	412	92
35	315	30	363	8	373	19	393	20	432	31

Table 3.6c Shrinkage strain from age 56 days to 119 days for air cured cylinders for mix #5 to mix #35

Time (Days)	Shrinkage Strain ($\mu\text{m/m}$)							
	56		77		98		119	
Mix #	ε	σ	ε	σ	ε	σ	ε	σ
5	320	20	370	44	430	30	480	26
6	353	58	423	61	447	50	490	36
7	450	30	507	60	543	57	587	61
8	310	33	355	40	408	32	457	34
9	282	10	310	23	370	30	412	24
10	407	130	472	146	517	133	562	133
11	355	21	385	21	440		475	21
12	425	35	485	35	535	35	515	21
13	525	49	580	71	620	85	680	85
14	492	12	540	15	620	23	663	25
15	455	69	508	61	568	80	637	81
16	315	103	333	124	393	124	412	138
17	325	70	375	28	417	63	478	25
18	410	58	440	58	477	76	505	74
19	453	44	488	45	563	62	580	46
20	423	73	463	92	523	73	563	63
21	432	71	455	78	510	75	492	71
22	390	35	417	25	498	14	547	48
23	383	45	428	38	497	38	580	45
24	377	49	428	57	513	59	568	51
25	338	60	378	61	448	67	505	62
26	395	10	477	26	517	25	597	18
27	403	36	475	35	500	35	557	73
28	362	66	417	58	460	67	532	40
29	298	43	373	55	418	71	482	89
30	347	45	402	50	458	53	512	58
31	367	43	395	36	440	58	532	64
32	348	20	395	41	440	35	517	33
33	298	10	345	15	412	3	493	34
34	448	72	497	59	557	57	657	63
35	447	36	480	48	525	43	613	47

Table 3.6d Shrinkage strain from age 2 days to 14 days for air cured cylinders for mix #36 to mix #66

Time (Days)	Shrinkage Strain ($\mu\text{m/m}$)									
	2		3		5		7		14	
Mix #	ϵ	σ	ϵ	σ	ϵ	σ	ϵ	σ	ϵ	σ
36	18	42	23	39	28	94	80	148	162	164
37	30	17	15	28	62	23	117	49	205	35
38	62	19	72	48	118	48	155	49	185	49
39	108	3	107	19	195	18	212	18	282	35
40	65	5	127	15	163	10	173	21	207	28
41	53	32	73	46	90	41	95	52	143	58
42	30	22	78	26	102	28	123	33	197	32
43	32	24	65	18	98	15	117	32	168	35
44	60	38	83	28	82	28	107	37	132	38
45	67	20	58	45	78	45	102	44	162	49
46	15	13	28	8	32	6	63	6	93	8
47	25	13	37	28	48	20	88	16	148	8
48	62	30	68	13	130	39	162	48	213	51
49	60	17	90	18	118	33	142	35	157	43
50	102	50	150	55	180	36	210	41	260	56
51	60	28	83	31	108	21	145	17	183	3
52	-3	50	5	15	8	33	25	35	85	26
53	63	16	107	25	143	16	148	8	218	29
54	53	18	72	34	145	30	147	39	222	26
55	62	10	87	16	163	15	145	22	225	17
56	103	8	113	13	150	9	177	31	277	23
57	83	10	70	26	73	21	100	39	208	34
58	82	13	85	0	92	10	115	20	217	8
59	43	38	57	37	138	55	175	54	267	58
60	58	8	35	17	67	33	97	25	188	3
61	110	82	133	83	180	84	202	60	313	60
62	15	40	55	31	110	31	138	23	247	58
63	43	36	67	28	103	40	137	40	235	31
64	122	35	193	47	217	18	252	20	335	31
65	8	26	38	39	90	15	103	24	217	31
66	118	28	175	30	235	22	268	26	388	51

Table 3.6e Shrinkage strain from age 21 days to 49 days for air cured cylinders for mix #36 to mix #66

Time (Days)	Shrinkage Strain ($\mu\text{m}/\text{m}$)									
	21		28		35		42		49	
Mix #	ϵ	σ	ϵ	σ	ϵ	σ	ϵ	σ	ϵ	σ
36	192	172	223	173	240	138	228	150	243	158
37	267	36	308	43	303	40	322	51	338	49
38	187	49	255	43	238	40	280	52	283	45
39	287	24	365	13	337	18	375	26	390	17
40	225	18	285	13	297	23	308	45	355	79
41	133	61	200	48	208	55	237	34	253	45
42	213	42	282	62	293	64	333	72	353	57
43	207	44	297	43	302	58	322	63	352	73
44	152	34	183	45	193	50	202	55	215	49
45	203	48	275	48	287	50	302	80	305	94
46	130	25	195	13	210	9	212	19	220	30
47	228	28	275	18	295	43	315	40	337	32
48	298	48	300	46	337	33	358	38	383	39
49	223	38	238	49	270	68	298	63	327	73
50	292	64	303	81	318	71	353	75	368	67
51	242	13	252	8	290	10	328	6	353	16
52	165	43	185	40	228	41	257	29	273	48
53	293	33	305	52	322	53	355	57	375	44
54	293	24	308	14	340	33	360	48	390	36
55	308	10	325	0	357	3	377	3	402	8
56	305	43	338	29	368	61	403	40	417	43
57	245	20	263	29	300	40	362	38	372	35
58	265	13	288	8	327	23	360	28	378	33
59	307	49	327	68	370	39	415	57	430	48
60	215	41	248	51	310	38	345	52	367	55
61	343	65	367	51	400	39	438	64	432	32
62	285	48	330	44	370	52	405	44	413	49
63	250	30	298	35	338	30	377	29	378	24
64	380	15	405	18	453	15	480	10	492	25
65	252	25	295	26	350	35	372	19	385	26
66	443	46	478	45	505	58	547	49	553	55

Table 3.6f Shrinkage strain from age 56 days to 119 days for air cured cylinders for mix #36 to mix #66

		Shrinkage Strain ($\mu\text{m/m}$)							
Time (Days)		56		77		98		119	
Mix #		ε	σ	ε	σ	ε	σ	ε	σ
36		260	149	282	161	315	163	380	179
37		357	56	397	64	440	61	517	65
38		330	54	362	63	415	58	493	40
39		433	10	480	26	528	6	625	10
40		385	75	423	67	453	88	532	86
41		273	55	318	43	363	33	430	28
42		417	49	463	62	533	64	617	71
43		373	80	433	65	517	74	598	85
44		228	41	260	44	272	68	318	60
45		313	101	383	94	438	103	548	112
46		247	20	327	56	388	40	442	24
47		375	23	467	39	537	26	605	10
48		390	44	450	26	510	36	633	42
49		325	64	383	60	438	55	552	61
50		372	72	453	86	498	78	603	80
51		363	33	435	33	468	33	577	45
52		298	64	387	75	418	64	497	57
53		382	64	455	61	493	59	568	70
54		403	32	495	44	540	58	650	72
55		412	13	502	16	568	10	663	15
56		445	71	518	68	567	71	663	74
57		368	40	472	33	508	48	600	43
58		393	26	477	25	517	28	610	20
59		452	51	517	42	572	41	678	42
60		385	30	457	32	512	40	602	32
61		430	26	502	19	527	33	625	35
62		448	55	548	55	593	60	717	83
63		402	29	498	25	543	43	660	38
64		497	41	577	29	600	30	712	30
65		407	30	485	40	570	31	665	18
66		550	48	645	52	705	44	808	55

Table 3.7a Shrinkage strain from age 2 days to 14 days for moist cured cylinders for mix #5 to mix #35

		Shrinkage Strain ($\mu\text{m}/\text{m}$)									
Time (Days)		2		3		5		7		14	
Mix #		ϵ	σ	ϵ	σ	ϵ	σ	ϵ	σ	ϵ	σ
5								-27	25	50	50
6								57	38	77	47
7								-13	51	33	72
8	-52	19	-63	46	-90	36	-100	39	-12	67	
9	-27	15	-40	30	-60	43	-97	37	-13	68	
10	-47	56	-55	13	-43	33	-58	29	27	25	
11	-30		-50		-50		-60		50		
12	240		210		190		130		500		
13			-10		-60		-70		10		
14	-23	20	-30	38	-33	60	-32	88	-7	138	
15	-48	40	-50	51	-87	99	-60	103	-12	77	
16	-27	55	-57	50	-60	73	-45	63	3	43	
17	-15	28	-32	3	-48	37	-60	60	-7	96	
18	-90	48	-130	65	-147	63	-148	62	-77	89	
19	-20	17	-22	33	-23	33	-15	10	43	30	
20	-5	49	-3	32	22	69	18	68	8	80	
21	-22	3	-15	13	0	13	22	60	-27	51	
22	-27	3	5	22	-15	46	-28	26	3	33	
23	-28	10	-45	20	-43	15	-57	42	-78	40	
24	-28	10	-45	20	-43	15	-57	42	-78	40	
25	-22	23	-35	35	-27	28	-32	12	-63	25	
26	-50	23	-17	30	-33	35	-62	48	-90	75	
27	-32	28	-23	26	-35	52	-55	25	-78	46	
28	-15	10	-47	20	-63	12	-67	28	-78	25	
29	-32	6	-33	6	-53	40	-70	51	-87	45	
30	13	33	-18	51	-2	45	-25	48	-25	87	
31	-15	35	-33	38	-65	46	-50	36	-118	56	
32	-67	25	-93	21	-128	34	-122	63	-152	65	
33	10	18	-22	16	-48	10	-50	26	-145	43	
34	10	28	13	35	-32	25	-52	33	-97	13	
35	-52	10	-63	33	-73	33	-82	26	-132	77	

Table 3.7b Shrinkage strain from age 21 days to 49 days for moist cured cylinders for mix #5 to mix #35

Time (Days)	Shrinkage Strain ($\mu\text{m/m}$)									
	21	28	35	42	49					
Mix #	ε	σ	ε	σ	ε	σ	ε	σ	ε	σ
5	123	46	117	58	103	64	97	76	77	59
6	103	51	103	58	90	79	47	47	63	68
7	87	49	37	179	73	187	50	140	53	155
8	33	75	47	55	33	65	32	50	15	62
9	-3	65	-12	63	-20	35	-8	38	-35	33
10	53	38	65	56	35	45	37	32	27	54
11	20		50		50		90		30	
12	360		360		350		320		290	
13	-10		-80		-110		-100		-180	
14	0	140	13	131	3	120	-17	130	-27	130
15	-38	106	-22	119	-23	98	-30	95	-70	100
16	-32	58	-35	70	-7	68	-63	98	-55	93
17	13	68	-7	104	18	68	20	58	-12	100
18	-77	75	-73	73	-68	83	-78	85	-112	105
19	27	33	37	28	35	18	23	20	3	16
20	-5	98	-40	95	-18	55	2	95	-33	44
21	-5	48	-18	40	5	43	-32	63	-37	68
22	-13	45	-42	35	-5	30	5	36	22	46
23	-75	31	-93	28	-73	29	-98	44	-100	35
24	-75	31	-93	28	-73	29	-98	44	-100	35
25	-78	40	-127	55	-82	48	-98	53	-92	39
26	-110	118	-107	114	-48	106	-50	120	-60	115
27	-102	38	-118	46	-110	45	-77	53	-58	58
28	-120	35	-107	38	-48	38	-57	28	-62	29
29	-140	69	-113	78	-80	80	-92	97	-92	99
30	-55	71	-43	57	-17	63	-23	47	-30	51
31	-152	68	-148	55	-125	49	-152	62	-148	68
32	-143	70	-122	50	-110	35	-138	45	-135	43
33	-115	61	-113	78	-93	88	-97	73	-95	84
34	-93	16	-65	22	-57	23	-58	8	-53	10
35	-97	67	-82	58	-83	56	-110	71	-103	61

Table 3.7c Shrinkage strain from age 56 days to 119 days for moist cured cylinders for mix #5 to mix #35

		Shrinkage Strain ($\mu\text{m/m}$)							
Time (Days)		56		77		98		119	
Mix #		ϵ	σ	ϵ	σ	ϵ	σ	ϵ	σ
5		77	59	63	46	77	59	73	57
6		50	44	63	49	60	36	20	44
7		63	152	60	159	63	142	63	165
8			57	12	46	47	39	52	39
9		-38	43	-48	21	-38	29	-13	31
10		12	49	22	61	18	63	38	69
11		40		80		80		110	
12		310		300		260		240	
13		-180		-160		-160		-180	
14		-32	124	-15	148	-20	140	-7	151
15		-55	96	-47	86	-35	100	-25	96
16		-68	105	-67	101	-105	107	-55	113
17		-13	105	2	114	3	80	17	83
18		-115	101	-105	106	-103	103	-107	101
19		7	26	10	15	12	16	20	9
20		-15	61	-18	57	-32	69	-23	58
21		-38	73	-20	63	-25	59	-25	75
22		15	59	28	32	33	32	28	36
23		-100	23	-95	23	-98	29	-25	43
24		-100	23	-95	23	-98	29	-25	43
25		-77	38	-88	49	-63	42	10	30
26		-28	111	-5	93	-15	110	45	110
27		-43	53	-28	71	-40	61	45	52
28		-43	49	-62	69	-68	51	12	53
29		-75	93	-77	75	-82	94	-57	68
30		-18	23	-20	40	-33	51	28	54
31		-115	87	-148	42	-158	56	-108	67
32		-127	43	-137	46	-138	30	-93	32
33		-57	75	-72	75	-57	71	-17	74
34		-2	12	-2	29	3	25	48	25
35		-75	84	-75	62	-90	79	-37	72

Table 3.7d Shrinkage strain from age 2 days to 14 days for moist cured cylinders for mix #36 to mix #66

Shrinkage Strain ($\mu\text{m/m}$)											
Time (Days)	2		3		5		7		14		
Mix #	ε	σ									
36	-25	58	-40	52	-35	56	-37	50	-78	33	
37	47	111	-2	103	-22	120	-13	137	-20	122	
38	-35	10	-42	6	-62	10	-23	21		30	
39	50	75	63	75	38	63	62	56	55	35	
40	-5	43	-33	60	-72	88	-87	108	-112	95	
41	-3	16	-25	30	-50	62	-43	36	-33	51	
42	-35	30	-28	42	-25	56	-38	53	-35	68	
43	-28	28	-143	136	-147	45	-133	61	-138	85	
44	2	23	-5	20	-5	26	-43	36	-42	26	
45	-93	38	-77	13	-120	23	-168	25	-163	16	
46	-47	58	-48	32	-82	35	-112	26	-173	81	
47	-23	92	-78	20	-95	26	-117	16	-122	21	
48	-23	55	-30	23	-80	55	-58	68	-57	74	
49	-32	29	-32	29	-73	50	-85	20	-82	55	
50	5	20	-5	36	-53	55	-55	35	-45	18	
51	-63	19	-75	53	-88	53	-75	65	-112	81	
52	-47	21	-53	15	-87	34	-87	39	-133	58	
53	-65	10	-83	16	-105	31	-110	23	-170	30	
54	18	34	7	45	-10	35	-67	39	-33	74	
55	-48	28	-40	39	-70	38	-110	72	-40	66	
56	-30	5	-18	35	-20	23	-72	63	-77	70	
57	-20	45	-18	55	-57	43	-68	55	-55	62	
58	-33	16	-23	25	-73	42	-72	20	-105	30	
59	-50	44	-60	30	-77	67	-78	63	-42	58	
60	2	12	-17	8	-17	24	-28	30	-10	23	
61	20	25	3	24	-8	28	-48	45	-35	71	
62	-53	30	-48	33	-58	19	-70	26	-40	13	
63	-18	38	3	71	-18	83	-37	67	5	62	
64	12	46	33	60	7	98	-40	108	-15	90	
65	-17	18	-48	31	-60	74	-75	62	-20	46	
66	27	16	2	38	-2	25	-40	40	-20	35	

Table 3.7e Shrinkage strain from age 21 days to 49 days for moist cured cylinders for mix #36 to mix #66

Time (Days)	Shrinkage Strain ($\mu\text{m/m}$)											
	21		28		35		42		49		Mix #	
	ϵ	σ	ϵ	σ	ϵ	σ	ϵ	σ	ϵ	σ		
36	-97	37	-48	40	-45	45	-60	54	-53	56		
37	-13	160	20	160	53	143	53	155	55	154		
38	-48	32	-18	28	-22	29	-40	18	-35	17		
39	7	38	45	30	28	39	17	14	20	33		
40	-147	118	-98	107	-98	103	-117	98	-125	103		
41	-60	74	-7	62	-8	64	-17	60	-2	77		
42	-20	22	25	36	28	53	28	32	52	28		
43	-105	88	-63	103	-58	88	-35	88	-23	103		
44	-42	20	-22	19	-33	31	-20	31	-10	23		
45	-147	23	-108	28	-95	18	-95	13	-83	19		
46	-113	78	-97	107	-87	109	-85	108	-68	113		
47	-73	33	-47	36	-42	31	-62	21	-45	20		
48	-12	55	-7	76	-27	80	5	80	22	58		
49	-45	58	-47	60	-68	70	-60	70	-47	91		
50	-30	35	-50	28	-73	16	-58	20	-53	28		
51	-85	76	-93	81	-93	98	-77	89	-88	81		
52	-88	80	-87	78	-78	88	-82	77	-67	68		
53	-125	31	-150	13	-138	18	-110	10	-100	25		
54	38	83	28	81	55	84	78	84	62	77		
55	3	46	12	51	20	35	27	24	13	8		
56	-82	43	-108	44	-105	48	-98	58	-122	64		
57	-28	56	-20	22	-20	18	10	35	7	38		
58	-72	38	-73	30	-62	40	-48	68	-50	79		
59	-52	78	-62	79	-57	78	-18	99	-57	94		
60	20	48	32	45	48	19	75	28	53	28		
61	-20	74	-35	64	-32	57	-18	84	-13	115		
62	-22	14	-23	20	-18	40	0	31	-2	38		
63	-18	70	-2	92	20	71	30	75	35	103		
64	-35	87	-27	128	-48	112	-30	98	-37	120		
65	-12	43	-3	38	35	51	32	56	35	68		
66	-18	28	-27	38	-22	38	-3	33	-45	22		

Table 3.7f Shrinkage strain from age 56 days to 119 days for moist cured cylinders for mix #36 to mix #66

Shrinkage Strain ($\mu\text{m/m}$)									
Time (Days)		56		77		98		119	
Mix #		ε	σ	ε	σ	ε	σ	ε	σ
36		-22	40	-40	46	-42	45	15	38
37		78	148	60	155	78	148	125	159
38		-25	25	-28	25	-55	66	-13	71
39		23	42	12	46	-3	45	40	56
40		-132	110	-138	106	-127	103	-88	88
41		15	77	37	61	40	60	98	55
42		48	29	27	52	48	38	88	45
43		-28	113	-20	131	7	118	67	98
44		-25	25	-22	33	-10	33	15	35
45		-80	15	-88	10	-70	5	-33	24
46		-42	122	-32	124	-12	108	32	90
47		-50	18	-68	13	-53	3	13	45
48		27	49	22	41	20	83	72	76
49		-50	94	-52	91	-18	92	27	83
50		-50	36	-80	43	-62	28	-20	48
51		-98	75	-113	92	-68	70	2	68
52		-65	65	-68	63	-42	63	-15	75
53		-103	32	-117	30	-77	40	-28	34
54		83	71	78	71	120	79	175	58
55		28	15	23	6	57	13	142	16
56		-118	75	-128	51	-95	61	-17	64
57		13	33	30	44	43	35	118	51
58		-40	66	-73	72	-87	102	28	129
59		-40	123	-52	138	-43	144	83	149
60		62	29	78	20	87	24	182	28
61		-2	38	-70	76	-72	62	23	107
62		-18	48	-7	58	7	63	105	71
63		-5	112	-5	100	28	89	108	78
64		-47	123	-58	120	-62	113	-18	135
65		38	73	53	73	127	69	180	85
66		-38	14	-75	26	-10	30	35	39

Table 3.8 Average and standard deviation values for concrete compressive strength at the age of 119 days for air cured and moist cured samples

Mix #	Compressive Strength (MPa)									
	Moist Cured		Air Cured		Mix #	Moist Cured		Air Cured		
	$\bar{\epsilon}$	σ	$\bar{\epsilon}$	σ		$\bar{\epsilon}$	σ	$\bar{\epsilon}$	σ	
5	40.00	2.12	35.00	1.38	36	31.60	1.28	20.65	1.70	
6	56.61	1.97	51.05	5.01	37	35.51	2.91	20.54	3.31	
7	53.92	6.28	45.86	7.57	38	45.70	3.23	37.61	1.97	
8	38.73	2.80	35.85	1.55	39	44.75	4.73	37.43	3.21	
9	37.43	1.37	30.11	4.47	40	47.53	4.47	42.99	0.42	
10	37.80	5.32	33.35	2.65	41	28.07	2.18	24.72	1.25	
11	51.98	0.00	42.53	3.14	42	32.06	1.05	28.25	1.15	
12	52.81	0.00	46.97	5.50	43	35.39	1.28	28.82	1.80	
13	49.20	0.00	45.03	5.11	44	51.04	1.51	44.28	1.81	
14	34.19	5.80	25.48	1.68	45	31.59	0.98	27.05	1.70	
15	29.37	1.77	25.29	3.01	46	40.62	0.45	33.21	0.80	
16	35.48	0.70	24.55	2.05	47	41.69	2.38	32.06	0.61	
17	35.85	0.83	26.87	0.16	48	42.55	5.41	33.56	1.32	
18	47.81	3.01	41.82	1.22	49	36.36	0.94	33.17	2.26	
19	48.45	2.84	43.17	1.60	50	90.65	5.03	70.60	3.10	
20	53.74	3.62	42.53	3.68	51	35.24	2.55	33.42	0.52	
21	45.86	1.39	31.31	3.22	52	20.27	1.00	17.30	0.12	
22	29.28	8.42	15.01	1.47	53	59.29	5.62	50.96	4.73	
23	53.64	0.74	46.69	1.93	54	40.95	1.29	33.74	1.54	
24	31.87	3.78	23.16	0.85	55	35.34	3.24	28.26	1.99	
25	35.67	0.70	22.61	1.37	56	69.39	0.70	58.01	7.74	
26	53.55	0.85	40.39	1.05	57	24.33	2.19	17.79	0.54	
27	47.99	0.64	37.24	3.74	58	23.73	1.11	19.18	0.41	
28	47.90	4.01	39.65	1.53	59	60.09	3.90	54.29	4.72	
29	39.47	2.37	23.81	2.26	60	23.29	1.67	16.62	0.84	
30	46.42	1.95	33.26	1.37	61	85.64	4.30	57.35	9.18	
31	32.15	3.70	25.20	1.78	62	33.19	3.24	30.02	0.28	
32	47.65	3.06	38.28	1.29	63	34.44	1.88	30.94	0.17	
33	45.86	2.17	36.81	1.86	64	82.03	2.18	69.78	6.34	
34	35.16	2.34	25.66	1.43	65	41.69	0.56	34.25	2.27	
35	49.20	5.28	34.43	2.43	66	77.89	4.18	73.05	6.75	

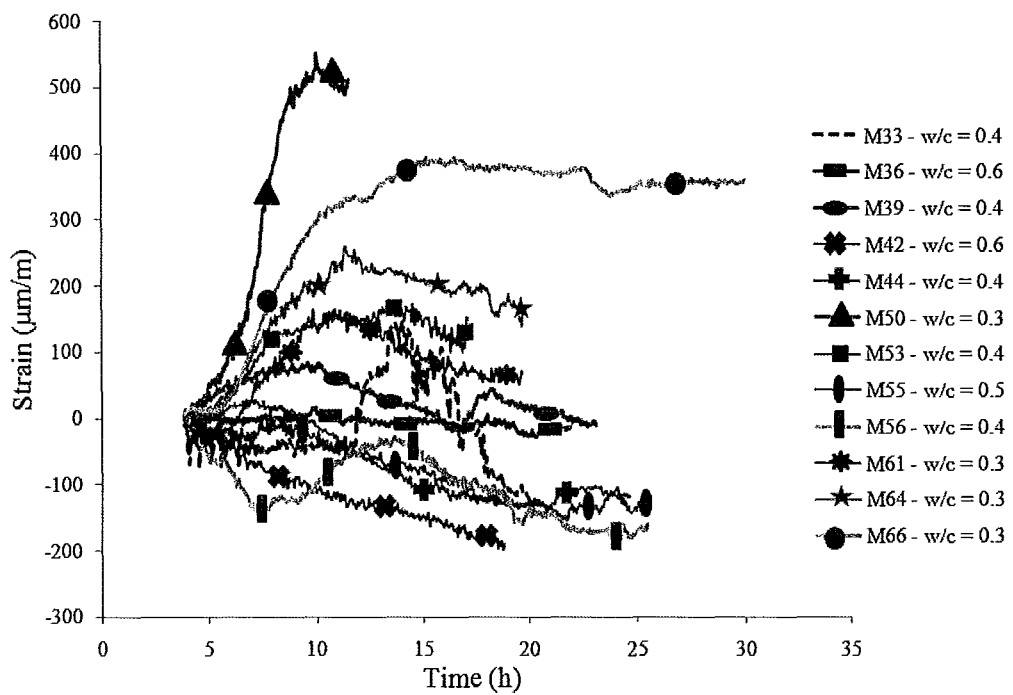


Figure 3.5 Strain versus time

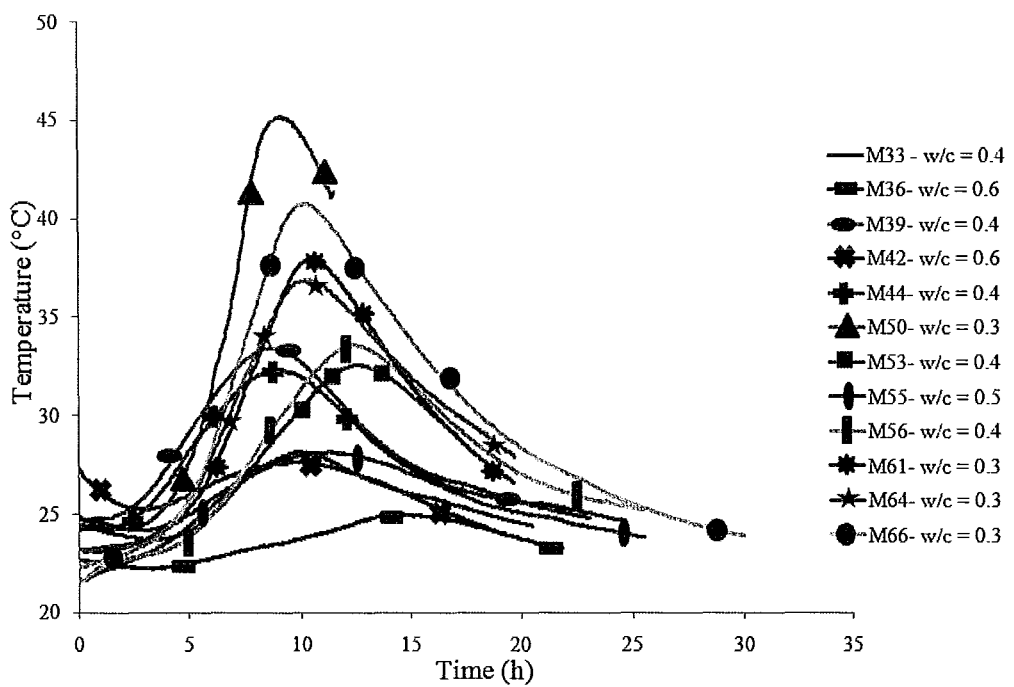


Figure 3.6 Temperature versus time

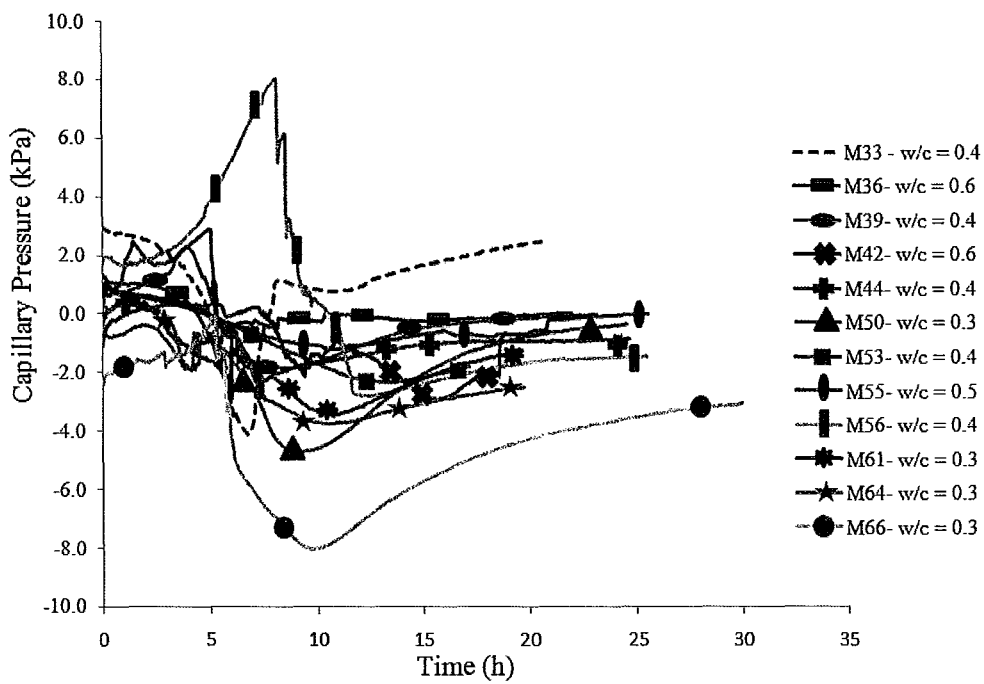


Figure 3.7 Capillary pressure versus time

Chapter 4

Analysis of Experimental Data

4.0 Introduction

Measured shrinkage strain for the air and moist cured samples were analyzed to determine the effects of the mixture design on shrinkage. A statistical analysis of the data was then carried out to determine the statistical significance of the variables. The effect of shrinkage strain on the concrete compressive strength was also evaluated.

4.1 Effect of Curing Regime on Shrinkage

Shrinkage strain in concrete was evaluated using two curing regimes, air and moist. According to the literature, when concrete is moist cured, drying shrinkage and plastic shrinkage become negligible in comparison to chemical shrinkage. However, air cured concrete is expected to experience both chemical and drying shrinkage. The air cured samples are expected to experience only chemical shrinkage for the first 24 hours before demoulding. Subsequently, the contribution of on-going shrinkage will mostly be due to

drying shrinkage. Moreover, it can be assumed that the contribution from chemical shrinkage will continue depending on the amount of free water available for hydration. On the basis of this analogy, the shrinkage for air cured concrete samples will provide measurements for both chemical and drying shrinkage, and those measurements for the moist cured samples will provide quantifications for the chemical shrinkage only.

Chemical shrinkage includes all possible types of shrinkage, except drying and plastic shrinkage. Accordingly, it is expected that moist cured samples experience the majority of their volume change in the first 7 days, whereas the air cured continue to experience volume change up to 119 days. The measured data presented in chapter 3 support this justification. Also, by examining the coefficient of co-variance given in Tables 4.1 to 4.4, it is possible to examine the variation in the measurements. The results, corresponding to both drying and chemical shrinkage given in Tables 4.1 and 4.2, indicate a high degree of variation after 2 and 3 days for most mixes and up to 7 days for a small number of mixes. Thereafter, the variation is less than 20%. However, the results, corresponding to chemical shrinkage, given in Tables 4.3 and 4.4, indicate that the variations in the measurements are not consistent for most mixes. The cause for the inconsistency goes back to the nature of chemical shrinkage. In chapter 2, it was stated that chemical shrinkage causes pores to develop inside the structure, whereas autogenous shrinkage causes a reduction in the volume of the sample. Hammer (1999) and Holt (2001) have shown that autogenous shrinkage occurs in the first 24 hours and that chemical shrinkage continues until all unhydrated particles react provided there is free water. Recognizing the inhomogeneity of the concrete structure, and its effect on hydration process, it is postulated that the random generation of the interior pores causes a sample to shrink in a random manner resulting inconsistency in the measured values for shrinkage. In contrast, drying shrinkage is due to the loss of water to the surrounding environment, which is uniform in comparison. This interaction is expected to yield a more behaved response as it is also observed in Tables 4.1 and 4.2. Another factor is the magnitude of the strains. As expected, significantly larger values were recorded for drying shrinkage in comparison to those for chemical shrinkage which were negligible.

In brief, the measured values for shrinkage confirm that strains due to chemical shrinkage are much smaller than those of drying shrinkage. Curing significantly influences the magnitude and type of shrinkage that occur in concrete. Drying shrinkage yields strains that range from 450 to 800 $\mu\text{m}/\text{m}$ after 119 days depending on the concrete mixture. Chemical shrinkage strains are found to be for most concrete mixtures less than 100 $\mu\text{m}/\text{m}$ after 119 days. Lastly, given the inconsistency in the measured strains for chemical shrinkage, the study will focus only on the drying shrinkage.

Table 4.1 Covariance values for drying and chemical shrinkage strains for mix #5 to mix #36

Time (Days)	Covariance (%)													
	2	3	5	7	14	21	28	35	42	49	56	77	98	119
Mix #														
5				16	7	11	7	8	8	5	6	12	7	6
6				45	28	19	15	16	16	16	16	14	11	7
7				21	8	3	4	5	13	10	7	12	10	10
8	62	285	160	77	37	27	24	16	11	10	11	11	8	7
9	12	218	34	11	14	12	10	17	12	2	4	7	8	6
10	93	53	1265	100	64	45	49	47	44	35	32	31	26	24
11	47	28	58	20			10	12	11	2	6	6		4
12	94	707	106	45	5		6	10	21	11	8	7	7	4
13	141			6	10	5	13	18	12	16	9	12	14	12
14	110	30	8	14	8	5	5	2	1	1	2	3	4	4
15	151	54	43	33	36	23	23	26	20	16	15	12	14	13
16	-104	332	125	101	40	31	33	52	51	38	33	37	32	34
17	126	402	108	29	39	38	7	7	10	8	22	7	15	5
18	52	25	15	13	12	16	15	9	13	12	14	13	16	15
19	205	90	9	11	6	13	14	8	9	11	10	9	11	8
20	27	33	40	32	19	15	8	17	17	14	17	20	14	11
21	10	9	2	2	12	19	18	16	14	16	16	17	15	14
22	63	65	104	36	24	13	14	8	3	4	9	6	3	9
23		11	16	17	10	11	10	12	13	14	12	9	8	8
24	14	34	20	17	5	3	16	6	12	11	13	13	12	9
25	83	142	44	24	14	13	14	9	16	14	18	16	15	12
26	57	40	20	15	15	9	8	4	7	4	3	5	5	3
27	50	30	15	17	19	14	9	13	12	8	9	7	7	13
28	19	25	32	21	17	19	10	14	17	17	18	14	15	8
29	120	75	44	21	6	14	15	15	12	12	14	15	17	19
30	43	71	42	14	17	5	12	15	15	14	13	12	12	11
31	68	20	43	35	8	10	10	11	6	11	12	9	13	12
32	68	113	20	23	17	15	8	11	8	7	6	10	8	6
33	18	50	7	19	12	7	5	7	10		3	4	1	7
34	145	131	133	90	39	27	23	18	21	22	16	12	10	10
35	54	11	17	6	15	10	2	5	5	7	8	10	8	8
36	229	166	333	184	101	90	77	58	66	65	57	57	52	47

Table 4.2 Covariance values for drying and chemical shrinkage strains for mix #37 to mix #66

Time (Days)	Covariance (%)													
	2	3	5	7	14	21	28	35	42	49	56	77	98	119
Mix #														
37	58	186	37	42	17	14	14	13	16	15	16	16	14	13
38	31	67	40	32	27	26	17	17	19	16	16	17	14	8
39	3	18	9	8	13	8	4	5	7	4	2	5	1	2
40	8	12	6	12	13	8	5	8	15	22	20	16	19	16
41	60	63	45	55	40	46	24	26	14	18	20	13	9	6
42	73	33	28	27	16	20	22	22	22	16	12	13	12	12
43	75	28	16	27	21	21	15	19	20	21	21	15	14	14
44	63	33	34	35	29	22	25	26	27	23	18	17	25	19
45	30	77	58	43	30	23	17	17	26	31	32	25	23	20
46	88	27	18	9	8	19	7	4	9	14	8	17	10	5
47	53	78	42	18	5	12	7	14	13	10	6	8	5	2
48	49	18	30	30	24	16	15	10	10	10	11	6	7	7
49	29	20	27	25	28	17	20	25	21	22	20	16	13	11
50	50	37	20	19	22	22	27	22	21	18	19	19	16	13
51	46	37	19	12	2	5	3	3	2	5	9	8	7	8
52	1502	300	390	140	31	26	22	18	11	18	22	19	15	11
53	25	24	11	5	13	11	17	17	16	12	17	14	12	12
54	33	47	21	26	12	8	5	10	13	9	8	9	11	11
55	17	19	9	15	8	3	0	1	1	2	3	3	2	2
56	7	11	6	17	8	14	9	17	10	10	16	13	13	11
57	12	38	28	39	16	8	11	13	10	9	11	7	9	7
58	15	0	11	17	4	5	3	7	8	9	7	5	5	3
59	87	65	40	31	22	16	21	11	14	11	11	8	7	6
60	13	49	49	26	2	19	21	12	15	15	8	7	8	5
61	75	62	46	30	19	19	14	10	15	7	6	4	6	6
62	265	57	28	16	23	17	13	14	11	12	12	10	10	12
63	83	41	39	30	13	12	12	9	8	6	7	5	8	6
64	29	24	8	8	9	4	4	3	2	5	8	5	5	4
65	308	101	17	23	14	10	9	10	5	7	7	8	5	3
66	23	17	9	10	13	10	9	11	9	10	9	8	6	7

Table 4.3a Covariance values for chemical shrinkage strains from age 2 days to 28 days
for mix #5 to mix #35

Time (Days)	Covariance (%)						
	2	3	5	7	14	21	28
Mix #							
5				94	100	37	49
6				67	62	50	56
7				385	217	57	489
8	37	73	40	39	576	226	118
9	57	76	71	38	509	1958	539
10	119	24	77	49	94	70	87
14	87	126	179	278	2065		985
15	84	101	115	172	656	277	549
16	207	88	121	139	1276	184	200
17	186	9	76	100	1447	512	1559
18	53	50	43	42	116	98	99
19	87	154	143	67	70	125	78
20	985	953	320	368	962	1952	238
21	13	88		275	192	964	220
22	11	436	306	91	976	340	84
23	37	44	35	73	51	42	30
24	37	44	35	73	51	42	30
25	104	100	103	36	39	52	43
26	46	181	105	78	84	107	107
27	87	110	149	45	59	37	39
28	67	43	18	41	32	29	35
29	18	17	76	72	52	50	68
30	250	279	2722	191	347	128	131
31	233	115	71	72	47	45	37
32	37	22	27	52	43	49	41
33	180	74	22	52	30	53	69
34	278	263	78	64	13	17	34
35	20	53	44	31	58	69	70

Table 4.3b Covariance values for chemical shrinkage strains from age 35 days to 119 days for mix #5 to mix #35

Time (Days)	Covariance (%)						
	35	42	49	56	77	98	119
Mix #							
5	62	78	76	76	73	76	78
6	88	101	107	87	78	60	218
7	255	280	291	240	265	224	261
8	196	159	416		398	83	75
9	173	450	94	111	43	76	229
10	129	88	202	421	282	345	180
14	3601	782	486	392	984	700	2263
15	418	318	143	175	185	285	386
16	1021	155	170	154	151	102	205
17	372	288	859	790	6817	2406	497
18	122	109	94	88	101	99	94
19	52	87	482	385	150	138	43
20	300	5679	131	410	310	219	250
21	854	200	186	190	313	236	300
22	600	721	214	393	113	96	128
23	40	44	35	23	24	30	173
24	40	44	35	23	24	30	173
25	58	54	42	49	55	66	304
26	219	241	192	390	1868	736	245
27	41	70	99	123	250	152	116
28	78	49	48	113	112	75	458
29	100	106	108	123	98	116	120
30	377	203	169	123	198	153	190
31	39	41	46	75	28	35	61
32	32	32	32	34	34	22	34
33	94	76	88	133	105	125	445
34	40	13	20	693	1758	740	51
35	67	64	59	111	83	88	197

Table 4.4a Covariance values for chemical shrinkage strains from age 2 days to 28 days
for mix #36 to mix #66

Time (Days)	Covariance (%)						
	2	3	5	7	14	21	28
Mix #							
36	231	131	161	137	42	38	83
37	239	6180	554	1030	608	1200	799
38	29	14	17	89		66	150
39	149	119	165	90	63	563	68
40	854	181	123	125	85	80	109
41	482	122	125	83	154	123	926
42	87	148	223	138	193	109	144
43	97	95	31	46	61	83	162
44	1353	400	529	83	62	48	87
45	41	16	19	15	10	15	25
46	125	67	43	23	47	69	110
47	393	26	27	14	17	45	78
48	237	76	69	116	130	474	1146
49	93	93	69	24	67	128	128
50	400	721	103	64	40	115	56
51	30	71	59	87	73	89	87
52	45	29	39	45	43	91	89
53	15	19	30	21	18	25	9
54	186	672	350	58	221	215	285
55	59	98	54	66	164	1394	438
56	17	193	115	88	91	53	40
57	225	299	75	81	114	198	109
58	48	108	57	28	29	53	41
59	89	50	87	80	139	150	128
60	693	46	142	106	229	238	143
61	125	709	330	93	203	368	182
62	57	69	32	37	33	67	87
63	205	2123	454	182	1249	383	5534
64	398	180	1463	271	603	248	481
65	105	63	123	83	229	364	1146
66	60	2272	1510	100	175	150	142

Table 4.4b Covariance values for chemical shrinkage strains from age 35 days to 119 days for mix #36 to mix #66

Time (Days)	Covariance (%)						
	35	42	49	56	77	98	119
Mix #							
36	100	90	105	187	115	109	252
37	268	290	280	189	259	189	127
38	135	45	49	100	89	119	533
39	137	87	164	180	398	1353	141
40	105	84	82	83	77	81	100
41	774	363	4612	513	167	150	56
42	189	112	53	60	195	79	51
43	151	253	440	400	656	1772	147
44	92	156	229	100	154	328	233
45	19	14	23	19	12	7	71
46	126	127	165	293	391	924	283
47	73	34	44	36	18	5	340
48	299	1609	267	185	188	416	106
49	103	117	195	187	176	500	312
50	22	35	52	72	53	45	238
51	105	116	92	76	81	103	4051
52	112	94	102	100	93	152	498
53	13	9	25	31	26	53	120
54	153	108	124	85	91	66	33
55	173	89	57	54	25	22	11
56	45	58	52	63	40	65	382
57	90	350	563	244	148	82	43
58	65	141	159	165	99	118	457
59	137	542	166	307	267	331	178
60	39	37	53	47	26	27	15
61	180	457	860	2272	108	87	460
62	219		2291	262	869	950	67
63	354	249	295	2234	2007	314	72
64	233	325	328	263	206	183	737
65	145	177	193	191	137	55	47
66	173	999	48	38	35	304	112

4.2 Effect of Concrete Mixture on Drying Shrinkage

Six variables were considered for this study, namely w/c, water content, maximum aggregate size, silica fume, GGBFS, and bulk volume of coarse aggregate. Their effects on drying shrinkage were examined. In order to isolate the parameters interaction effects as well as the effects of dominant parameters, a set of graphs exhibiting the relation between each variable and the shrinkage strain with the other variables being constant were explored.

The effects of GGBFS addition on shrinkage strain is shown in Figure 4.1. After 119 days, it is observed that increasing the replacement level of GGBFS enhances the shrinkage strain. These results are expected given GGBFS has lower specific gravity in comparison with OPC (ACI Committee 226, 1994). Moreover, these results concur with those reported by Chern and Chan (Omar et al., 2008).

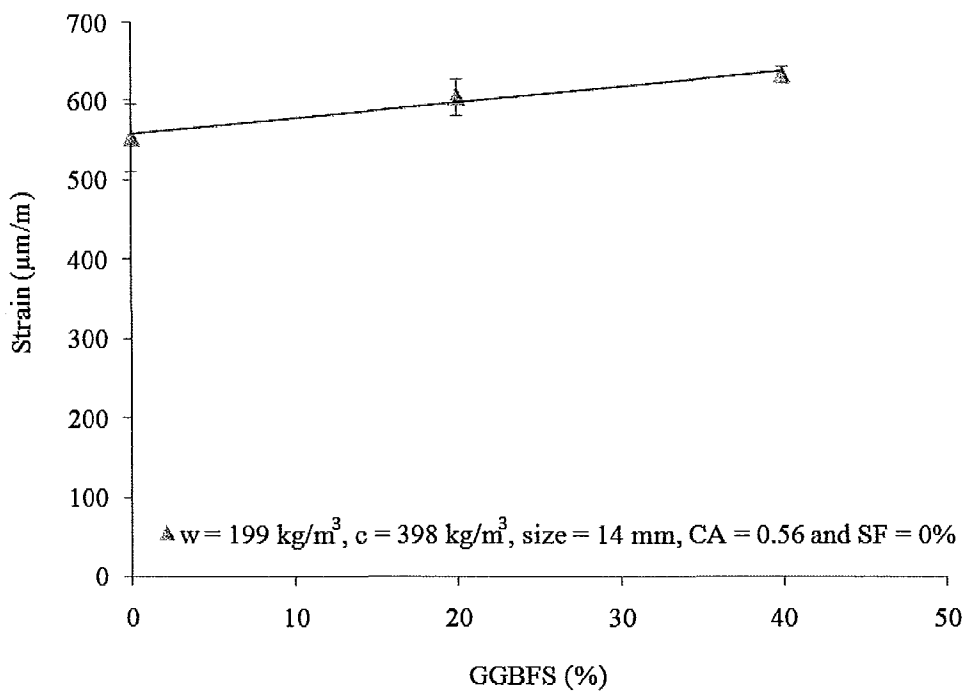


Figure 4.1 Effect of GGBFS addition on shrinkage at the age of 119 days

The combined effect of GGBFS and SF as cement replacement on shrinkage strain is shown in Figure 4.2. The measured shrinkage strains for these mixtures are high, where the

smallest value exceeds 450 $\mu\text{m}/\text{m}$. Comparing the strain of mixes with 0.4 w/c and 0.69 CA volume to those with 0.6 w/c and 0.57 CA volume, one observes that there are approximately the same despite the use of SF and GGBFS as cement replacement. Also comparing the strains of mixes with 0.4 w/c and 0.57 CA volume to those with 0.6 w/c and 0.57 CA volume, one observes that the latter has a higher value and that it decreases to the same level of the 0.6 w/c mixtures when the cement was partially replaced with SF and GGBFS. This shows that the addition of SF and GGBFS only to the mixtures with 0.4 w/c results in a reduction in shrinkage strains. Also, comparing the strains of mixes with 0.5 CA volume and 14 mm maximum CA size to those of 0.57 CA volume and 20 mm maximum CA size, one observes that replacing cement with SF and GGBFS has led to a decrease only to the latter mixtures. From these observations, it can be deduced that the effect of replacing cement with SF and GGBFS on shrinkage strains is minimal with the exception of the mixtures containing 0.4 w/c, 0.57 CA volume and 20 mm maximum CA size, where the values are found to decrease. Furthermore, comparing these results to those shown in Figure 4.1, one can deduce SF as cement replacement has different effect on shrinkage strains in comparison to GGBFS, where the former yields a decrease in strains and the latter an increase in the shrinkage strains. These results do concur with the results reported in the literature (Li and Yao, 2001; Haque, 1996).

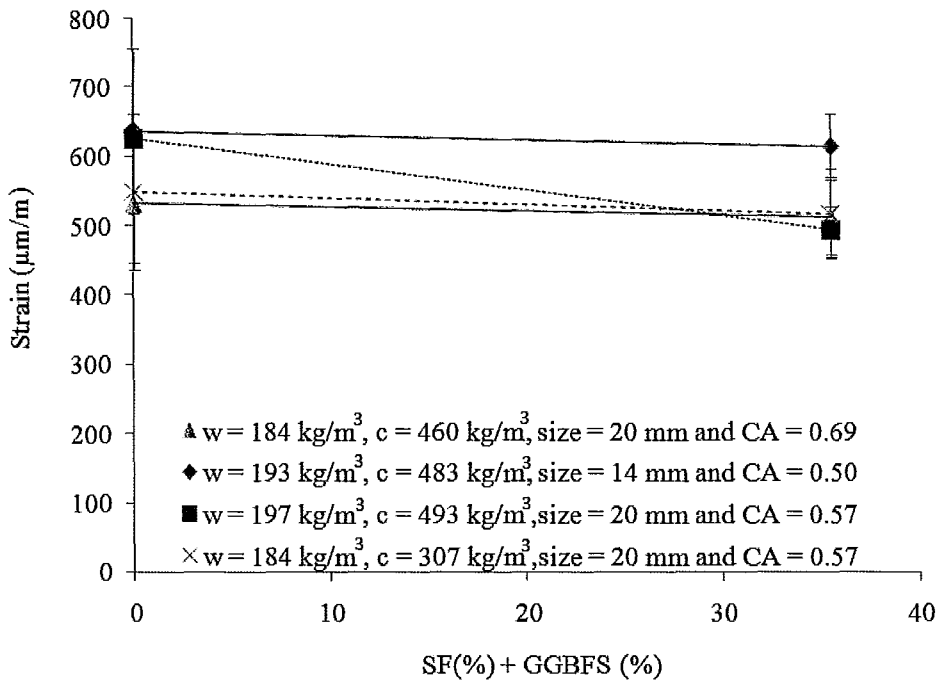


Figure 4.2 Effect of GGBFS and SF addition on shrinkage at the age of 119 days

The effects of the coarse aggregate volume on shrinkage strain are shown in Figure 4.3. The results indicate that increasing the amount of coarse aggregate volume leads to a decrease in shrinkage strain. This response agrees with the data reported in the literature (Omar et al., 2008).

Water reducing agent effects on shrinkage are shown in Figure 4.4. The results indicate that the addition of WRA results in a reduction in shrinkage. This finding is consistent with the literature where Polycarboxylate Ether (PCE) based WRA has been shown to reduce the shrinkage strain because PCE reduces the capillary pressure (Heirman et al., 2007).

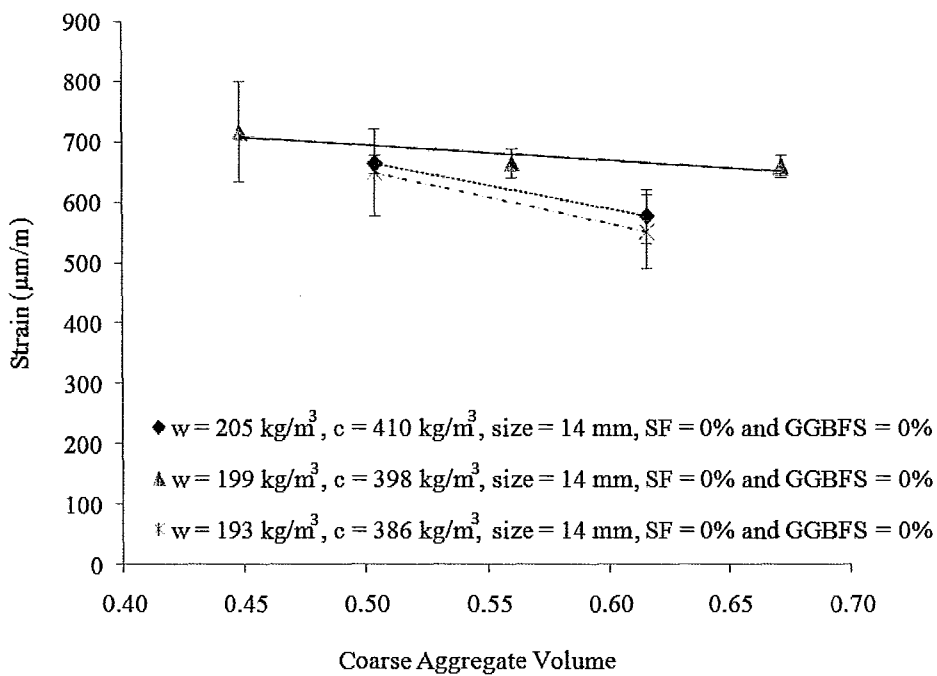


Figure 4.3 Effect of coarse aggregate volume on shrinkage at the age of 119 days

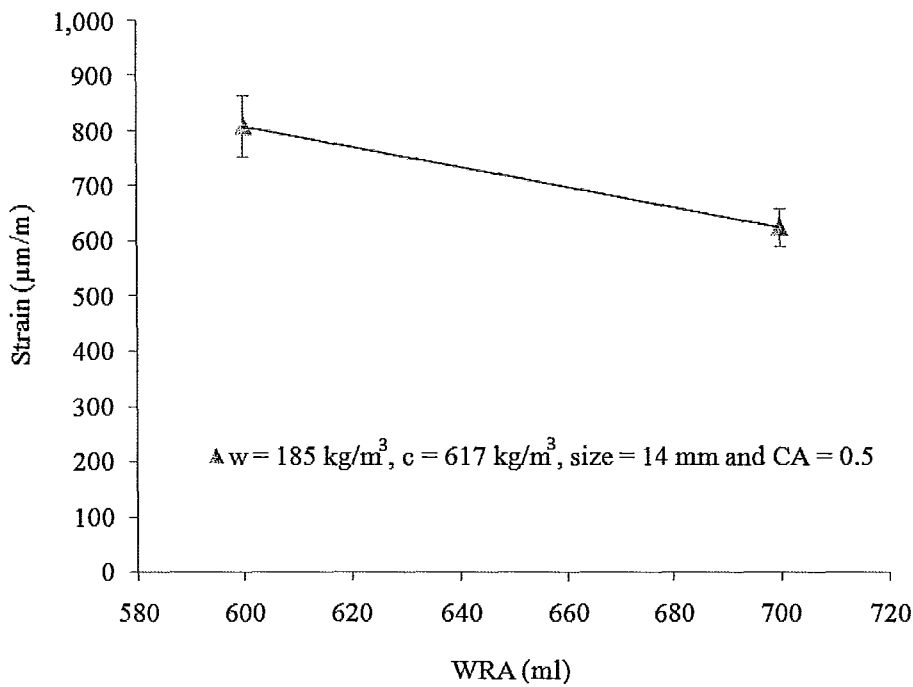


Figure 4.4 Effect of water reducing agent on shrinkage at the age of 119 days

The results collectively show that replacing cement with GGBFS has led to an increase in shrinkage strains. However, replacing cement with SF yielded opposite results, i.e. a reduction in shrinkage strains. Increase in the coarse aggregate maximum size, the coarse aggregate volume or the amount of WRA has resulted in a decrease in shrinkage strains. The results have also shown that an increase in the cement content or w/c has resulted in an increase in shrinkage strains. All these trends are consistent with the data reported in the literature (Omar et al., 2008).

4.3 Autogenous Shrinkage

Measurements of the early age autogenous shrinkage strains are analysed in term of their relation with time, temperature, and capillary pressure. The concrete mixtures used to study autogenous shrinkage strain are divided into three groups corresponding to their w/c, namely 0.3, 0.4 and greater than or equal to 0.5. This grouping is intended to isolate the effects of w/c from the other parameters, since w/c is the dominant factor affecting autogenous shrinkage (Tazawa et al., 1999; Holt, 2001). Tables 4.5 to 4.7 show the mix design studied corresponding to three groups.

Table 4.5 Group I - Concrete mixtures with w/c = 0.3

Mix #	w kg/m ³	size mm	CA	WRA ml	VEA ml	Cementitious kg/m ³
50	185	14	0.50	800	400	617
61	185	14	0.50	700	300	617
64	180	14	0.50	600	300	600
66	185	14	0.50	600	300	617

Table 4.6 Group II - Concrete mixtures with w/c = 0.4

Mix #	w kg/m ³	size mm	SF %	GGBFS %	CA	WRA ml	VEA ml	AEA ml	Cementitious kg/m ³
33	197	20	5.6	30	0.57	-	-	35	493
39	197	20	0.0	0	0.57	-	-	35	493
44	193	14	0.0	0	0.50	-	-	35	483
53	185	14	0.0	0	0.50	700	400	0	463
56	185	14	0.0	0	0.50	500	300	0	463

Table 4.7 Group III - Concrete mixtures with w/c = 0.5 and w/c = 0.6

Mix #	w/c	w kg/m ³	size mm	SF %	GGBFS %	CA	Cementitious kg/m ³
36	0.6	197	20	5.6	30	0.69	328
42	0.6	193	14	0.0	0	0.62	322
55	0.5	193	14	0.0	0	0.50	386

Going through the results of the mixes #44 and #55 in Figures 4.5 to 4.7 and comparing them to the data in Tables 4.6 and 4.7, one can notice that the temperature increases as the amount of cementitious materials in the mixtures increases. However, given that the w/c for mixes #44 and #55 is 0.4 and 0.5, respectively, the autogenous shrinkage strain and capillary pressure for both mixes are very similar after 20 h. For mix #44, one observes an increase in autogenous shrinkage for the first 5 hours followed by swelling. The same pattern is observed for the capillary pressure. Mix #55, whose w/c is 0.5, is found to only experience swelling.

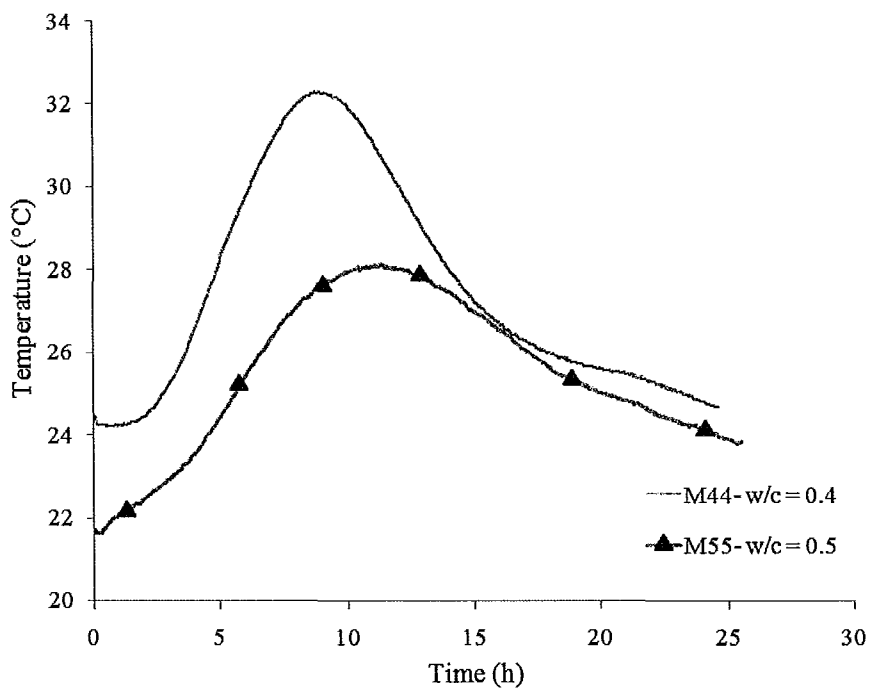


Figure 4.5 Temperature versus time for mixes #44 and #55

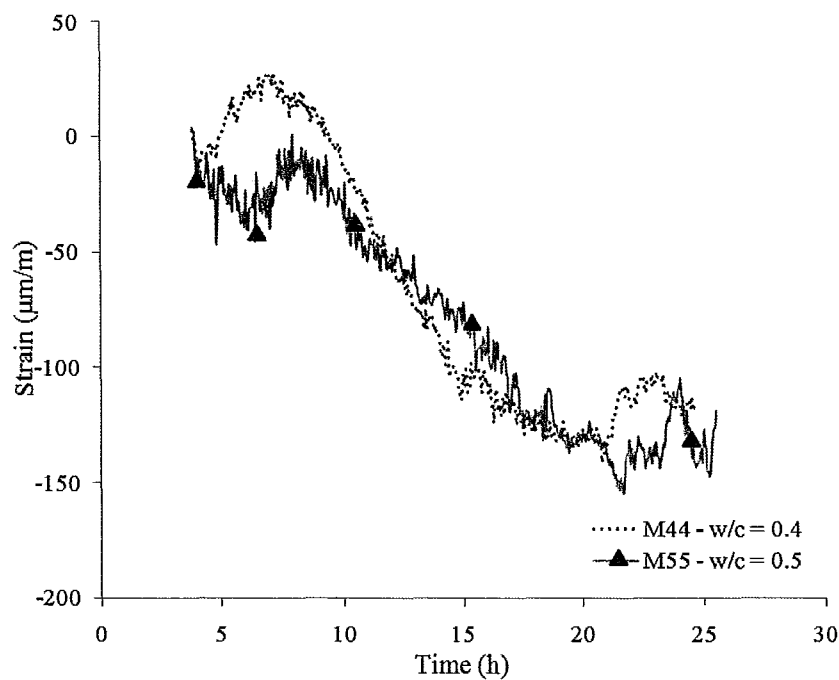


Figure 4.6 Autogenous shrinkage strain versus time for mixes #44 and #55

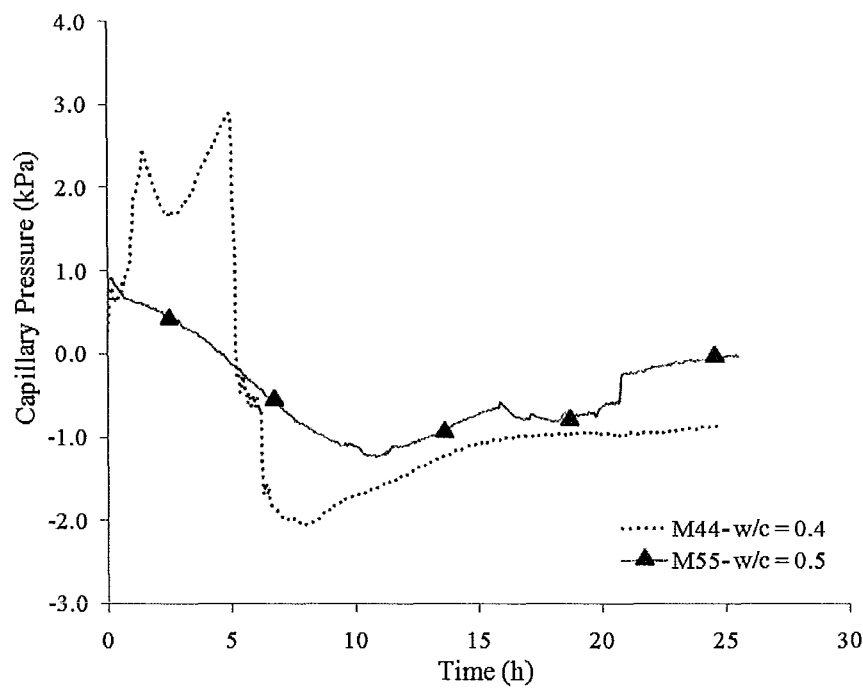


Figure 4.7 Capillary pressure versus time for mixes #44 and #55

Comparing mixes #61 and #66 in Table 4.5 with Figures 4.8 to 4.10; one observes that a small increase in the amount of water reducing agent has led to a decrease in autogenous shrinkage strain, temperature and capillary pressure. Although water reducing agent formulated using Polycarboxylate Ether (PCE), similar to the one used in this experimental program, tends to decrease autogenous shrinkage (Heirman et al., 2007), the observed results reveal a larger than expected difference in the magnitude of autogenous shrinkage strain and pressure for the two mixes. Figure 4.9 and Figure 4.10 show the same trend for the autogenous shrinkage and capillary pressure, respectively. A difference of approximately 300 $\mu\text{m}/\text{m}$ is recorded after 20 h. This difference cannot be attributed solely to WRA but perhaps could be due to chemical interaction between WRA and VEA.

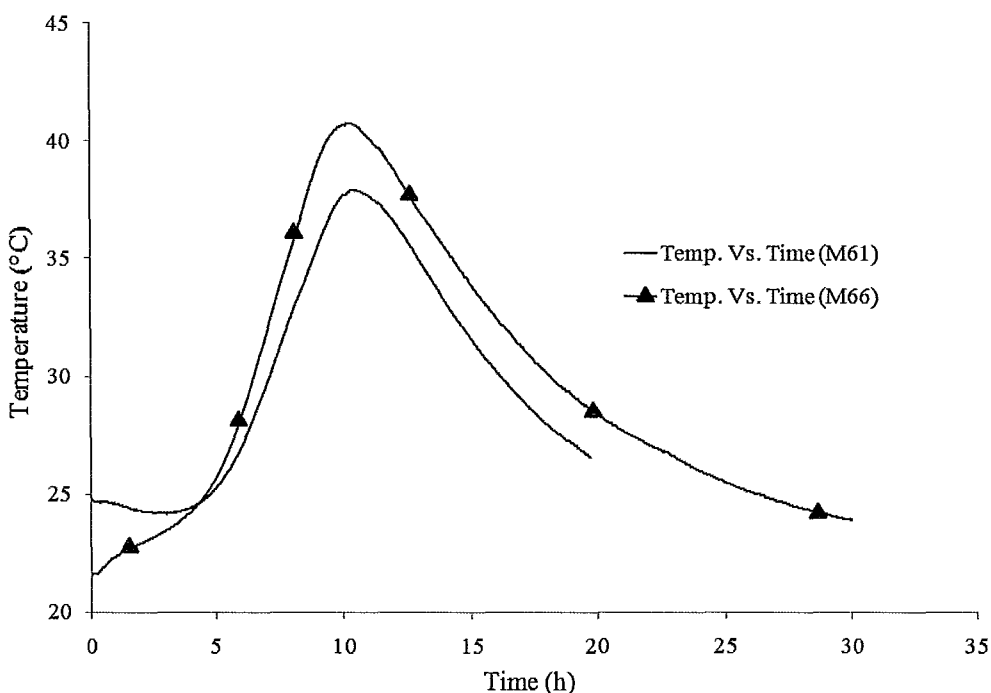


Figure 4.8 Temperature versus time for mixes #61 and #66

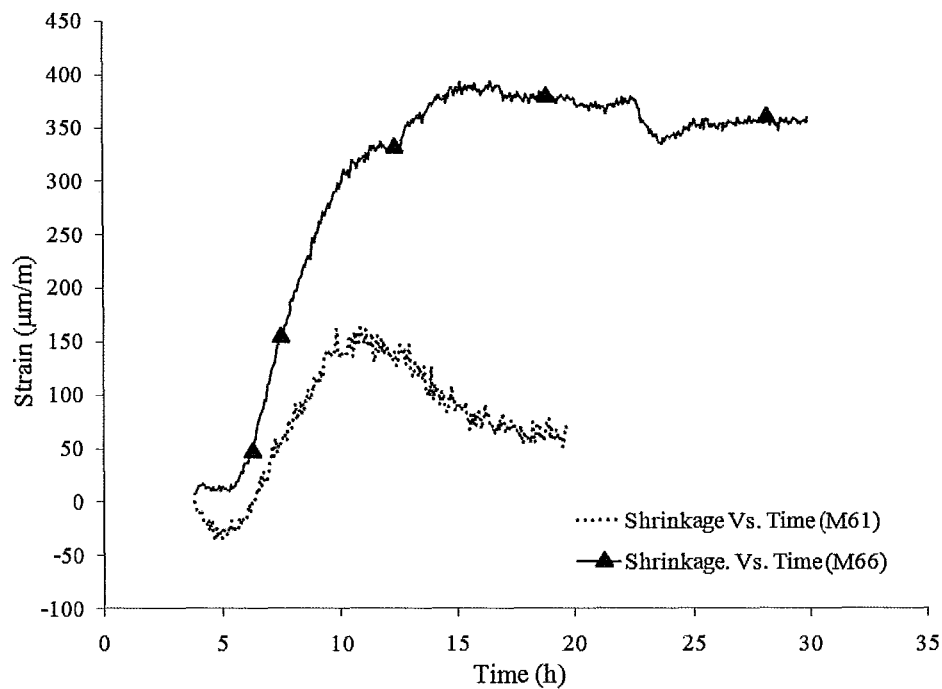


Figure 4.9 Autogenous shrinkage strain versus time for mixes #61 and #66

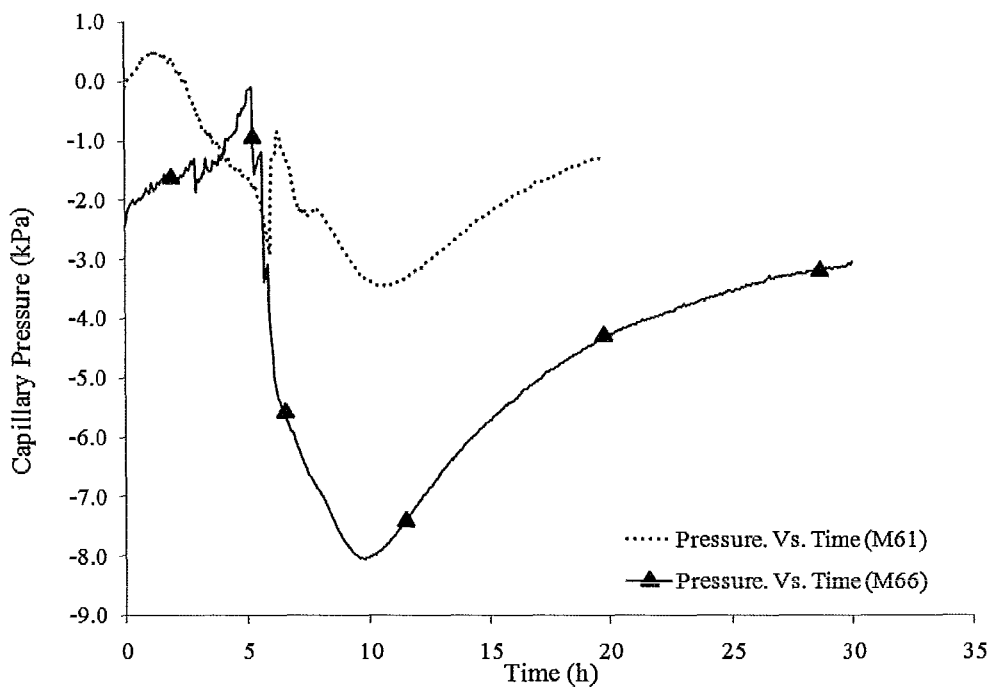


Figure 4.10 Capillary pressure versus time for mixes #61 and #66

Figure 4.11 to Figure 4.13 show the effect of increasing the amount of WRA and VEA on temperature, autogenous strains and capillary pressure. The addition of these admixtures has resulted in a significant increase in the peak temperature and autogenous shrinkage. Although difference in the autogenous shrinkage between the two mixes is expected, the measured values and trend reveal a greater influence than previously reported. The behaviour can be again attributed to the chemical interaction that is negatively impacting the strains when the amount of these chemical admixtures is increased. Further investigation is warranted for mixes listed in Group I as some of the recorded measurements are not easily explained.

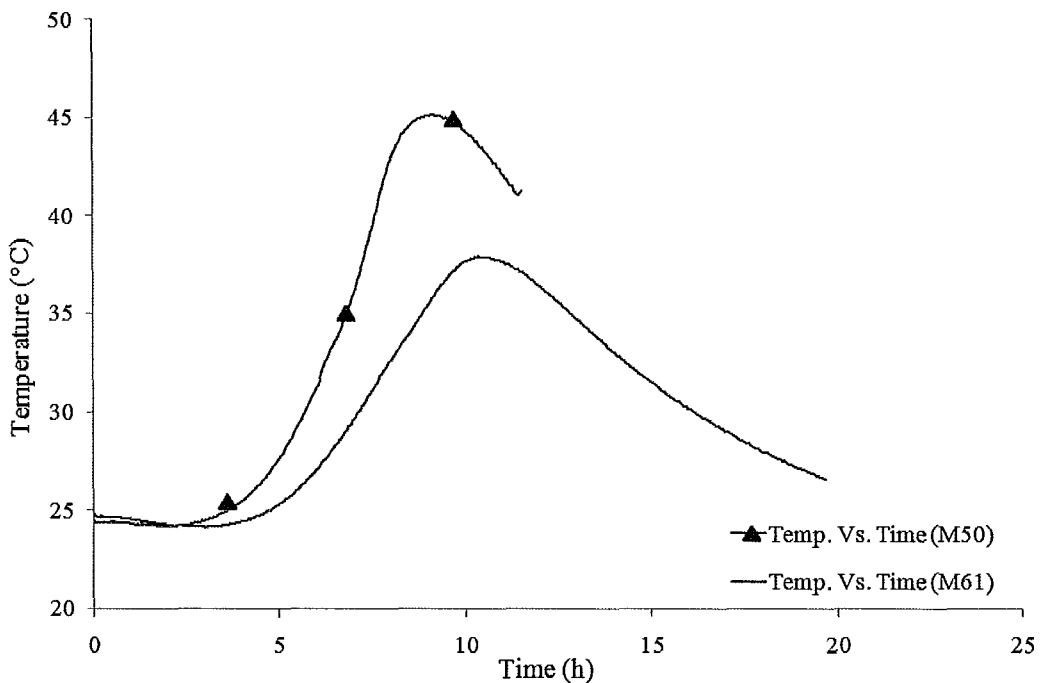


Figure 4.11 Temperature versus time for mixes #50 and #61

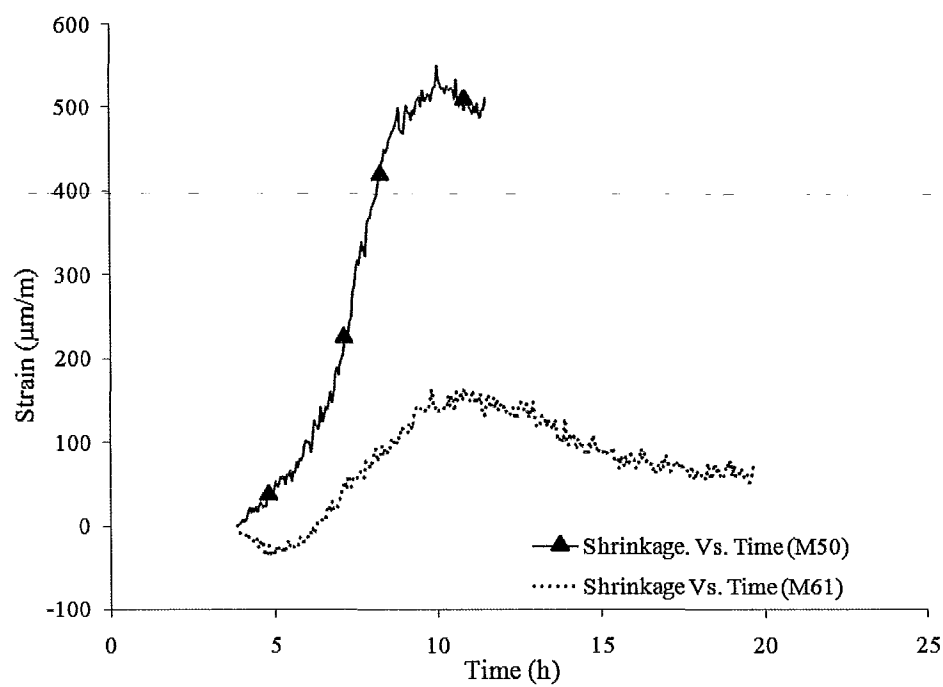


Figure 4.12 Autogenous shrinkage strain versus time for mixes #50 and #61

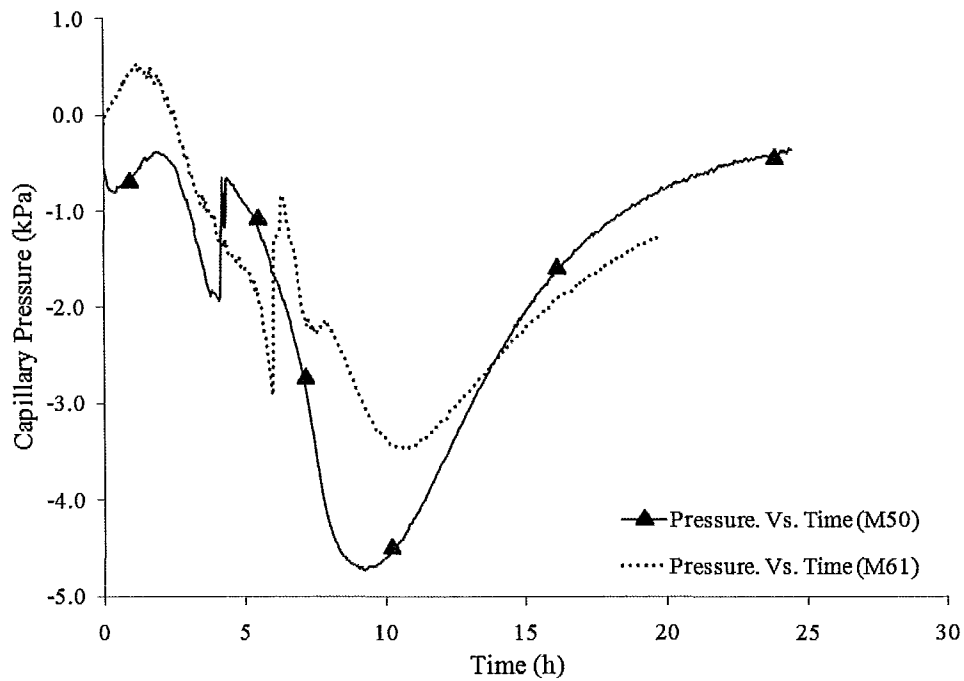


Figure 4.13 Capillary pressure versus time for mixes #50 and #61

By comparing mixtures proportions of mixes #53 and #61 in Tables 4.5 and 4.6 and the corresponding results in Figures 4.14 to 4.16, it can be observed that increasing the amount of cementitious material by 25% in mix #61 yielded higher temperature. According to the literature, the autogenous shrinkage strain and capillary pressure values must be much higher for mix #61 in comparison to mix #53. The results do show that an increase in VEA content to 400 ml is triggering a considerable increase in autogenous shrinkage strains to the point that they exceeded those recorded for mix #61 by 100% after 15 h. The measured capillary pressure, however, does not yield the same increase for mix #53. These results confirm previous observations that increasing VEA to 400 ml is resulting in a substantial increase in autogenous shrinkage even for 0.4 w/c mixtures. This phenomenon has dwarfed the effects of cement paste content and w/c.

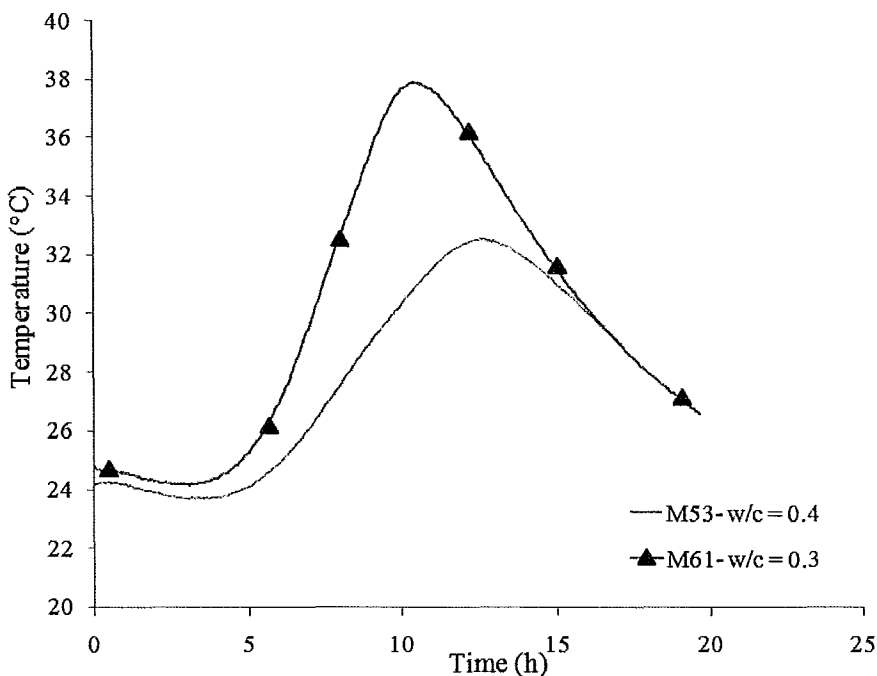


Figure 4.14 Temperature versus time for mixes #53 and #61

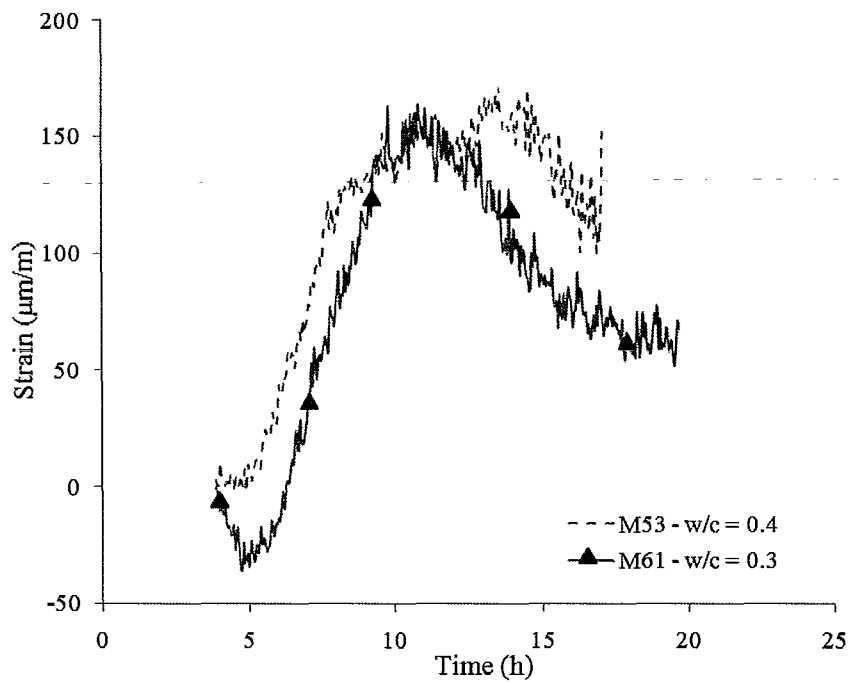


Figure 4.15 Autogenous shrinkage strain versus time for mixes #53 and #61

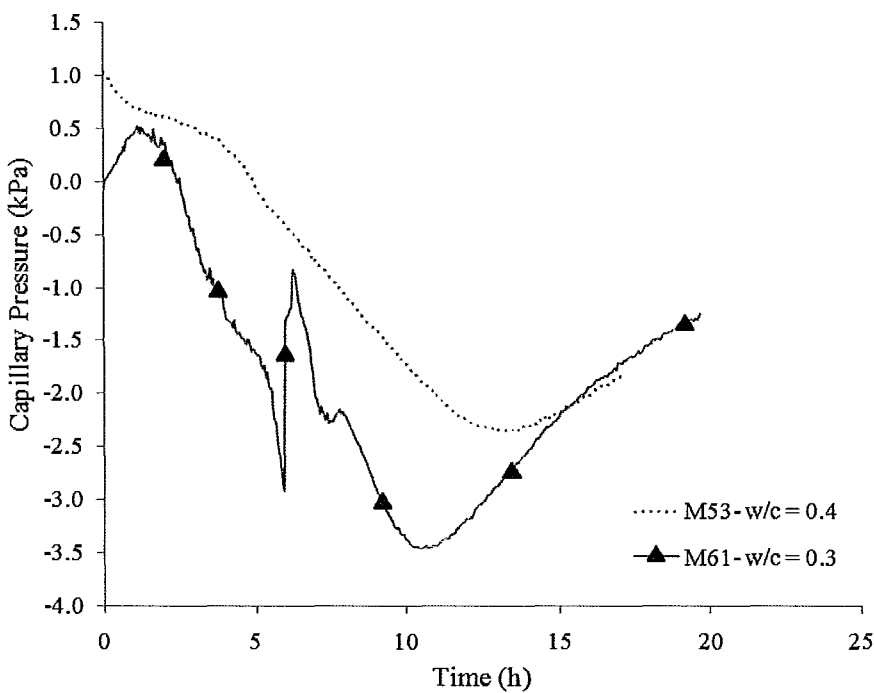


Figure 4.16 Capillary pressure versus time for mixes #53 and #61

By investigating mixes #39 and #44 proportions in Table 4.6 and the corresponding results in Figures 4.17 to 4.19, couple observations can be made. The small increase in cement content has led to an increase in peak temperature. Both mixes have a 0.4 w/c and experience shrinkage for the first 5 h to 15 hours. After 24 hours, mix #39 is found to experience relatively zero shrinkage and mix #44 swelling. The effect of coarse aggregate volume on autogenous strains, which according to the literature should reduce strains, is not apparent. The relation between strains and capillary pressure continues to follow the same trend.

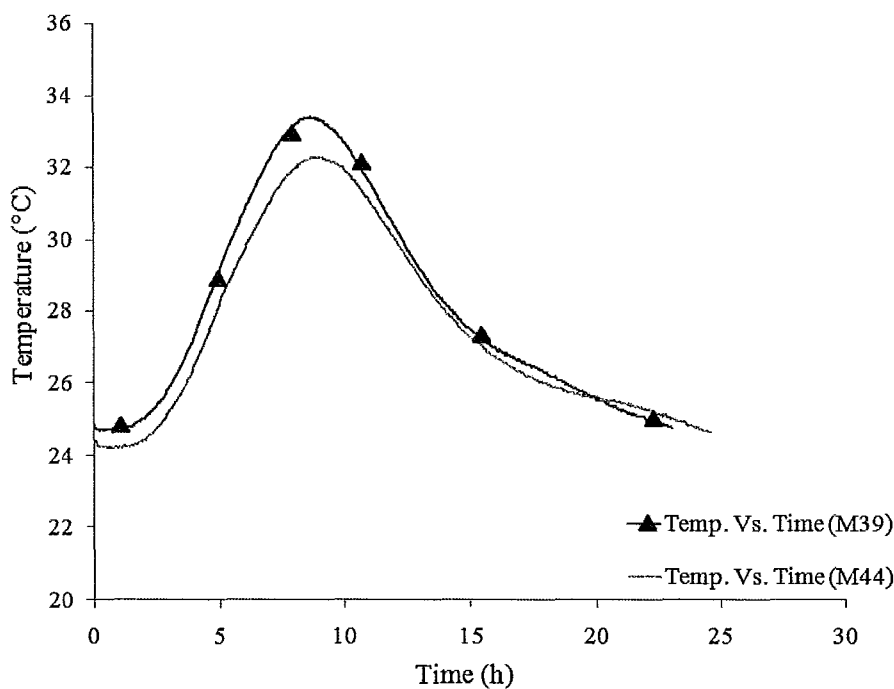


Figure 4.17 Temperature versus time for mixes #39 and #44

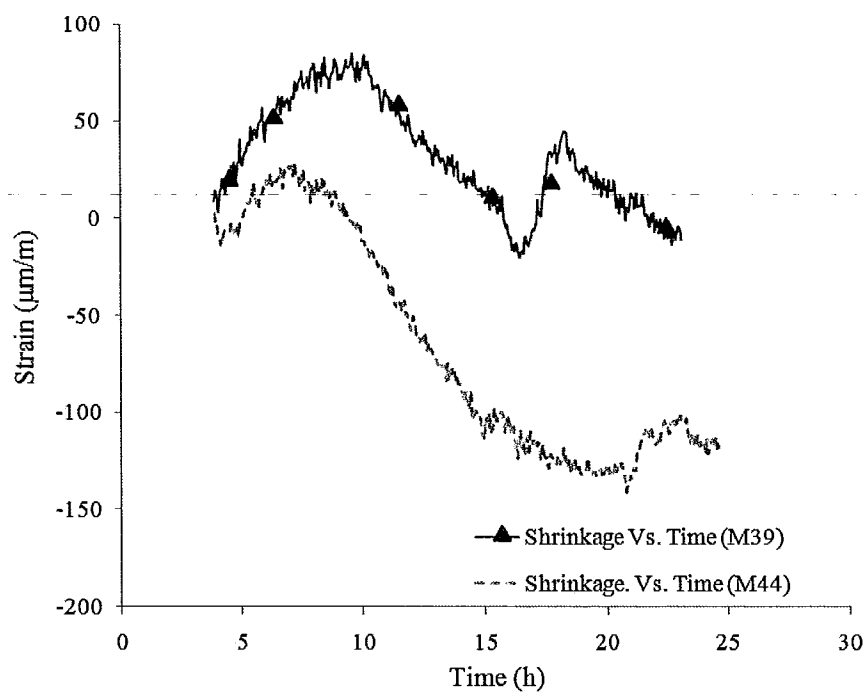


Figure 4.18 Autogenous shrinkage strain versus time for mixes #39 and #44

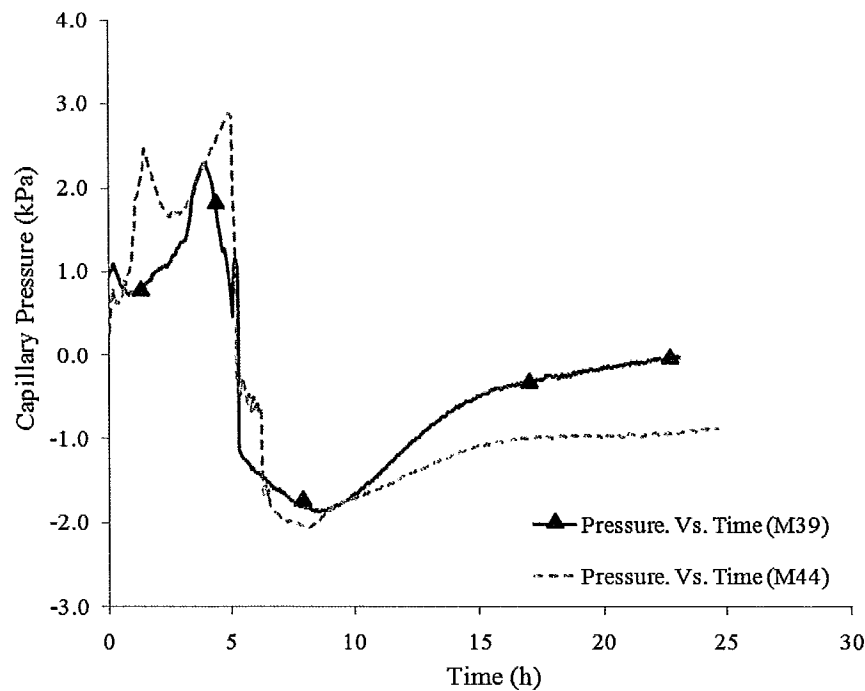


Figure 4.19 Capillary pressure versus time for mixes #39 and #44

Investigating mixes #64 and #66 grouped in Table 4.5 and whose results are shown in Figures 4.20 to 4.22, it can be stated that by increasing the amount of cementitious material, autogenous shrinkage strain, temperature and capillary pressure are found to increase. Although both mixtures have identical composition including their w/c, an increase in the cement content which implies an increase in the cement paste has led to a significant increase in autogenous shrinkage at 30 h. This is consistent with the literature.

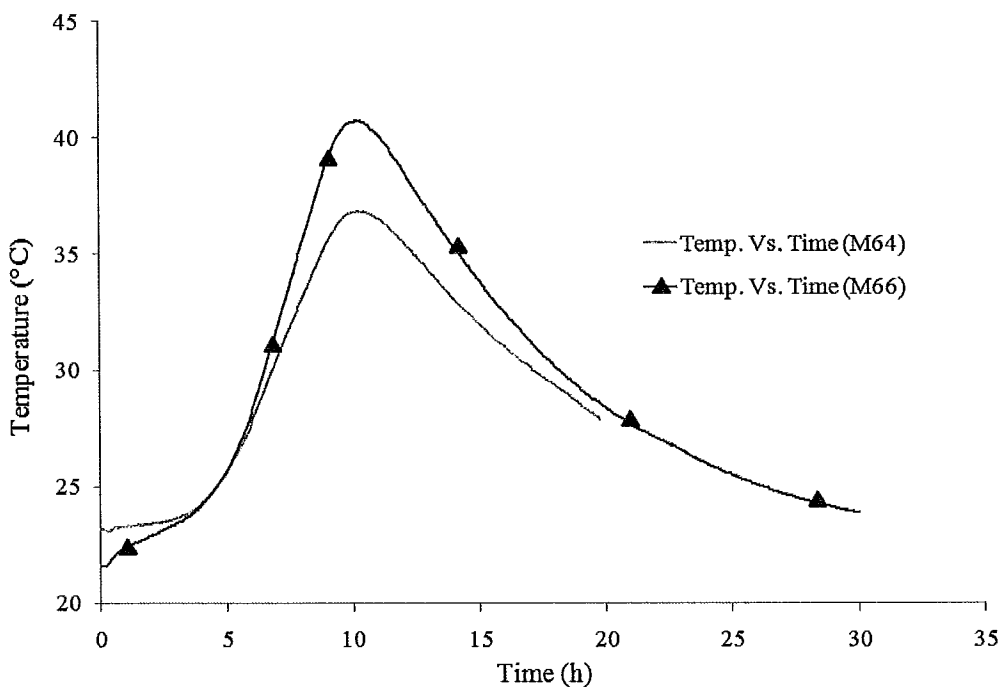


Figure 4.20 Temperature versus time for mixes #64 and #66

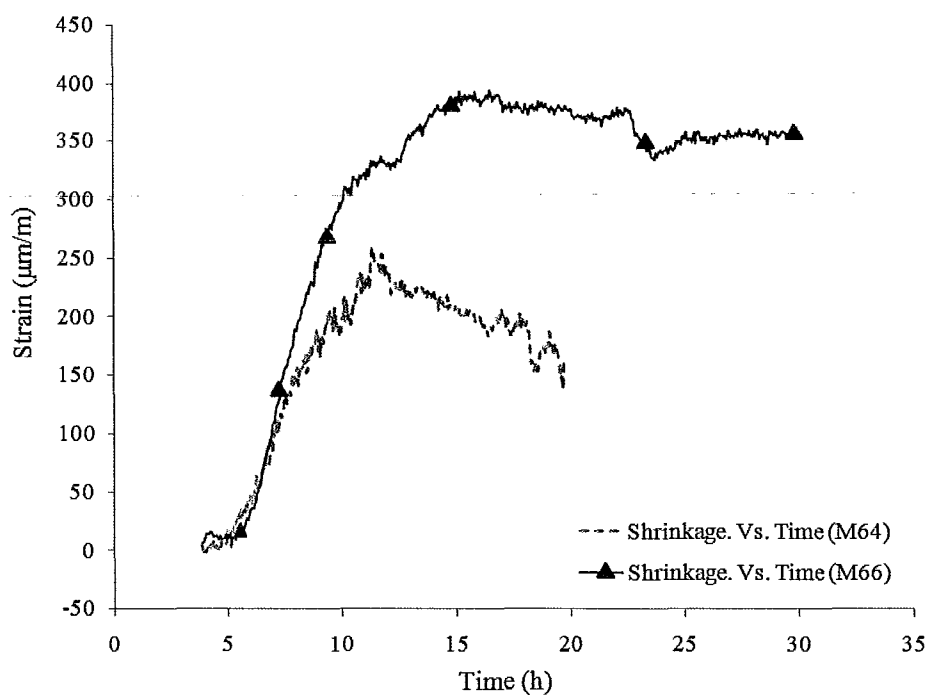


Figure 4.21 Autogenous shrinkage strain versus time for mixes #64 and #66

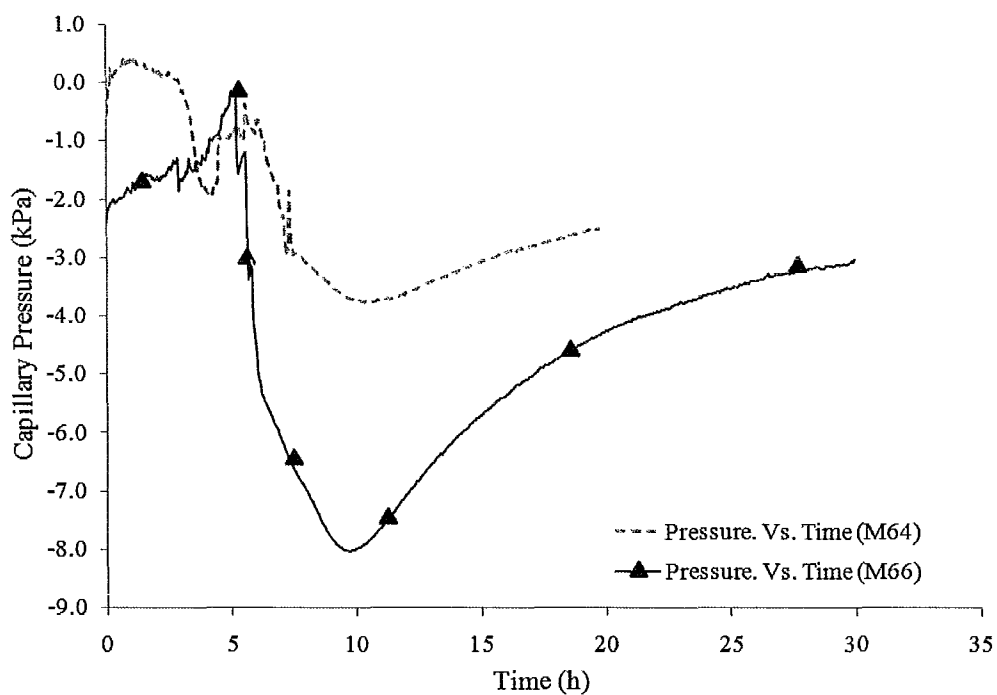


Figure 4.22 Capillary pressure versus time for mixes #64 and #66

In brief, the results from the autogenous shrinkage strain experiment indicate that the test set up developed was adequate for the intended purpose. The results confirmed that a decrease in w/c and an increase in cement paste content yield an increase in autogenous strains. The results have also revealed that mixing different types of chemical admixtures and their amount can negatively and significantly influence the magnitude of autogenous shrinkage strain. The effect of coarse aggregate volume on autogenous strain was either negligible or most likely dwarfed by other effects. Mixtures whose w/c is 0.5 or greater are found to experience swelling instead of shrinkage after 24 hours with the exception of those mixtures that contain large amount of WRA and VEA.

4.4 Effect of Curing Conditions and Shrinkage Strain on Compressive Strength of Concrete

The compressive strength of air cured and moist cured cylinders were tested at the age of 119 days. A plot of compressive strengths, shown in Figure 4.23, reveals that the compressive strengths of air cured cylinders were on average 10% lower than those of moist cured. These results indicate that the effect of curing on the concrete compressive strength is less than 10% provided the concrete is adequately cured for the first 24 hours. These results also indicate that the corresponding shrinkage has minimal effects on the compressive strength. These results support the current practice, i.e., drying shrinkage has negligible effect on the compressive strength of concrete.

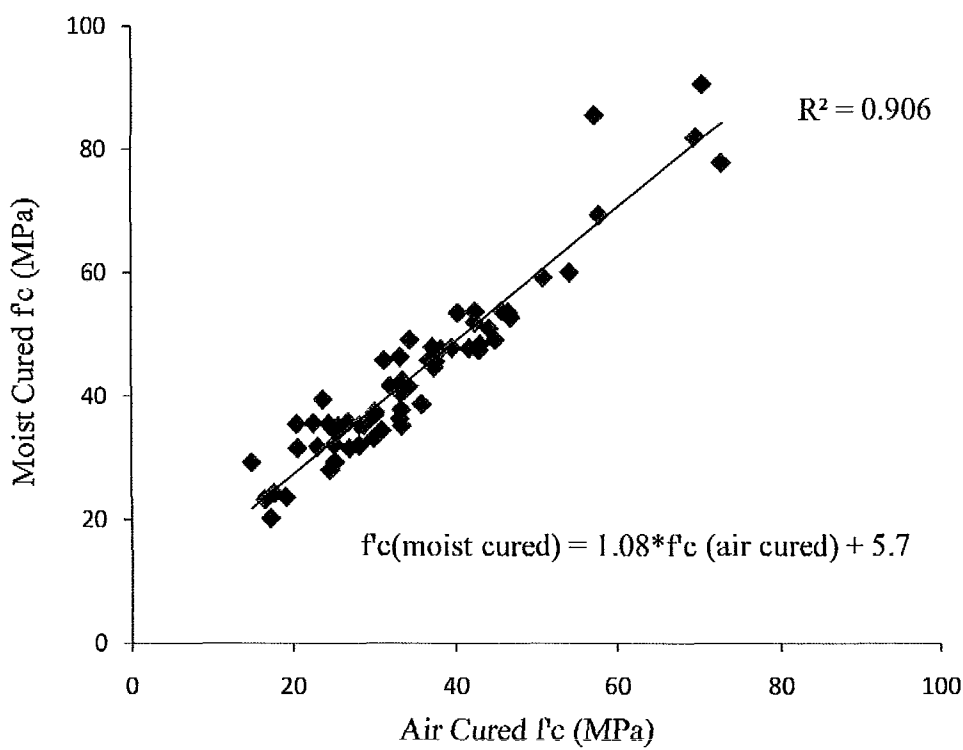


Figure 4.23 Concrete compressive strength of moist cured versus air cured cylinders

4.5 Statistical Analysis

4.5.1 Complete shrinkage regression models

Statistical analyses were carried out to determine the significance of the parameters studied, namely, w/c, w, size, SF, GGBFS, and CA. To meet this objective, models were developed by considering the effects of main parameters and the interaction of two and three variables, as well as incorporating non-linear relations such as square, exponential, and logarithmic functions. The best fit models for shrinkage strains at each age were selected based on high correlation of coefficients and low covariance indicator (Montgomery and Runger, 2003). The parameters, which are considered to have significant effect on the response, were those having a confidence interval excluding zero with a probability of more than 90% or 95%.

Table 4.8 identifies the parameters that are deemed to be significant with either a 90% confidence level or 95% confidence level, along with the corresponding coefficients at different concrete ages. By examining Tables 4.8 and 4.9, the following observations can be drawn. For both 90% and 95% confidence levels, 10 parameters are found to be statistically significant for at least 4 of the 6 recorded measurements for shrinkage, namely CA, w/c^2 , CA^2 , $w/c*SF$, $w/c*GGBFS$, $size*SF$, $size*CA$, $w/c*w*size$, $w/c*SF *GGBFS$, and $w/c*SF*CA$. These results indicate that the parameters w/c, CA, size, and the addition of mineral mixtures are the predominant. These observations are consistent with what has been reported in the literature. Closer examination shows that an increase in w/c, SF and GGBFS content results in an increase in shrinkage strain; however, an increase in CA volume and size result in a decrease in shrinkage strain. These results conform to the data reported in the literature. An interesting finding is the three level interactions between w/c, CA, and SF. The results indicate that the interaction between w/c, SF and GGBFS leads to an increase in shrinkage, whereas the interaction between w/c, SF and CA results in a decrease in shrinkage strain. Moreover, these results show the complex and non-linear interactions between the concrete mixtures and shrinkage strain. These results, which conform to the findings in the literature, add to the confidence level for using the regression model.

Table 4.8 Regression models for total shrinkage strain

Parameters	90% Confidence Level						95% Confidence Level					
	Time (days)						Time (days)					
	3	7	14	28	56	119	3	7	14	28	56	119
Constant	44	111	175	282	362	539	44	113	175	284	377	548
w/c	-44					-26		-52				
w				-18	-27							-29
size				-12	-34	-34						-31 -28
SF			15	22		-15			15	21		
CA	-16	-19	-54	-52	-63	-82	-16	-19	-54	-68	-63	-80
w/c*SF	36	21	28	37	18		36	18	28	35		
w/c*GGBFS	30	13	30	22	27		30		30	24	25	
w*size			-25	-16					-25			
w*CA						-62						-61
size*SF		-10	-13	-15	-17	-15		-10	-13	-13	-15	
size*CA		-26	-63	-37	-58	-97		-26	-63	-55	-59	-94
SF *GGBFS	13		-20		-22		13		-20		-22	
SF *CA	-18						-18					
w/c ²	46	37	78	38	27		46	31	78	33		
CA ²		42	117	58	99	135		43	117	79	92	129
w/c*w*size			-34	-51	-47	-61			-34	-41	-40	-51
w/c*w*SF	-23	-23					-23	-23				
w/c*w*GGBFS	-21						-21					
w/c*size*GGBFS					18	22						
w/c*SF *GGBFS	34	30	36	28			34	26	36	28		
w/c*SF *CA	-29	-34	-39	-36	-33		-29	-34	-39	-33		
w/c*size*CA				-22	-34				-25	-53		

The evaluation of the regression models can be seen in Table 4.9. The covariance values, which are a gauge of the model efficacy, are larger for the 90% confidence level than for the 95% confidence level. The correlation values are however found to be lower for the 95% in comparison to the 90% confidence interval. This implies that adding more parameters to the model results in a better fit to the data due to the added flexibility. However, it does not mean that the predictions are better for future estimations or measurements. Of interest is the drop in correlation with the age of concrete for the 90% confidence level model with a

corresponding drop in the covariance. The same observations do apply to the 95% confidence interval model.

Table 4.9a Statistical indicators for total shrinkage strain with 90% confidence level

Statistical Indicators	90% Confidence Level					
	Time (Days)					
	3	7	14	28	56	119
Correlation (R^2)	0.90	0.94	0.92	0.92	0.88	0.86
Standard Covariance	22.0	24.1	21.2	10.9	9.5	9.4

Table 4.9b Statistical indicators for total shrinkage strain with 95% confidence level

Statistical Indicators	95% Confidence Level					
	Time (Days)					
	3	7	14	28	56	119
Correlation (R^2)	0.90	0.94	0.92	0.89	0.82	0.80
Standard Covariance	22.0	23.1	21.2	9.3	7.2	7.3

Shrinkage regression models $\epsilon(\mu\text{m}/\text{m})$ for the 90% confidence level can be expressed using the data in Table 4.8. For the 28 days, the expression is as follows:

$$\begin{aligned} \epsilon(28 \text{ days}) = & 282 - 18 * w - 12 * \text{size} + 22 * \text{SF} - 52 * \text{CA} + 37 * \frac{w}{c} * \text{SF} + 22 * \frac{w}{c} \\ & * \text{GGBFS} - 16 * w * \text{size} - 15 * \text{size} * \text{SF} - 37 * \text{size} * \text{CA} + 38 * \left(\frac{w}{c}\right)^2 \\ & + 58 * \text{CA}^2 - 51 * \frac{w}{c} * w * \text{size} + 28 * \frac{w}{c} * \text{SF} * \text{GGBFS} - 36 * \frac{w}{c} * \text{SF} \\ & * \text{CA} - 22 * \frac{w}{c} * \text{size} * \text{CA} \end{aligned} \quad (4.1)$$

4.5.2 Shrinkage regression models excluding variables interaction

To study the effects of variables interaction on the models predictions, the 95% regression model was derived for the 28 days and accounting only for the six main variables, i.e. interactions between variables were not considered. This model is assessed in Chapter 5 with particular attention to the scattering of data. The regression model $\epsilon'(\mu\text{m}/\text{m})$ is represented by Eq. 4.2 and is found to have a correlation factor of 0.66 and standard

covariance equal to 3.98. These results indicate that modeling shrinkage strain without considering the interaction of the different variables is not sufficient in capturing all the effects.

$$\varepsilon'(28 \text{ days}) = 297 - 32 * \frac{W}{C} + 20 * SF - 33 * CA \quad (4.2)$$

4.5.3 Complete shrinkage regression including chemical admixtures

The statistical analysis were repeated to account for the six main variables (w/c, w, size, SF, GGBFS and CA), their interaction, and the effects of chemical admixtures, namely water reducing agent (WRA), viscosity enhancing agent (VEA) and air entraining agent (AEA). The corresponding 95% regression model $\varepsilon''(\mu\text{m}/\text{m})$ is represented in Eq. 4.3 and is found to have has a correlation factor of 0.80 and standard covariance equal to 8.47.

$$\begin{aligned} \varepsilon''(28 \text{ days}) = & 237 - 47 * \frac{W}{C} - 65 * CA - 69 * WRA - 24 * AEA + 33 * \frac{W}{C} * SF - 42 \\ & * size * CA - 20 * SF * GGBFS + 56 * \left(\frac{W}{C}\right)^2 + 72 * CA^2 - 52 * \frac{W}{C} * SF \\ & * CA \end{aligned} \quad (4.3)$$

Through Eq. 4.3, one can deduce that the addition of water reducing agent and air entraining agent to the mixtures reduces shrinkage strain, whereas the viscosity enhancing agent is not statistically significant. The water reducing agent “Glenium 7500” used in the experimental program is based on the polycarboxylate technology (BASF, 2007b). The polycarboxylate reduces the surface tension and reduces therefore the drying shrinkage. It shall be noted that many of the shrinkage reducing agent are based on the polycarboxylate products - Rheoplus 800S (BASF, 2008). Air entraining agent causes the expansion of air pores (Kronlöf et al., 1995), which leads to a decrease in shrinkage strain. Therefore the findings in Eq. 4.3 agree with the literature.

Chapter 5

Evaluation of Concrete Shrinkage Strain Prediction Models

5.0 Introduction

A review of the literature reveals that there are seven models that codes and standards in North America, Japan, and Europe have adopted for estimating shrinkage strains in concrete. These models are: ACI - 209 (Bhal and Jain, 1996), JSCE 2002 (Sakata and Shimomura, 2004), B3 (Hui Kiang, 2006), CEB-FIP 1990 (Omar et al., 2008), EHE (Gómez and Landsberger, 2007), GL 2000 (Gardner and Lockman, 2001), and Eurocode 2 (Omar et al., 2008). The predictive capacities of these models are evaluated in this chapter using data gathered from the experimental program. These predictive models are evaluated statistically by examining the following statistical indicators: residual squared, error percentage, and coefficient of variation.

5.1 Shrinkage Strain Predictions Models

Concrete shrinkage models are intended to provide an estimate of shrinkage strain. The predicted values according to the seven models and the two regression models versus the mean measured strains plus and minus standard deviation are displayed in Figures 5.1 to 5.5 for the concrete at the ages of 3 days, 14 days, 28 days, 56 days, and 119 days, respectively.

Results of Figures 5.1 show that none of the prediction models with the exception of the current regression models were able to reasonable estimate the shrinkage strain in concrete 3 days after placement. These results were expected as these predictive models are intended to estimate the long term shrinkage in concrete. The regression models, developed specifically from the experimental data, do provide a good estimate of shrinkage strain when the concrete is still young.

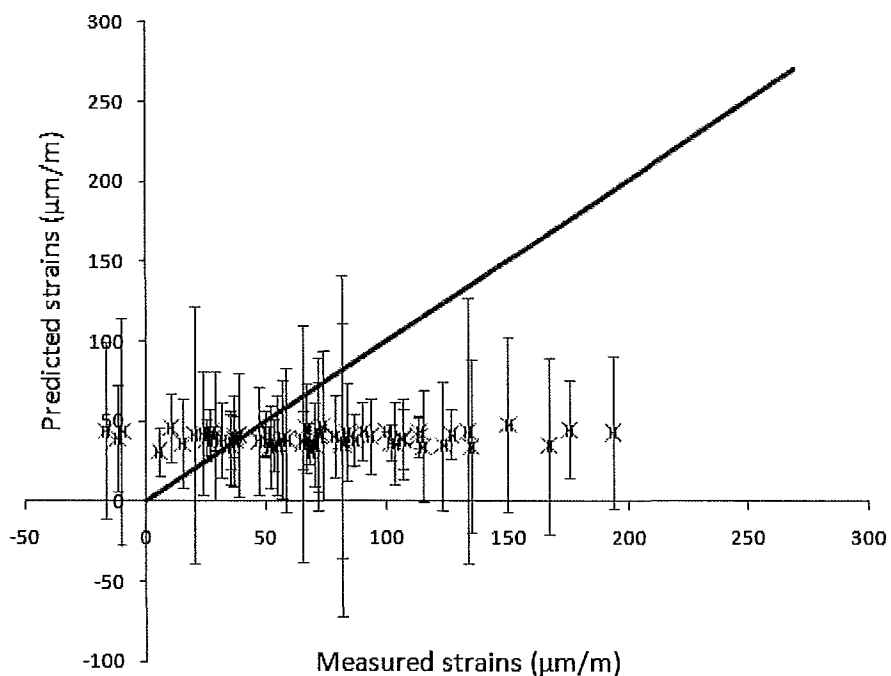


Figure 5.1a ACI - 209 Model – Predictions of shrinkage strains versus measured values for 3 days concrete

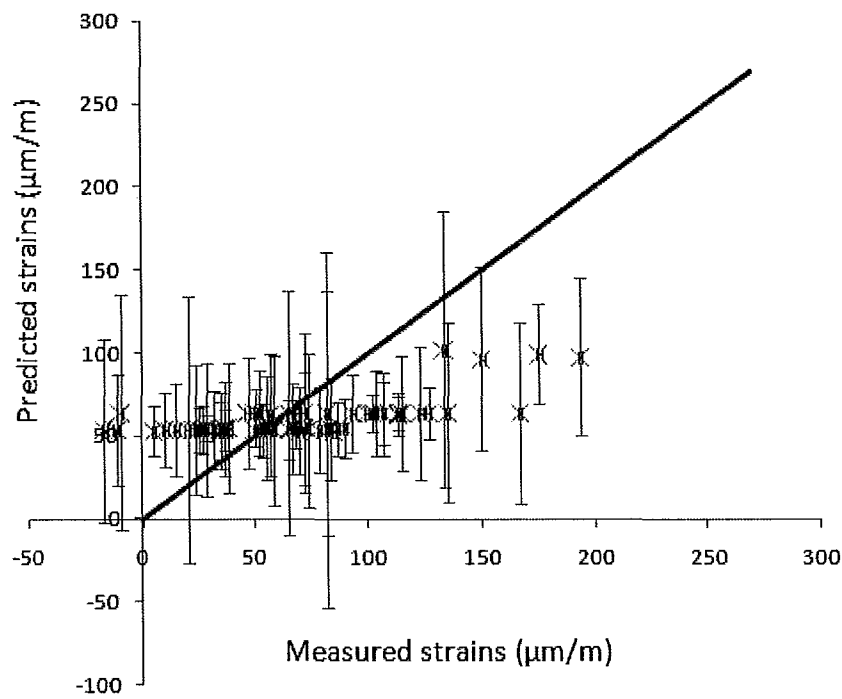


Figure 5.1b JSCE 2002 Model – Predictions of shrinkage strains versus measured values for 3 days concrete

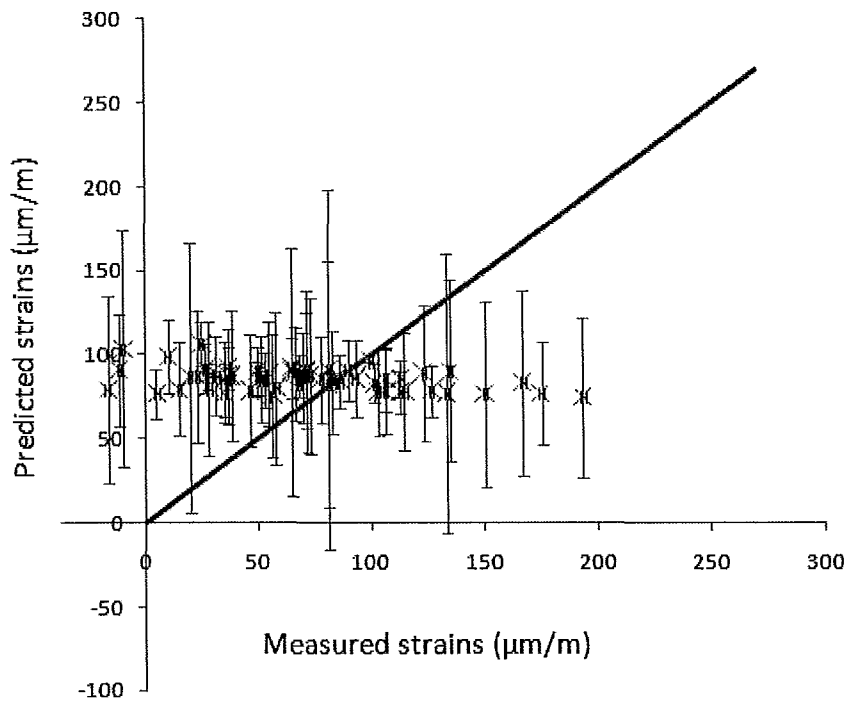


Figure 5.1c B3 Model – Predictions of shrinkage strains versus measured values for 3 days concrete

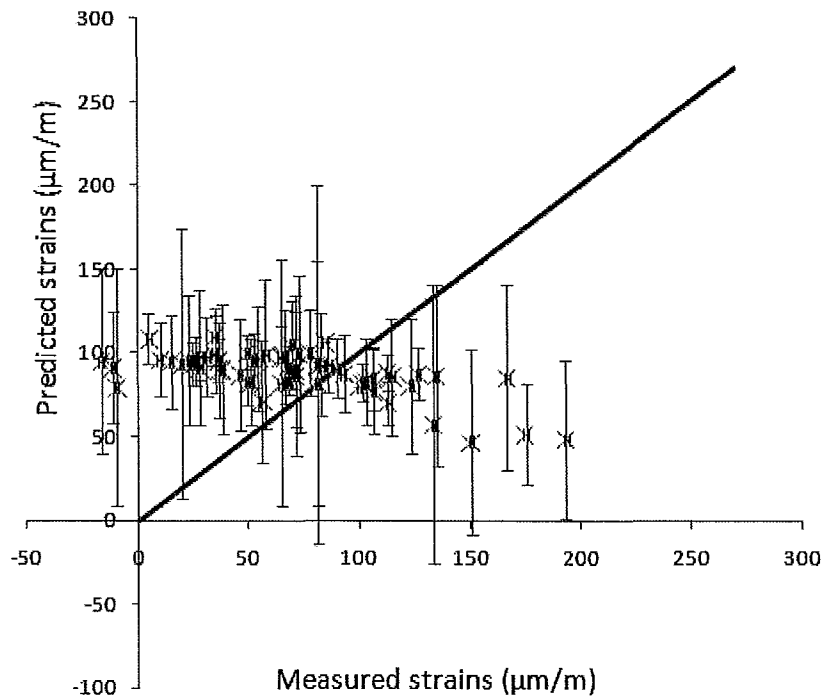


Figure 5.1d CEB – FIP 1990 Model – Predictions of shrinkage strains versus measured values for 3 days concrete

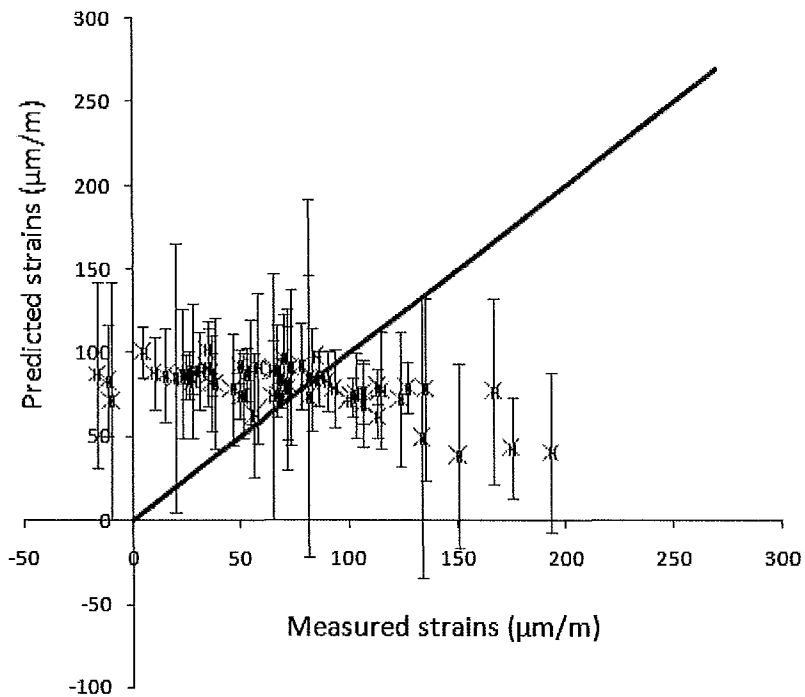


Figure 5.1e EHE Model – Predictions of shrinkage strains versus measured values for 3 days concrete

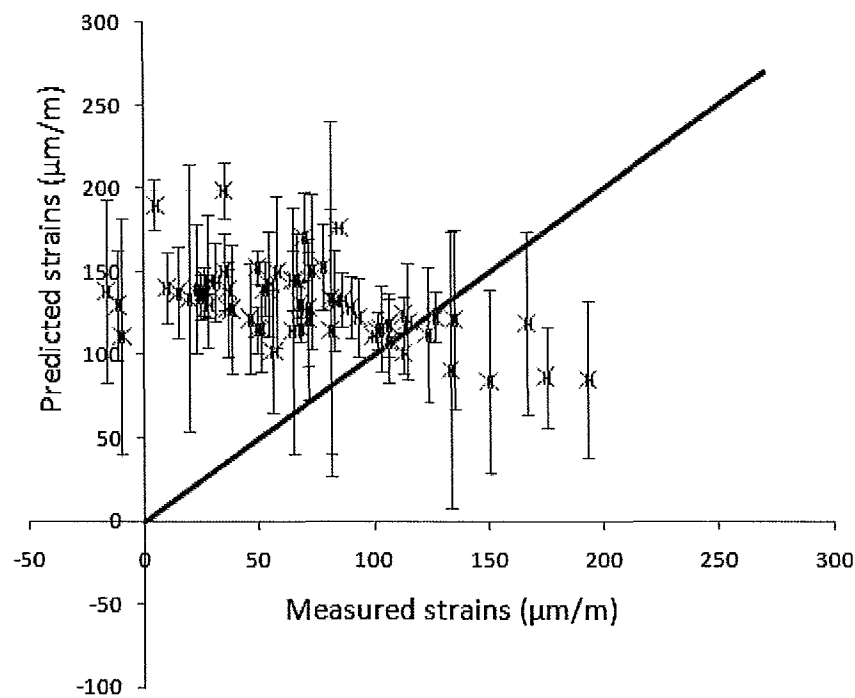


Figure 5.1f GL 2000 Model – Predictions of shrinkage strains versus measured values for 3 days concrete

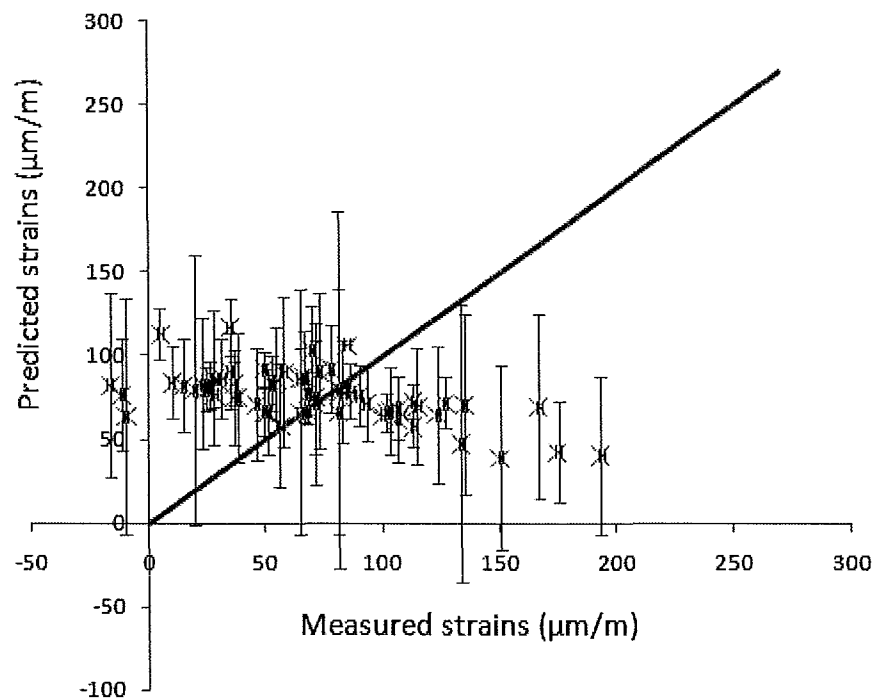


Figure 5.1g Eurocode 2 Model – Predictions of shrinkage strains versus measured values for 3 days concrete

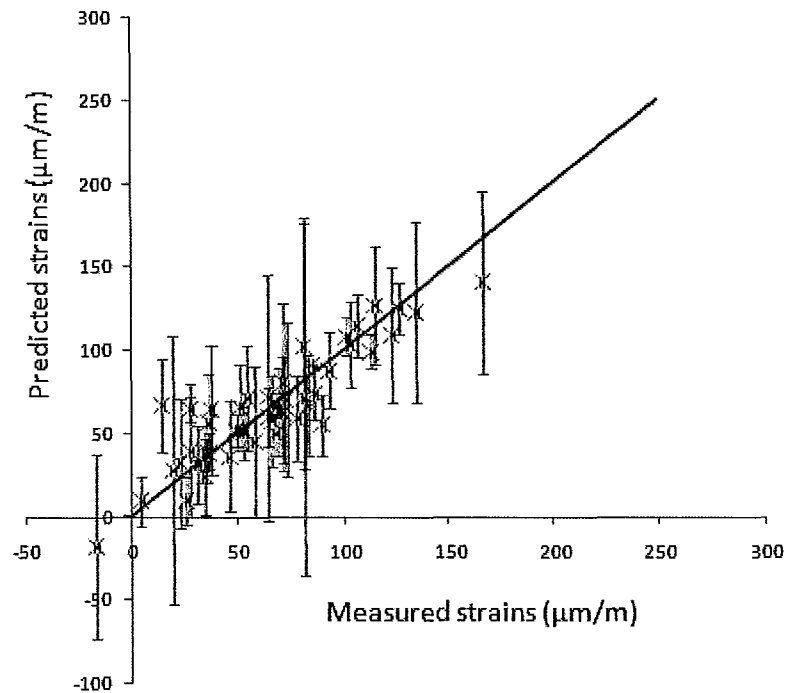


Figure 5.1h Regression model (90% Confidence level) – Predictions of shrinkage strains versus measured values for 3 days concrete

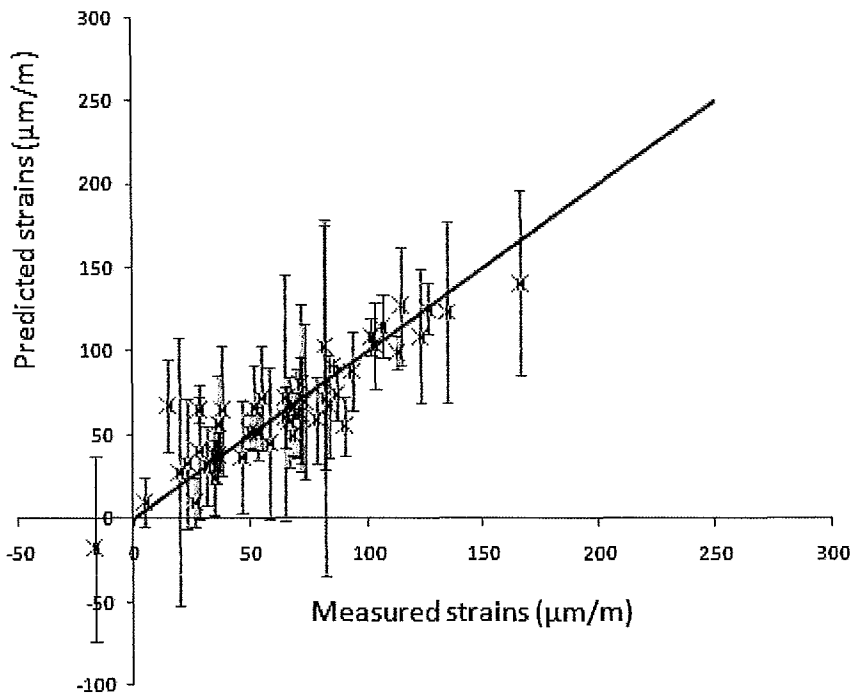


Figure 5.1i Regression model (95% Confidence level) – Predictions of shrinkage strains versus measured values for 3 days concrete

Figures 5.2 show that the models' predictions are improving after 14 days but still not reliable to be used as good estimates for shrinkage strain. Of the predictive models, the B3, CEB-FIP 1990 and EHE are found to better represent the measured values in comparison to the others. The regression models, as expected, continue to provide a good estimate of the concrete shrinkage strain at the age of 14 days.

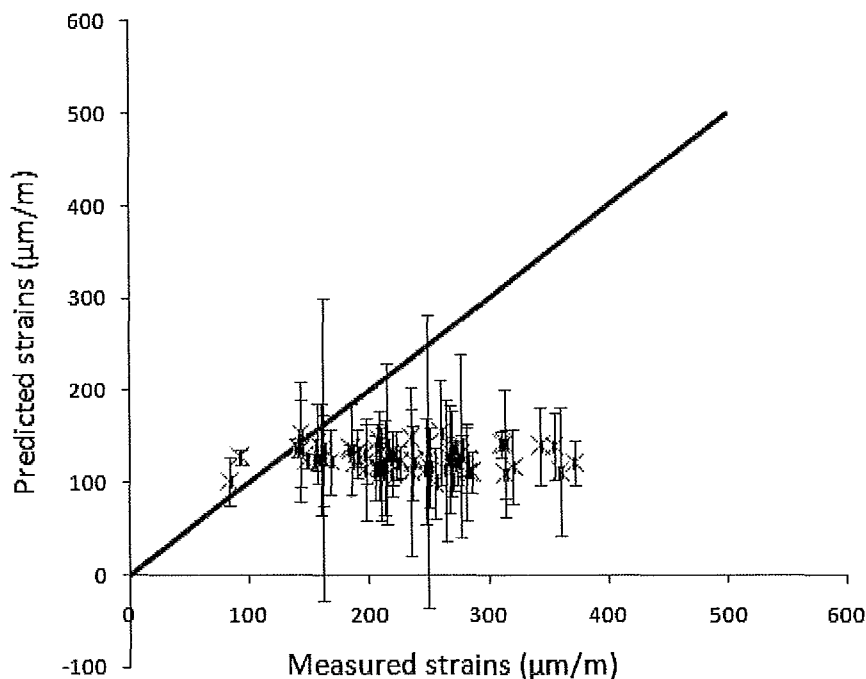


Figure 5.2a ACI - 209 Model – Predictions of shrinkage strains versus measured values for 14 days concrete

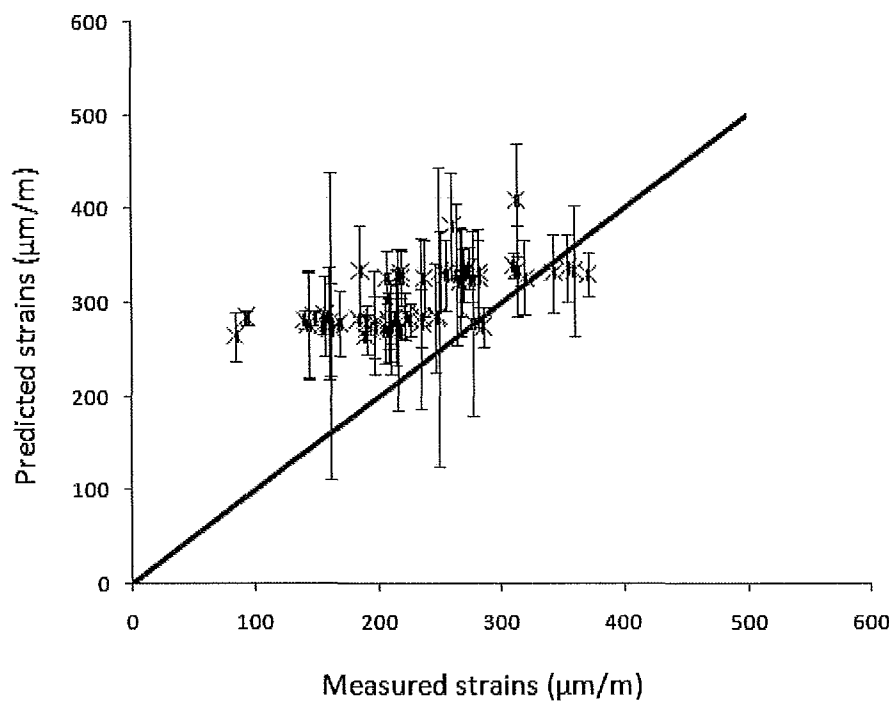


Figure 5.2b JSCE 2002 Model – Predictions of shrinkage strains versus measured values for 14 days concrete

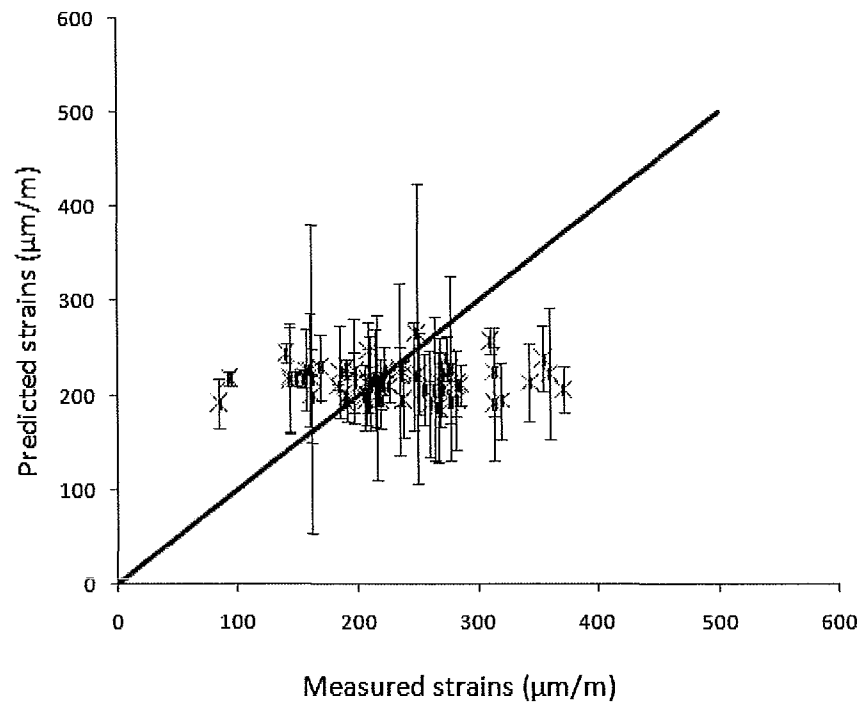


Figure 5.2c B3 Model – Predictions of shrinkage strains versus measured values for 14 days concrete

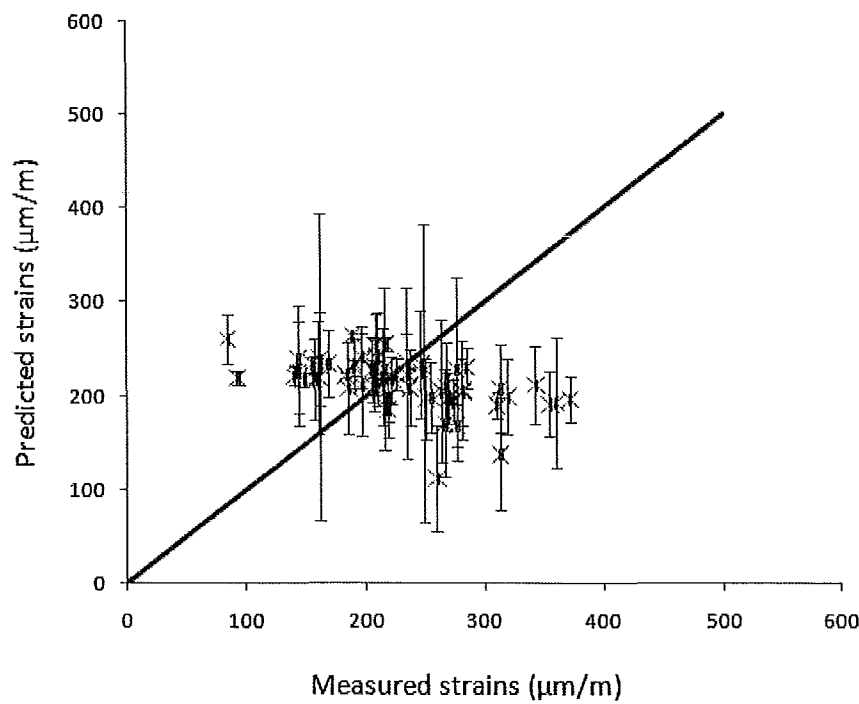


Figure 5.2d CEB – FIP 1990 Model – Predictions of shrinkage strains versus measured values for 14 days concrete

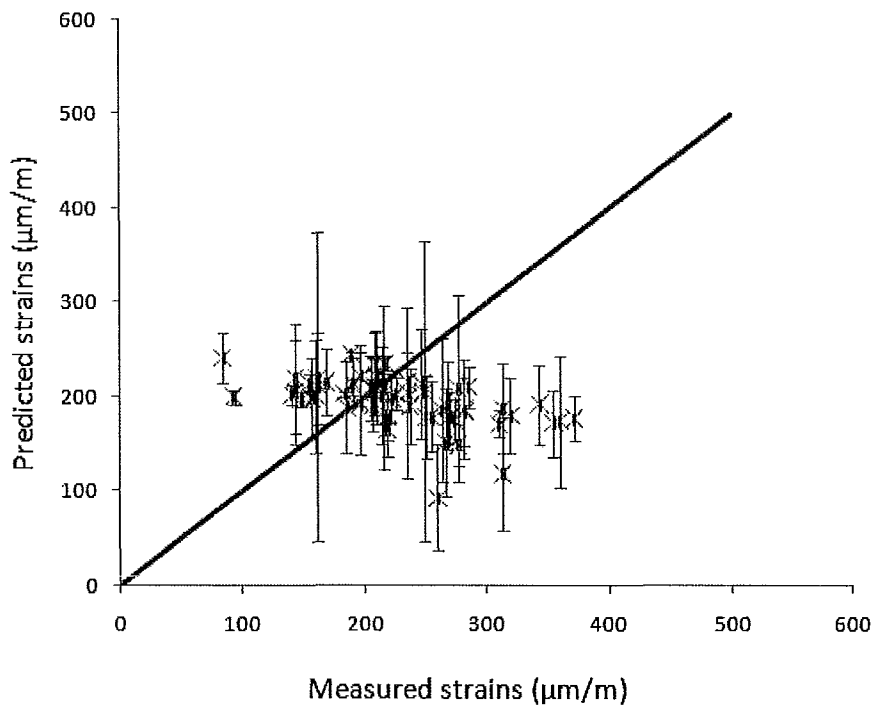


Figure 5.2e EHE Model – Predictions of shrinkage strains versus measured values for 14 days concrete

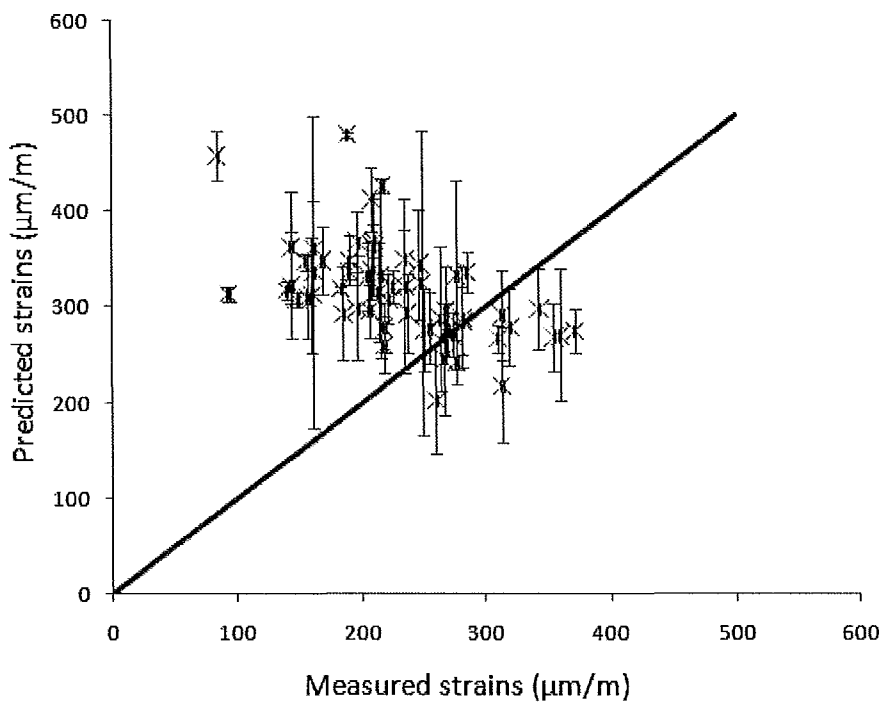


Figure 5.2f GL 2000 Model – Predictions of shrinkage strains versus measured values for 14 days concrete

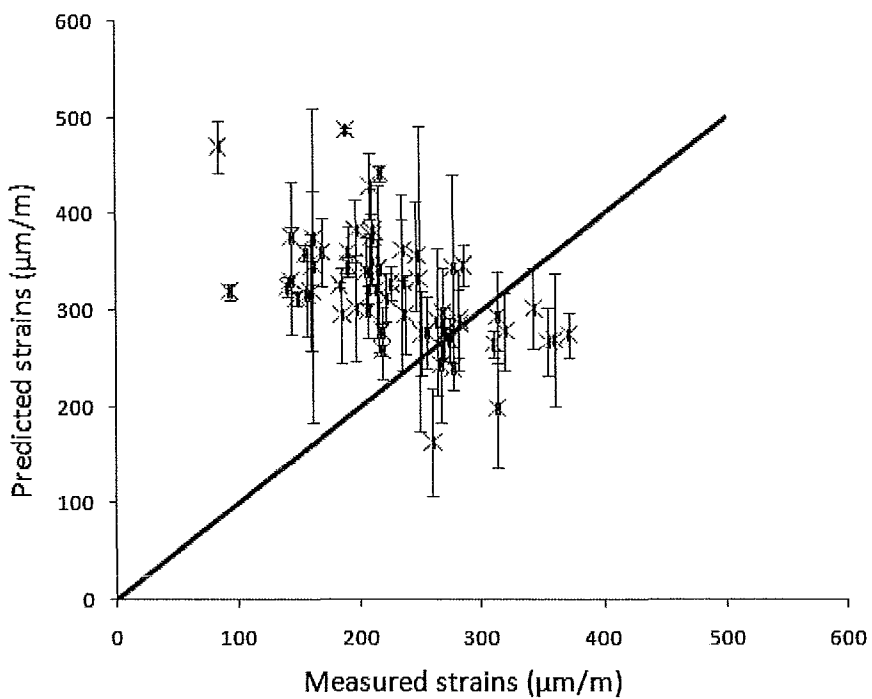


Figure 5.2g Eurocode 2 Model – Predictions of shrinkage strains versus measured values for 14 days concrete

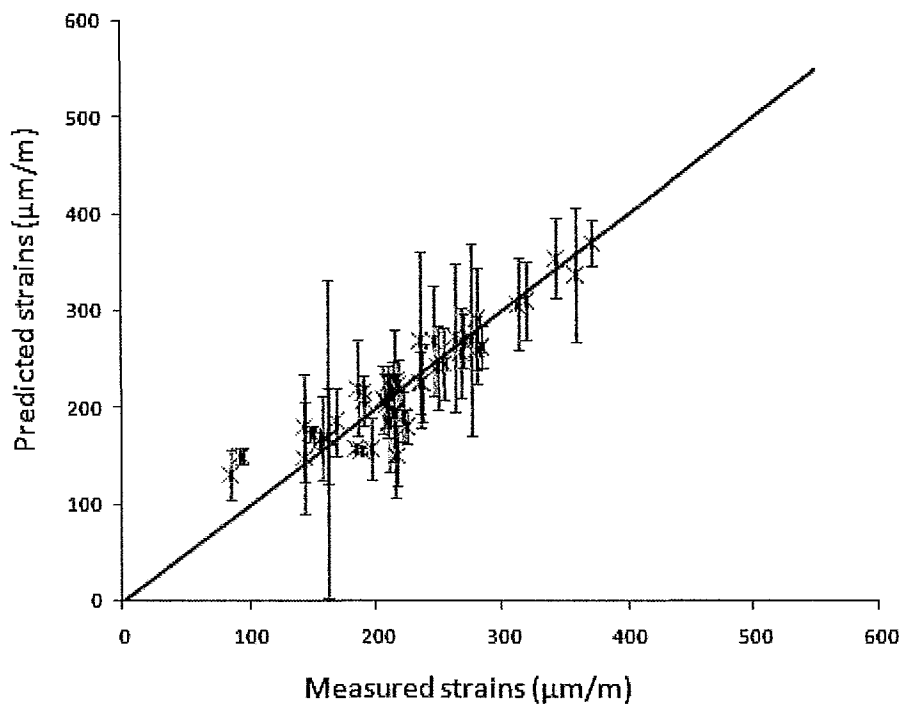


Figure 5.2h Regression model (90% Confidence level) – Predictions of shrinkage strains versus measured values for 14 days concrete

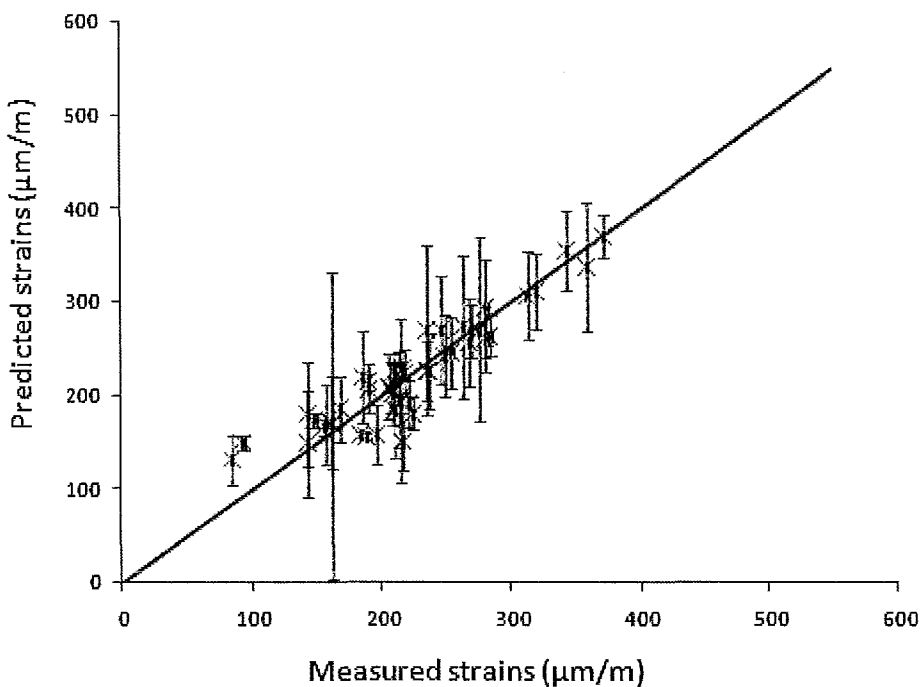


Figure 5.2i Regression model (95% Confidence level) – Predictions of shrinkage strains versus measured values for 14 days concrete

Results shown in Figures 5.3 reveal that ACI – 209, B3, CEB-FIP 1990 and EHE provide an improved estimate of shrinkage in comparison to JSCE 2002, GL 2000 and Eurocode 2 models, whose predictions overestimate the measured ones after 28 days. Moreover, the 90% regression model and 95% regression model continue to capture the behavior of the concrete. Figure 5.3j shows the predictions obtained using the regression model without the interaction terms. The results still do indicate a good fit, however one also observes that a higher degree of scatter in comparison to Figure 5.3i.

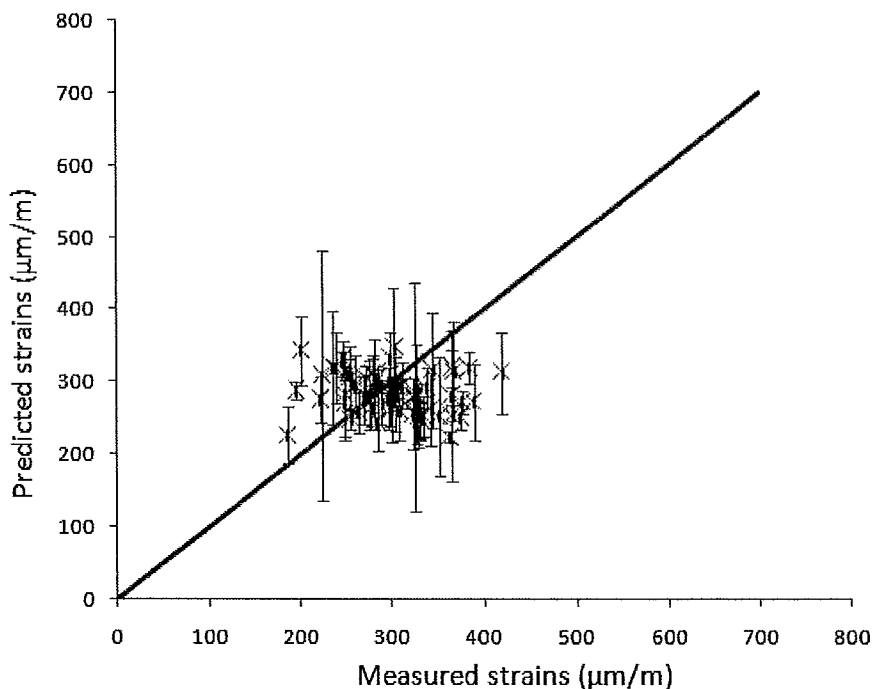


Figure 5.3a ACI - 209 Model – Predictions of shrinkage strains versus measured values for 28 days concrete

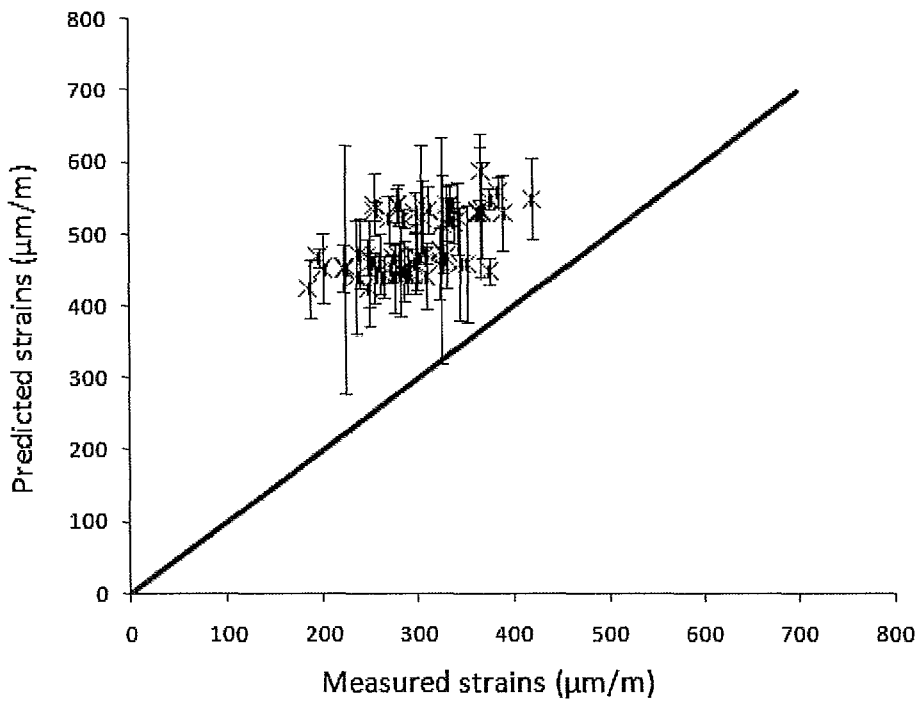


Figure 5.3b JSCE 2002 Model – Predictions of shrinkage strains versus measured values for 28 days concrete

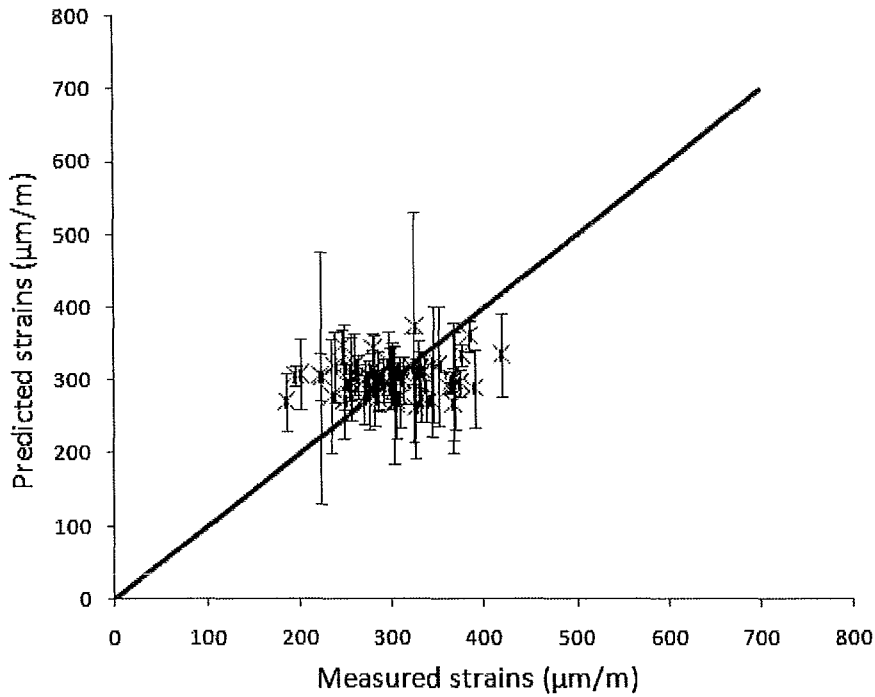


Figure 5.3c B3 Model – Predictions of shrinkage strains versus measured values for 28 days concrete

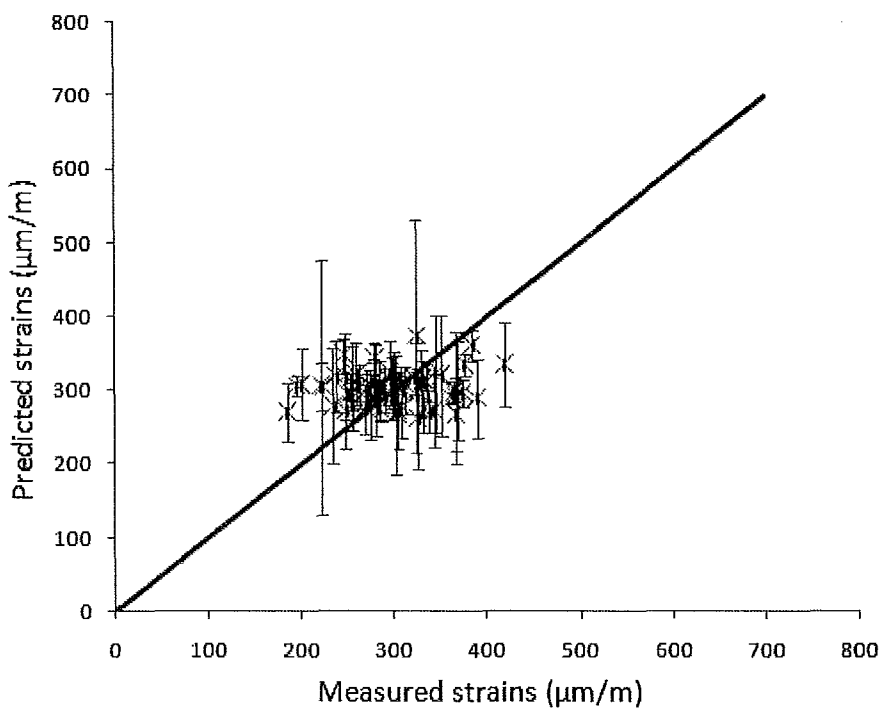


Figure 5.3d CEB – FIP 1990 Model – Predictions of shrinkage strains versus measured values for 28 days concrete

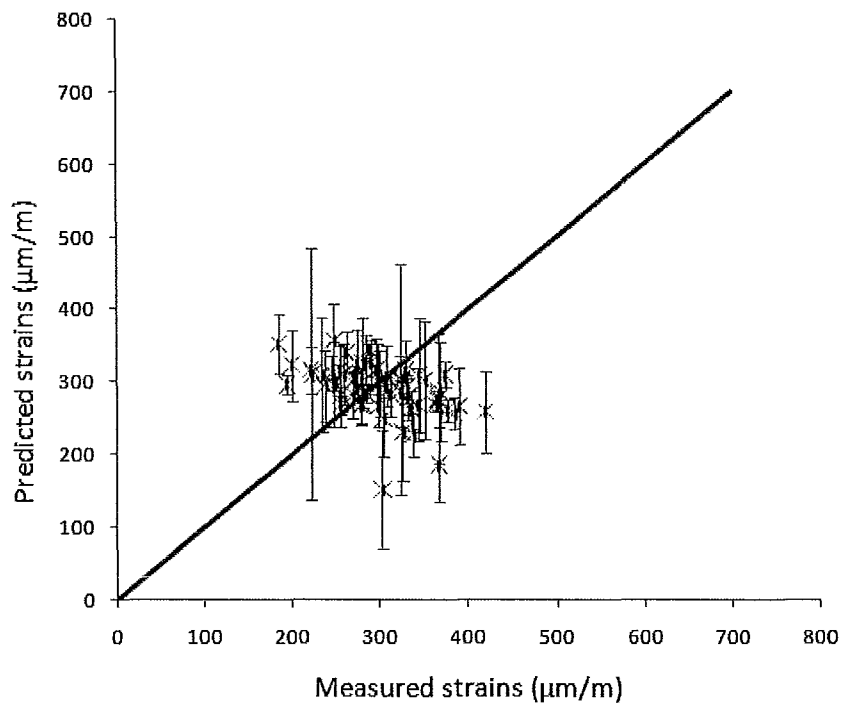


Figure 5.3e EHE Model – Predictions of shrinkage strains versus measured values for 28 days concrete

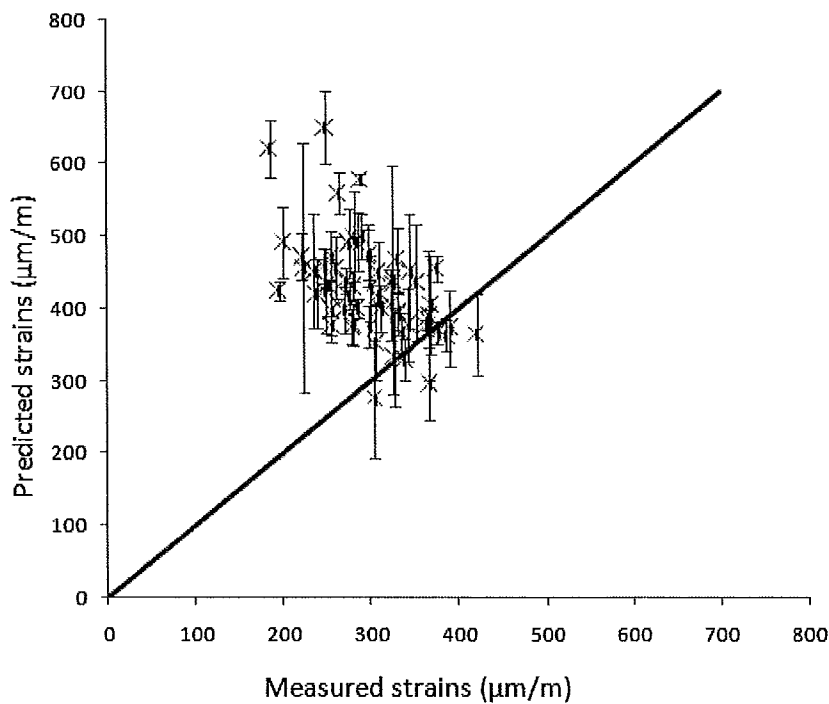


Figure 5.3f GL 2000 Model – Predictions of shrinkage strains versus measured values
for 28 days concrete

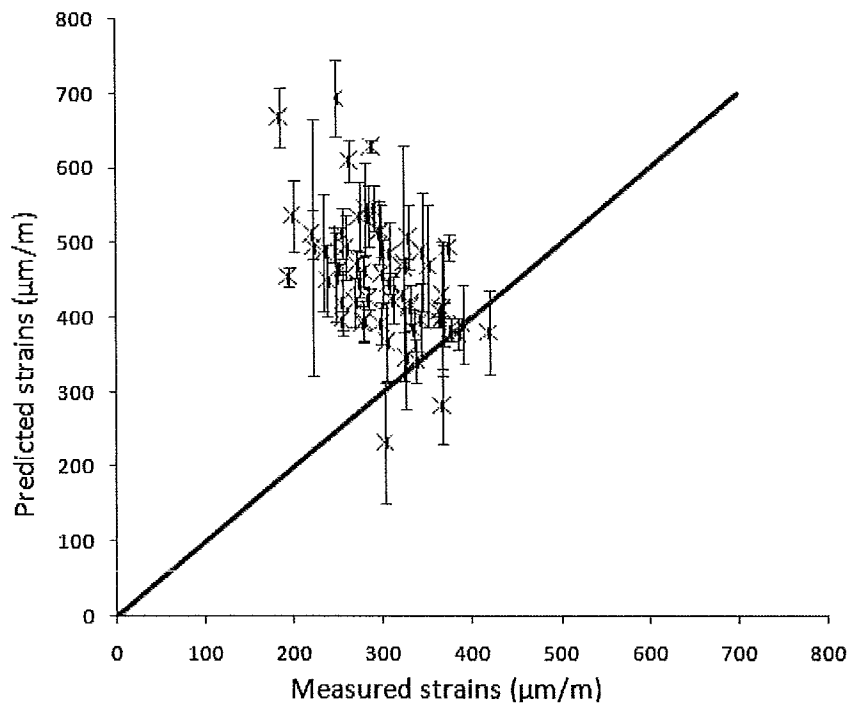


Figure 5.3g Eurocode 2 Model – Predictions of shrinkage strains versus measured
values for 28 days concrete

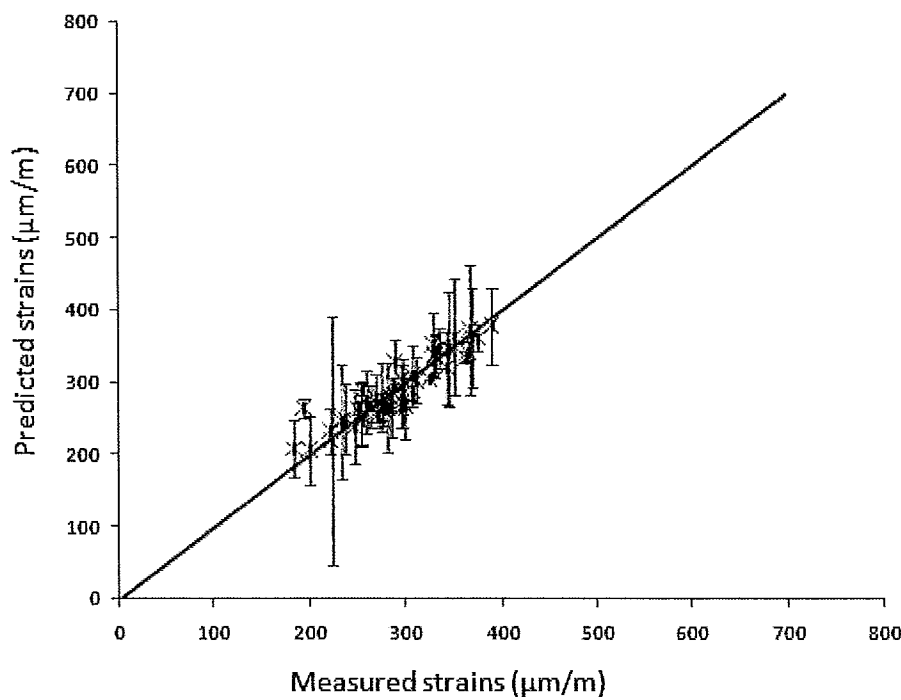


Figure 5.3h Regression model (90% Confidence level) – Predictions of shrinkage strains versus measured values for 28 days concrete

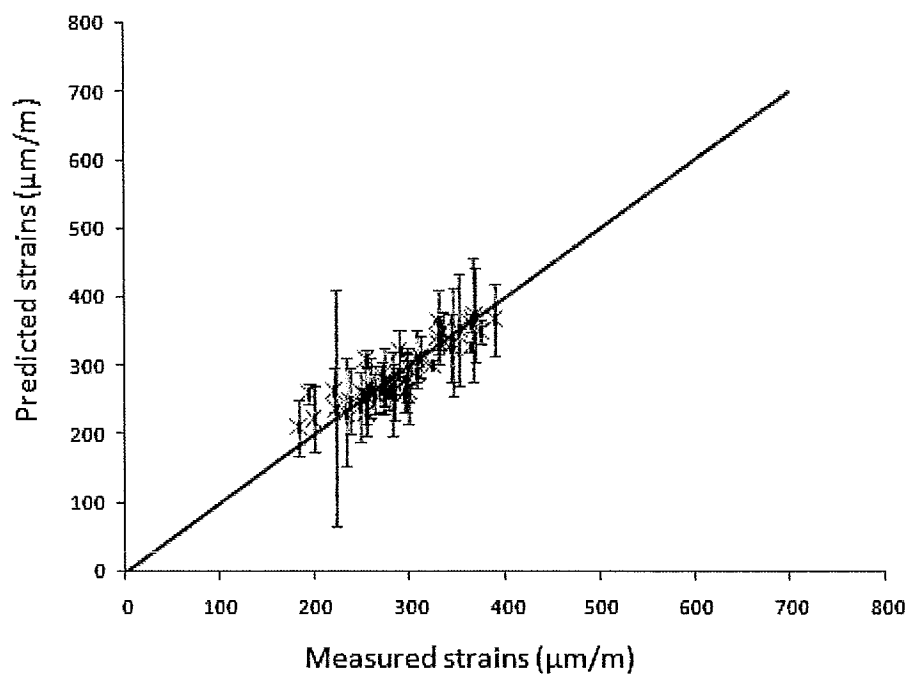


Figure 5.3i Regression model (95% Confidence level) – Predictions of shrinkage strains versus measured values for 28 days concrete

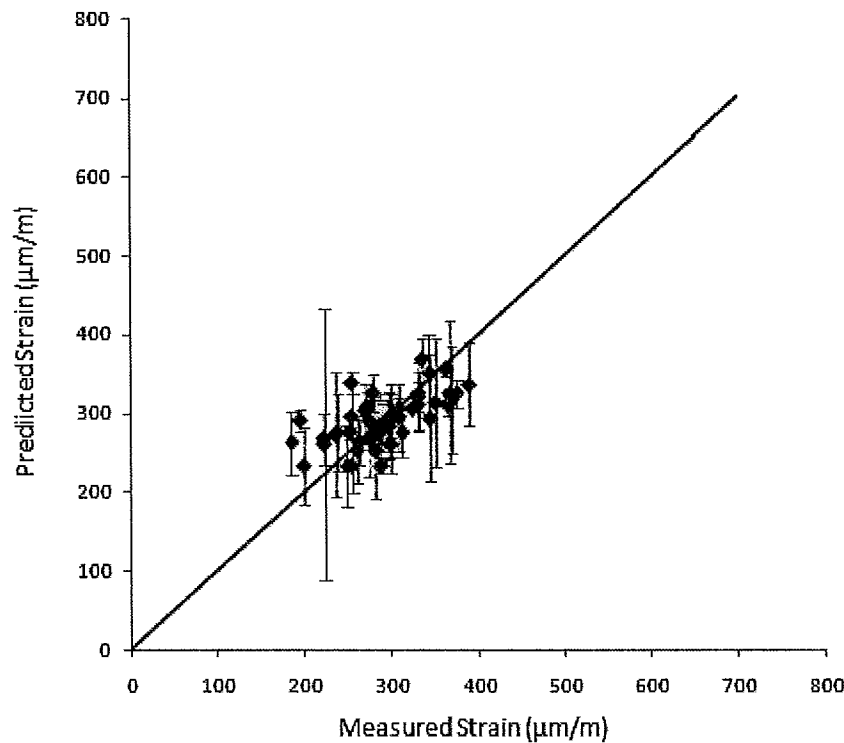


Figure 5.3j Regression model (95% Confidence level – without interaction parameters)
– Predictions of shrinkage strains versus measured values for 28 days concrete

For the results shown in Figures 5.4 for 56 days old concrete, the trend is somewhat similar to the 28 days predictions. CEB - FIP 1990 and EHE models predictions are found to be the most representative whereas ACI – 209 and B3 models slightly overestimate, GL 2000 and Eurocode 2 models overestimate and JSCE model well overestimates the measured values. The regression models continue to provide a good estimate of the concrete shrinkage strain.

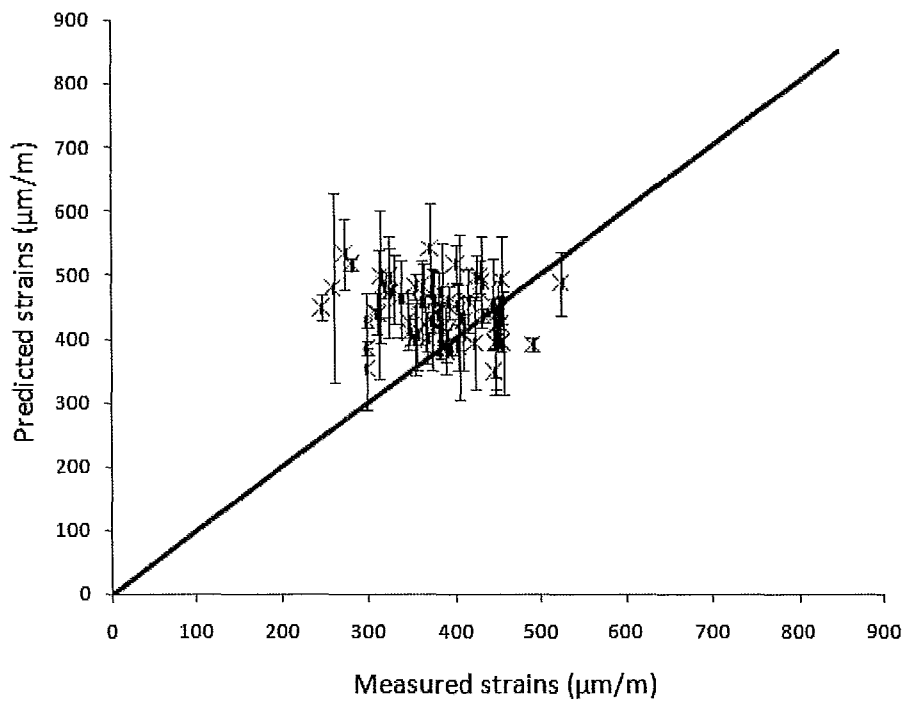


Figure 5.4a ACI - 209 Model – Predictions of shrinkage strains versus measured values
for 56 days concrete

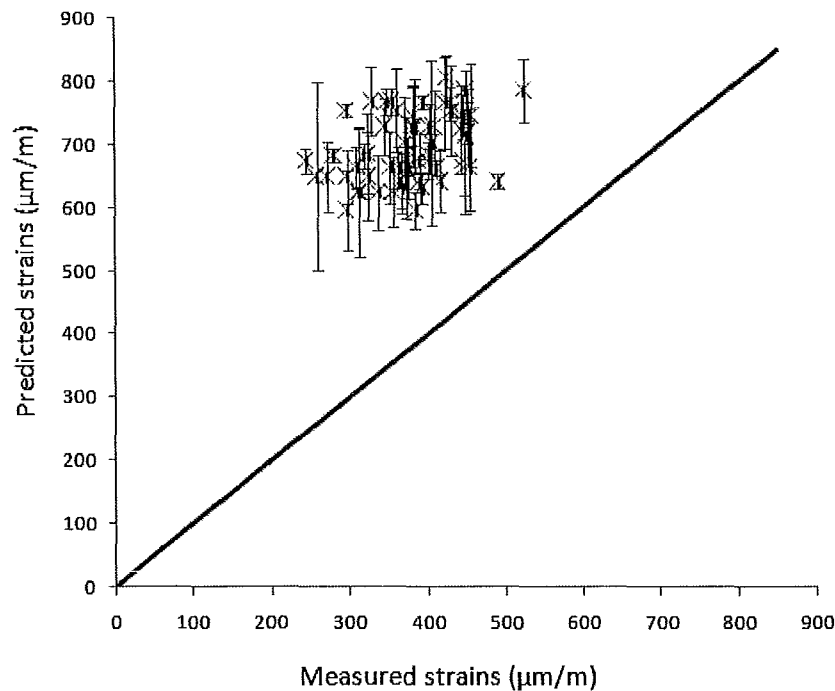


Figure 5.4b JSCE 2002 Model – Predictions of shrinkage strains versus measured values
for 56 days concrete

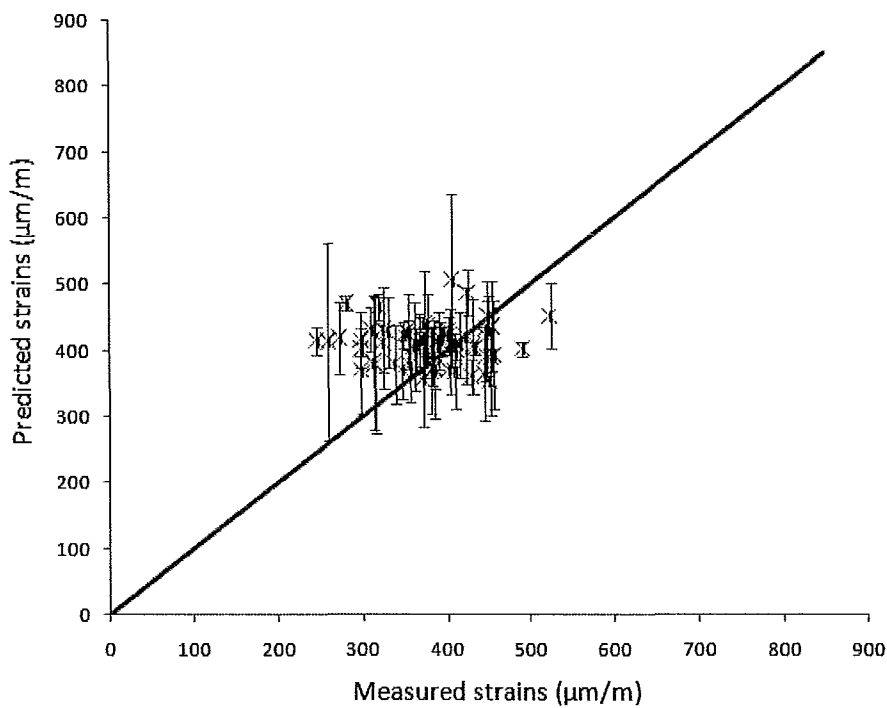


Figure 5.4c B3 Model – Predictions of shrinkage strains versus measured values for 56 days concrete

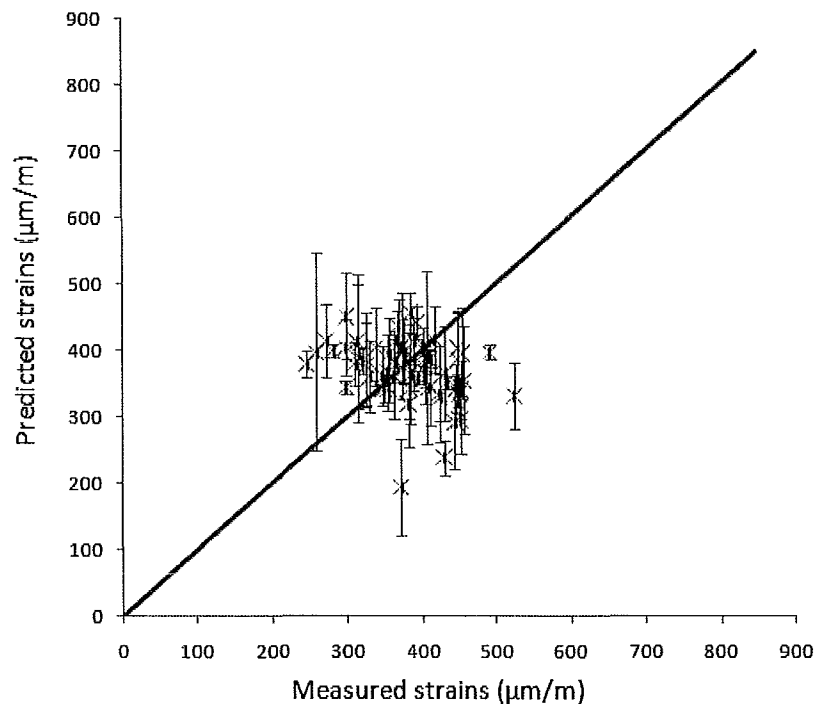


Figure 5.4d CEB – FIP 1990 Model – Predictions of shrinkage strains versus measured values for 56 days concrete

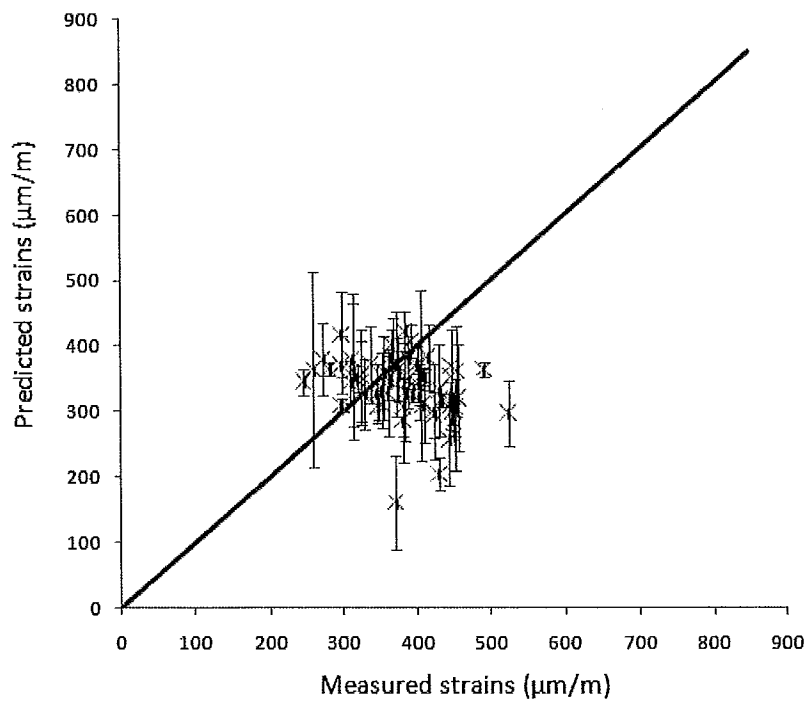


Figure 5.4e EHE Model – Predictions of shrinkage strains versus measured values for
56 days concrete

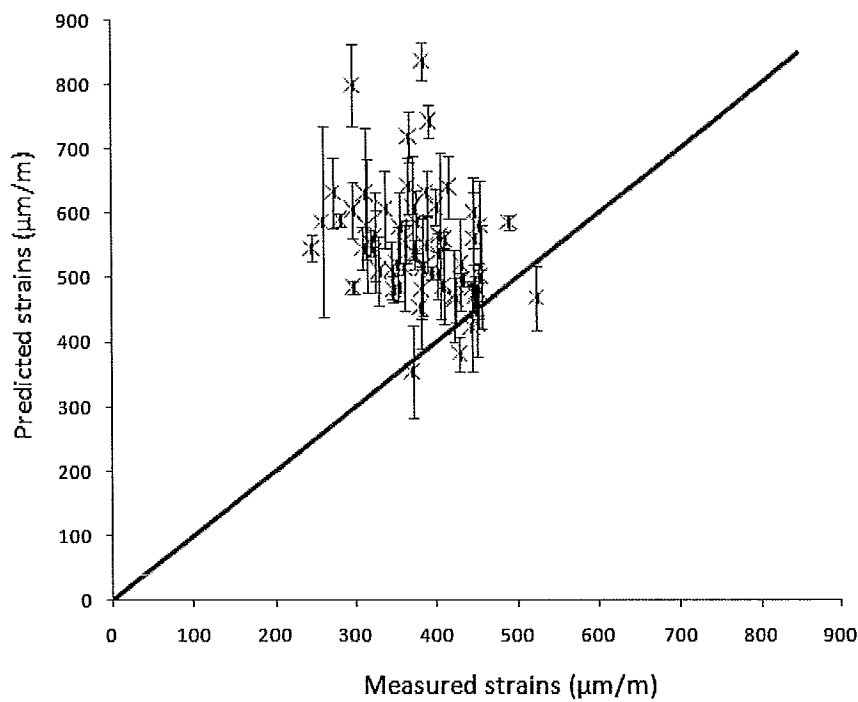


Figure 5.4f GL 2000 Model – Predictions of shrinkage strains versus measured values
for 56 days concrete

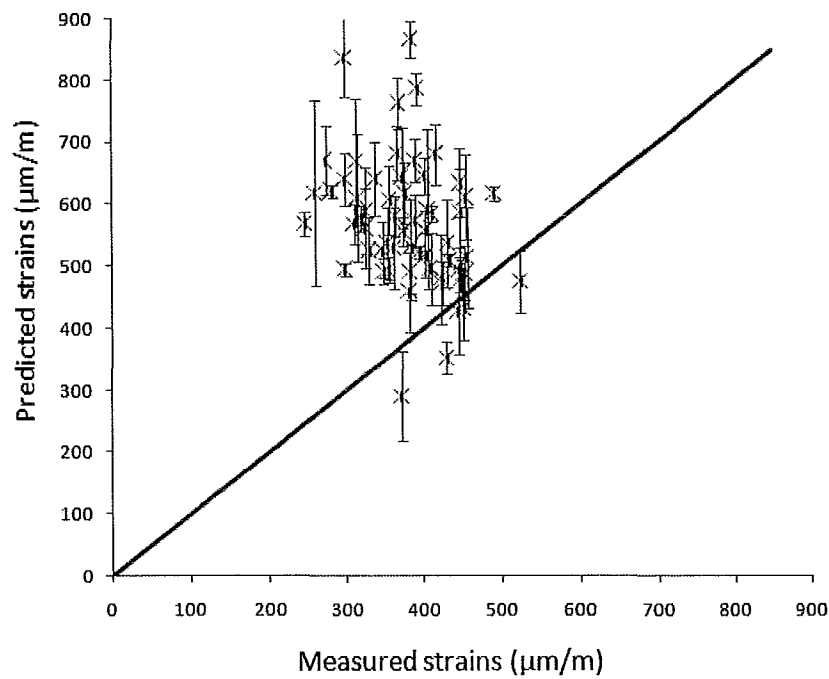


Figure 5.4g Eurocode 2 Model – Predictions of shrinkage strains versus measured values for 56 days concrete

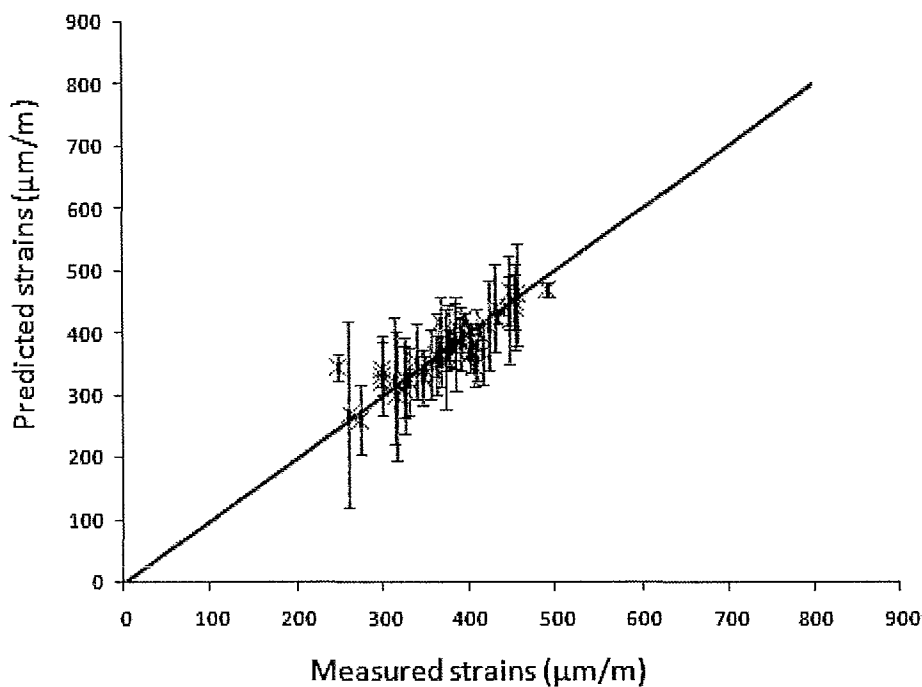


Figure 5.4h Regression Model (90% Confidence level) – Predictions of shrinkage strains versus measured values for 56 days concrete

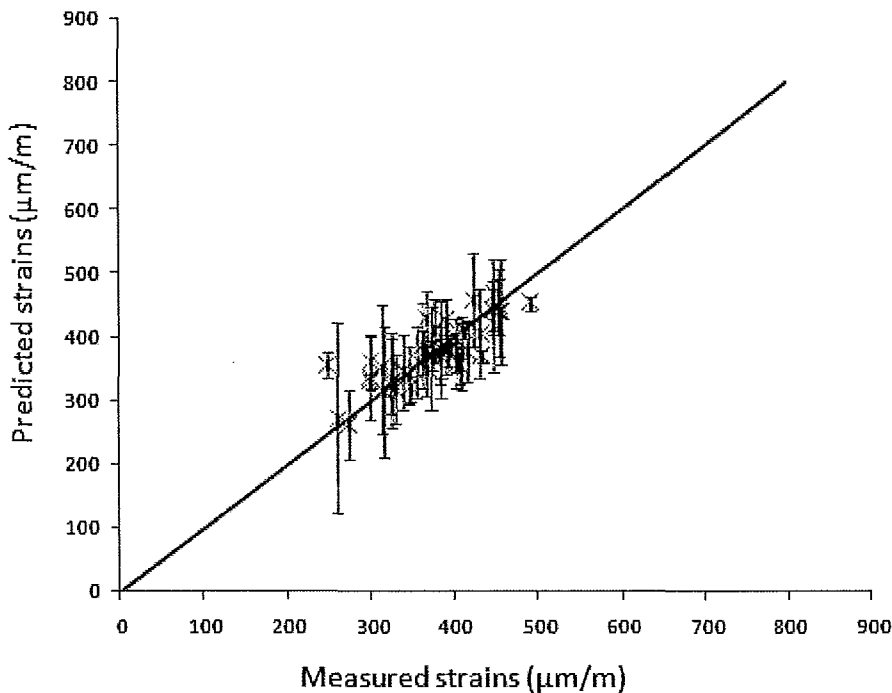


Figure 5.4i Regression Model (95% Confidence level) – Predictions of shrinkage strains versus measured values for 56 days concrete

From Figures 5.5, corresponding to the age of 119 days, ACI – 209 and B3 models are found to yield values that are comparable to the measured values. CEB-FIP 1990 and EHE models predictions slightly underestimate the measured values. GL 2000 and Eurocode 2 predictions slightly overestimate the measured values, whereas JSCE 2002 model predictions overestimate the measured values. Both regression models provide good prediction of shrinkage strain.

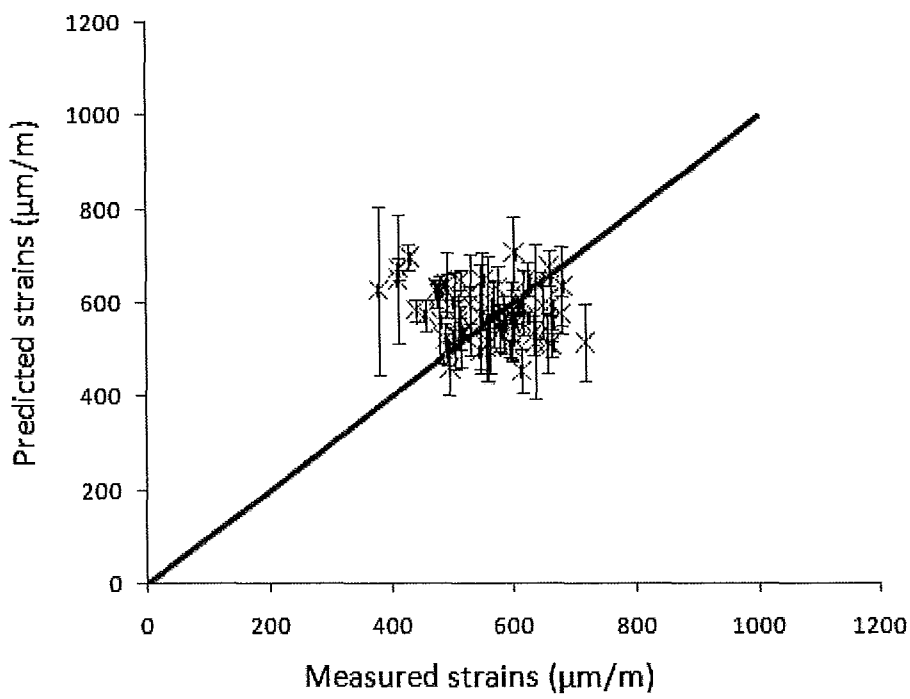


Figure 5.5a ACI - 209 Model – Predictions of shrinkage strains versus measured values for 119 days concrete

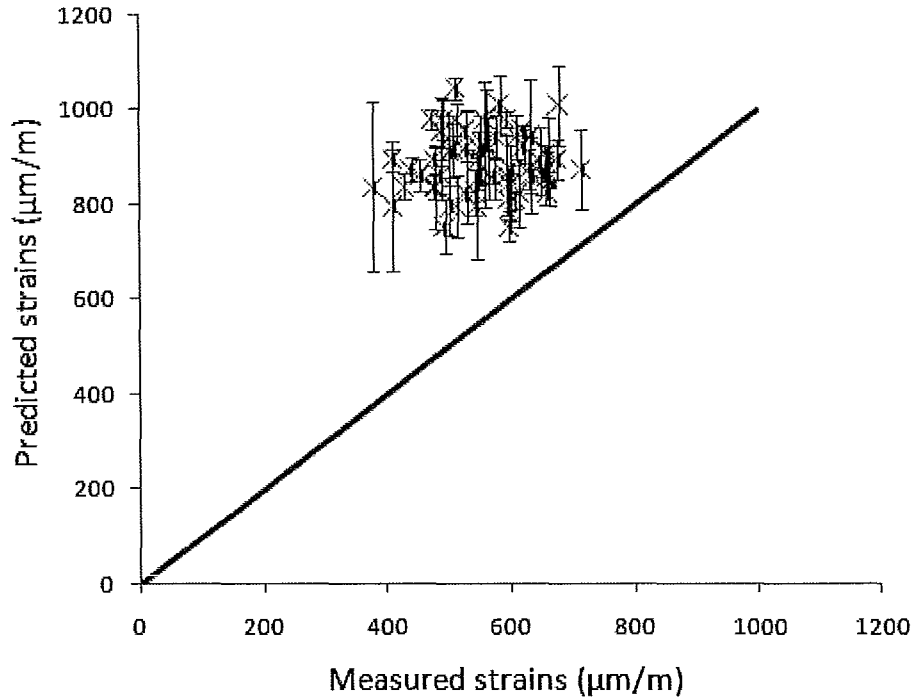


Figure 5.5b JSCE 2002 Model – Predictions of shrinkage strains versus measured values for 119 days concrete

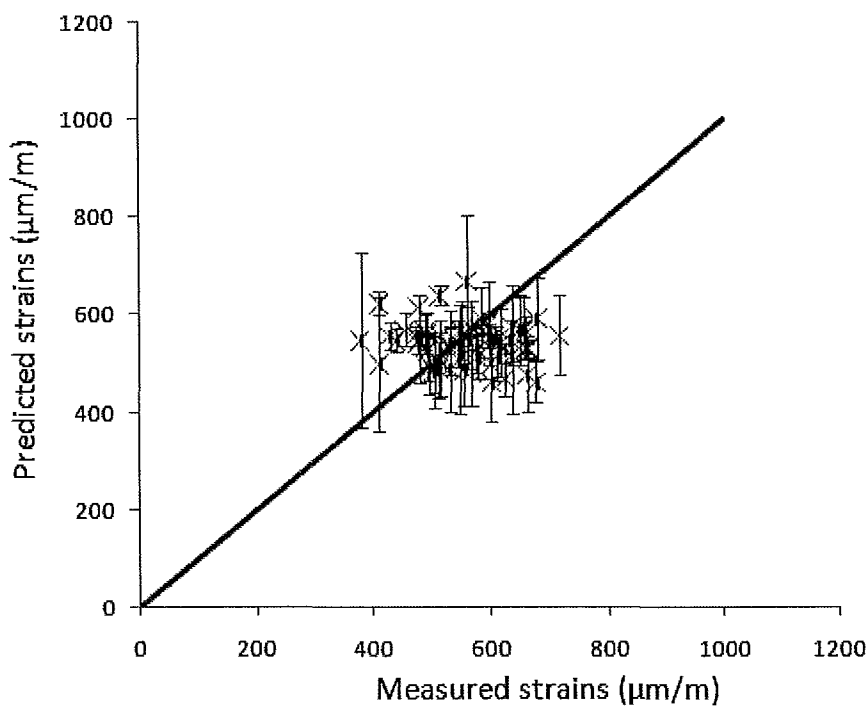


Figure 5.5c B3 Model – Predictions of shrinkage strains versus measured values for 119 days concrete

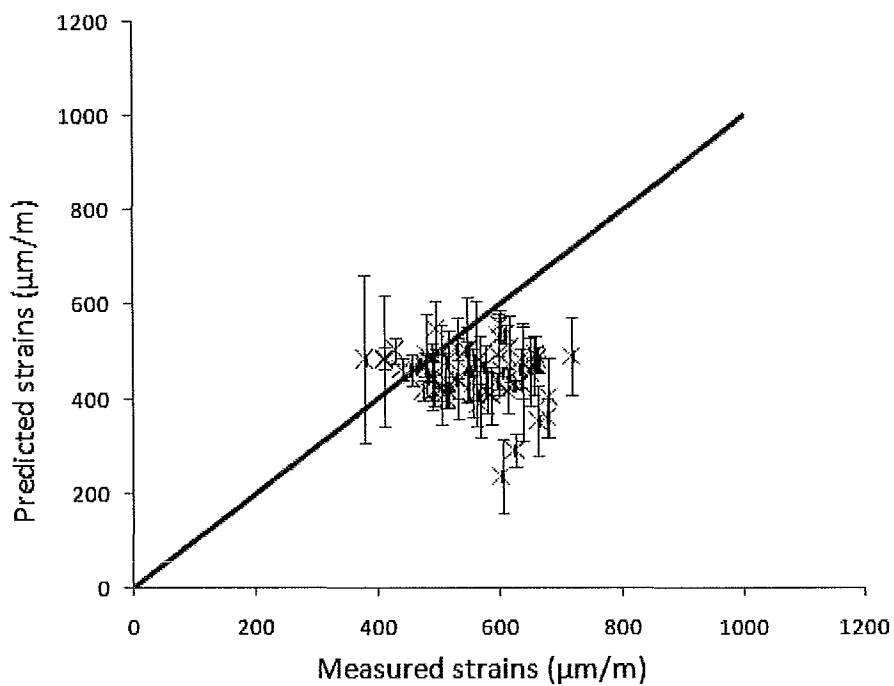


Figure 5.5d CEB – FIP 1990 Model – Predictions of shrinkage strains versus measured values for 119 days concrete

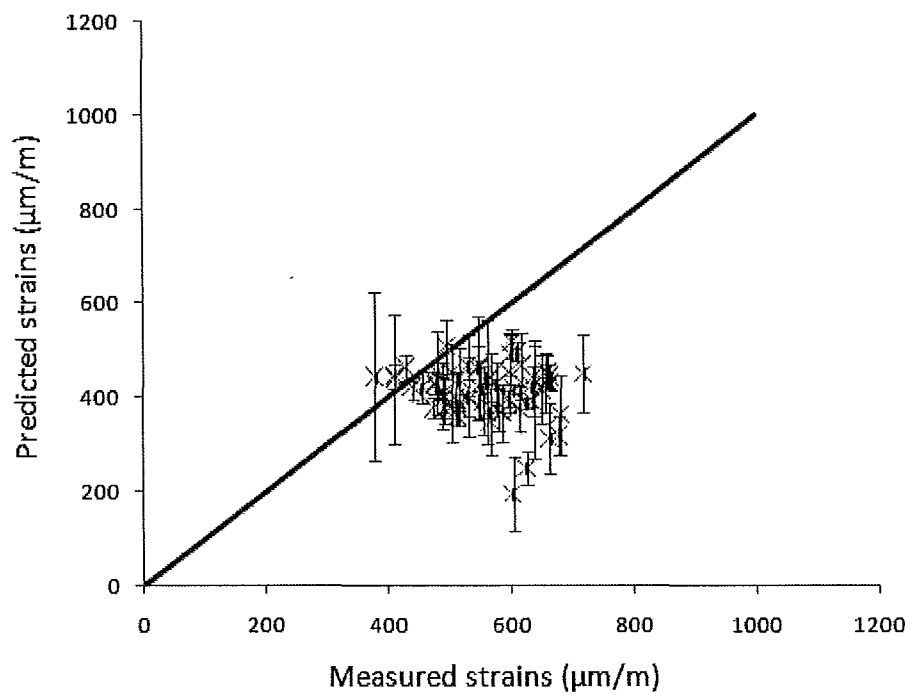


Figure 5.5e EHE Model – Predictions of shrinkage strains versus measured values for
119 days concrete

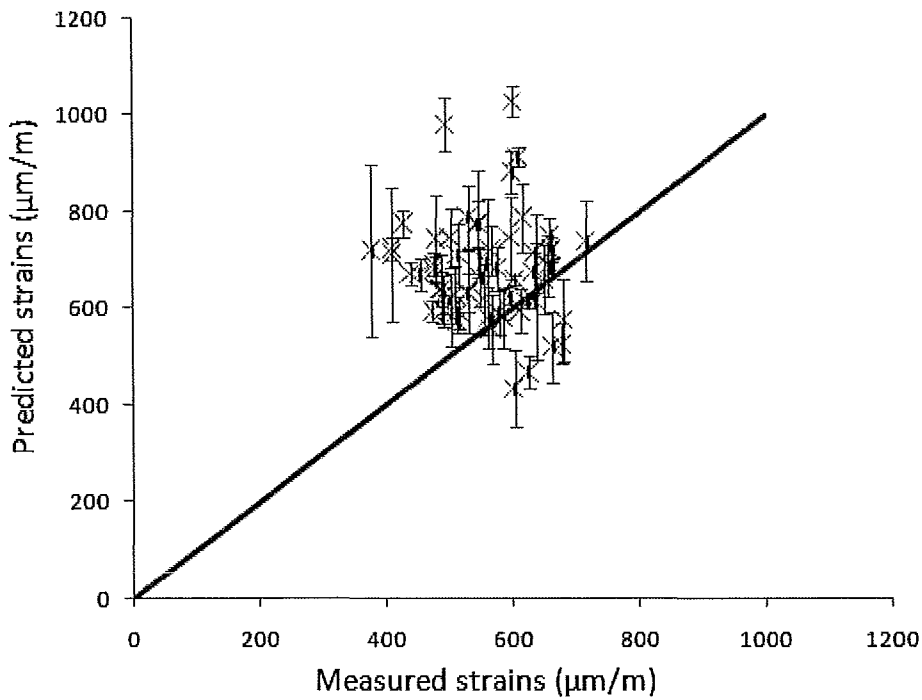


Figure 5.5f GL 2000 Model – Predictions of shrinkage strains versus measured values
for 119 days concrete

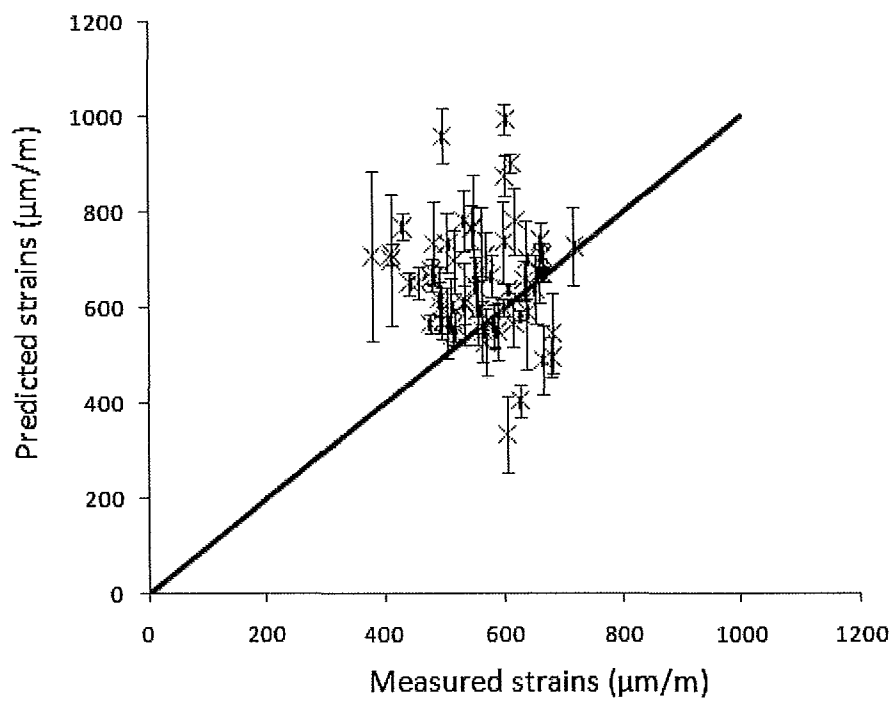


Figure 5.5g Eurocode 2 Model – Predictions of shrinkage strains versus measured values for 119 days concrete

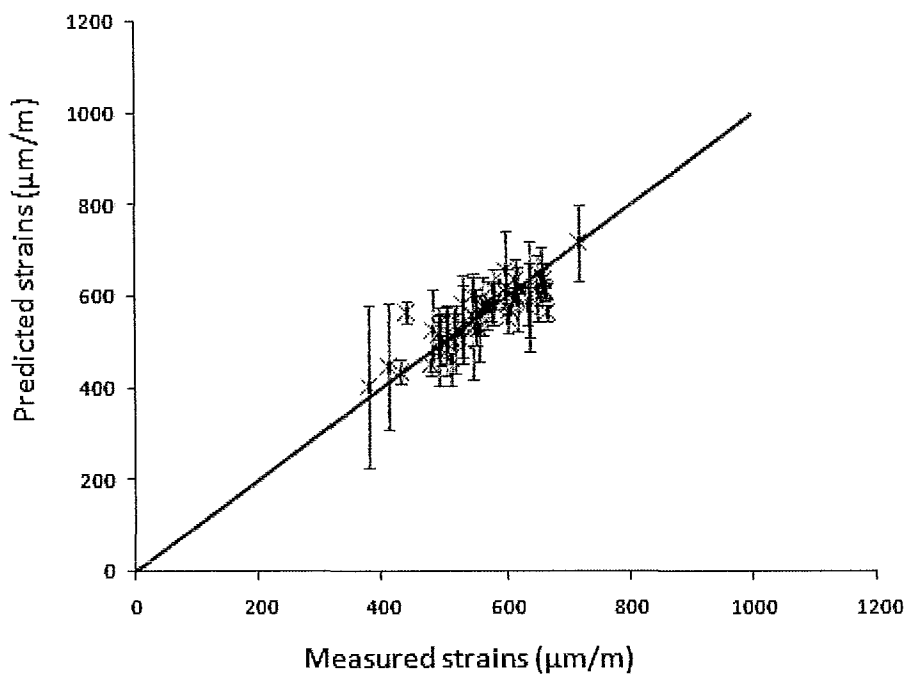


Figure 5.5h Regression model (90% Confidence level) – Predictions of shrinkage strains versus measured values for 119 days concrete

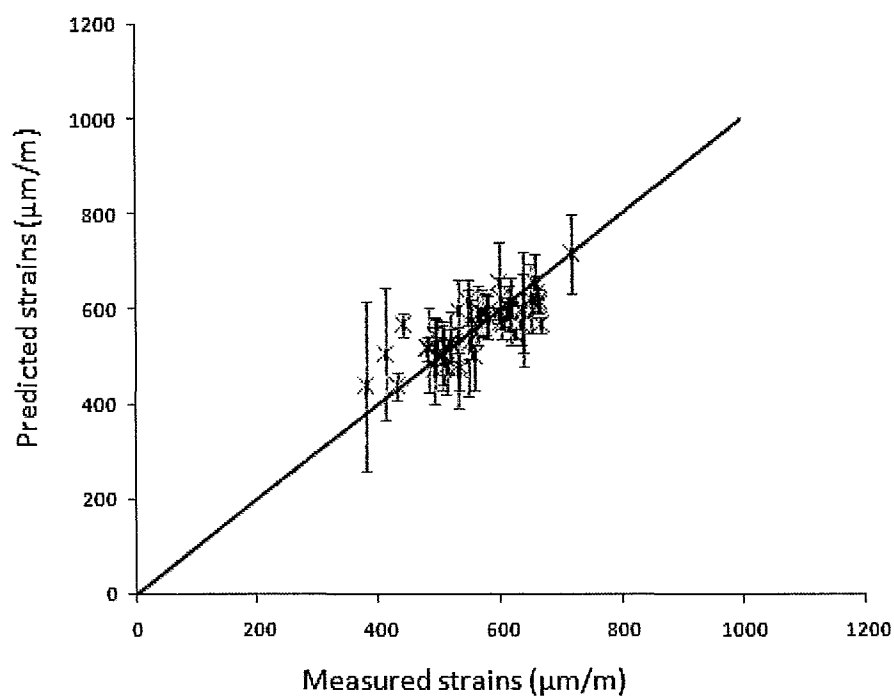


Figure 5.5i Regression Model (95% Confidence level) – Predictions of shrinkage strains versus measured values for 119 days concrete

5.2 Statistical Indicators

5.2.1 Residual Squared, R_e^2

The residual squared is the sum of the square of the difference between the predicted and measured values (Omar et al., 2008). The model yielding the minimum value is said to have the best fit for the experimental data.

5.2.2 Error Percentage

The error percentage method is based on the residual analysis and can be obtained from the following relation (Omar et al., 2008):

$$E(\%) = \frac{R_e}{c} \cdot 100 \quad (5.1)$$

where c is the mean value of the measured shrinkage strain. The error percentages for the different points are summed and the best fit model is the one yielding the lowest error percentage value.

5.2.3 Coefficient of Variation

The coefficient of variation is an important gauge to measure the accuracy of the different prediction models. The coefficient of variation for each prediction model at specified age is calculated. The model yielding the minimum value of coefficient of variation best fit the experimental data. Time interval considered in this study are: 2 days, 3 days, 5 days, 7 days, 14 days, 21 days, 28 days, 35 days, 42 days, 49 days, 56 days, 77 days, 98 days and 119 days. The formula for the coefficient of variation is expressed as follows (Gómez and Landsburger, 2007):

$$V_m = \sqrt{\frac{1}{N} \sum V_i^2} \quad (5.2)$$

$$V_i = \frac{1}{d} \cdot \sqrt{\sum \frac{(d - d')^2}{n - 1}} \quad (5.3)$$

where N is the number of time intervals, d is the measured value, d' the predicted value, \bar{d} the average measured value, and n the number of measured points.

5.3 Model Predicted Values

The results of the predictive models and the regression models were assessed statistically using the three statistical indicators. The corresponding results are given in Tables 5.1 to 5.4.

Table 5.1 Models assessment according to the residuals squared method ($\times 10^{-8}$)

Time (Days)	ACI - 209	JSCE 2002	B3	CEB - FIP 1990	EHE	GL 2000	EC2	Reg. Model 95%	Reg. Model 95%
2	11	11	13	14	13	27	11		
3	16	8	15	19	18	42	18	1	1
5	30	11	21	28	27	66	38		
7	41	12	21	32	33	78	57		
14	95	50	32	51	58	110	130	2	3
21	49	140	32	55	63	150	190		
28	27	240	25	50	59	170	240	1	2
35	33	350	31	56	67	200	270		
42	42	450	36	63	75	230	310		
49	55	560	39	64	76	260	330		
56	64	640	40	63	76	270	330	3	3
77	79	780	50	85	110	280	320		
98	77	820	51	100	140	270	280		
119	73	730	74	180	250	220	220	6	7
Sum	690	4800	480	860	1100	2400	2700		
Rank	2	7	1	3	4	5	6		

From Table 5.1, it is observed that B3 model ranks first with a relatively slight difference with ACI - 209 and CEB-FIP 1990 models. Performance of EHE model, which is based mainly on the CEB-FIP 1990 model, is found to yield substantially different results according to residuals squared method. GL2000 and Eurocode 2 appear to be in the same accuracy

range, while the JSCE is the least fitting of the measured data among the seven models. The regression models, on the other side, are found to fit best the experimental data.

Table 5.2 Models assessment according to the error percentage method (%)

Time (Days)	ACI - 209	JSCE 2002	B3	CEB - FIP 1990	EHE	GL 2000	EC2	Reg. Model 95%	Reg. Model 90%
2	-1	-4	-19	-18	-18	-15	-15		
3	-20	-1	38	53	47	99	49	10	11
5	41	53	71	80	72	132	97		
7	26	24	28	35	32	63	52		
14	26	27	16	20	20	39	41	4	5
21	15	36	14	17	17	35	40		
28	11	42	11	14	14	33	39	2	3
35	12	47	11	14	14	32	38		
42	13	50	11	14	14	33	38		
49	15	53	12	13	13	33	38		
56	15	54	11	13	13	32	36	2	2
77	14	52	11	12	13	28	30		
98	12	47	9	12	14	24	24		
119	10	39	10	14	17	18	17	2	3
Sum	232	542	234	292	282	585	525		
Rank	1	6	2	4	3	7	5		

When implementing the error percentage method, whose results are given in Table 5.2, one can observe that ACI - 209 model ranks first with a slight difference with B3 model. The EHE model and CEB-FIP 1990 model appear to be similar in accuracy. The other three methods yielded poorer results with similar level of accuracy. The regression models predictions provide the best representation for the measured shrinkage strain values.

Closer examination of the results given in Table 5.3, one can note that B3 best represents the data followed by the ACI - 209 method. The CEB-FIP 1990 and EHE are very similar in term of their accuracy according to this method. For the remaining three predictive models, they rank last with the GL2000 being the least fitting model. Similar to the previous results,

the regression models provide the best predictions for the shrinkage strain. This is expected as these regression models are developed specifically for these test data.

Table 5.3 Models assessment according to the coefficient of variation method ($\times 10^{-2}$)

Time (Days)	ACI - 209	JSCE 2002	B3	CEB - FIP 1990	EHE	GL 2000	EC2	Reg. Model 95%	Reg. Model 90%
2	105	99	118	132	122	252	105		
3	59	30	53	69	64	155	64	3	4
5	43	16	29	41	39	95	55		
7	32	9	16	25	25	60	44		
14	29	15	10	16	18	34	39	0.8	0.8
21	11	30	7	12	14	32	42		
28	5	46	5	10	11	33	5	0.3	0.2
35	5	53	5	8	10	30	42		
42	6	61	5	9	10	31	41		
49	7	69	5	8	9	32	41		
56	7	72	4	7	9	30	38	0.4	0.3
77	7	66	4	7	9	24	27		
98	5	56	3	7	10	18	19		
119	4	38	4	9	13	11	11	0.4	0.3
Sum of V_i^2	325	661	269	360	364	838	573		
Vm	48	69	44	51	51	77	64		
Rank	2	6	1	3	4	7	5		

A summary of the model assessment is given in Table 5.4. The assessment reported in the literature was amended in Table 5.5 to include the results of Table 5.4. This assessment concur with what has been reported in the literature, namely that model B3 provides the best estimate for shrinkage strain followed by ACI - 209, CEB – FIP 1990, GL 2000, EHE then Eurocode 2.

Table 5.4 Models assessment summary

	ACI - 209	JSCE 2002	B3	CEB-FIP	EHE	GL2000	EC 2
Re ²	2	7	1	3	4	5	6
E(%)	1	6	2	4	3	7	5
Vm	2	6	1	3	4	7	5
Overall	2	7	1	3	4	6	5

Table 5.5 Ranking of shrinkage models

	Shrinkage Models					
	ACI - 209R	B3	CEB-FIP	EHE Model	EC 2	GL 2000
Bazant	3	1	2			
Al-Manaseer	3	2	4			1
Gardner	3	2	4			1
McDonald	1	2	3			
Gómez.	1	2	3	5		4
Kiang	5	1	2		4	3
Current Study	2	1	3	4	5	6
Average	2.6	1.6	3	4.5	4.5	3
Overall Ranking	2	1	3	5	5	4

Chapter 6

Conclusions and Recommendations

6.0 Summary

An experimental program was undertaken to study the effects of concrete mixture and curing regime on shrinkage strain, as well as the effects of shrinkage on concrete compressive strength. The parameters investigated are w/c, water content, maximum aggregate size, silica fume percent replacement, GGBFS percent replacement, and coarse aggregate volume. In this study, a new test setup was developed to study the relation between autogenous shrinkage strain, concrete temperature and capillary pressure with considerations given to the concrete mixture.

The study also included the assessment of the proposed predictive models for shrinkage strains as well as the development and assessment of regression models for shrinkage strain based on the experimental data. This elaboration enabled the identification of parameters and parameters interaction's influence on shrinkage strain.

6.1 Conclusions

On the basis of the results obtained from the experimental program, analysis of the experimental results and assessment of the models proposed to predict shrinkage of concrete, the following conclusions are drawn.

Concrete drying and chemical shrinkage

1. Magnitude and type of shrinkage strain are highly dependent on the curing regime.
2. Moist cured samples exhibit chemical and autogenous shrinkage.
3. Strains due to chemical shrinkage are inconsistent and much smaller in comparison to drying shrinkage.
4. Air cured samples exhibit chemical, autogenous and drying shrinkages.
5. Strains due to drying shrinkage are found to range from 450 to 800 $\mu\text{m/m}$.
6. Strains due to chemical shrinkage are found less than 100 $\mu\text{m/m}$.
7. Increasing coarse aggregate volume and size reduces the magnitude of shrinkage strain.
8. Increasing the amount of cement content increases the magnitude of shrinkage strain.
9. Increasing the amount of water to cement ratio increases the magnitude of shrinkage strain.
10. Addition of water reducing agent and/or air entraining agent reduces the magnitude of shrinkage strain.
11. The significant parameters affecting the shrinkage strain are, CA, w/c², CA², w/c*SF, w/c*GGBFS, size*SF, size*CA, w/c*SF*GGBFS, w/c*w*size, and w/c*SF*CA.
12. The behavior of concrete shrinkage strain is non-linear in relation to the composition of concrete.
13. The interaction between w/c, SF and GGBFS leads to an increase in shrinkage strain.
14. The interaction between w/c, SF and CA volume results in a decrease in shrinkage strain.
15. The interaction between w/c, water content, and size of aggregate results in a decrease in shrinkage strain.

Concrete autogenous shrinkage

1. Mixtures with w/c less than 0.4 yields autogenous shrinkage strain.
2. Increase in the capillary pressure is observed to precede the development of autogenous shrinkage strain.
3. Proposed test setup to measure autogenous shrinkage is found to yield data that are consistent with the literature.
4. Increasing amount of cementitious materials in the mixture whose w/c is less than 0.4 increases the magnitude of autogenous shrinkage and capillary pressure.
5. Increasing amount of cementitious materials in all the mixture increases the magnitude of the hydration temperature.
6. Addition of water reducing agent concentration decreases the autogenous shrinkage strain, temperature, and capillary pressure.
7. Addition of viscosity enhancing agent increases autogenous shrinkage strain and capillary pressure.
8. Interaction between GGBFS and SF leads to a decrease in autogenous shrinkage strain.
9. An increase in coarse aggregate volume reduces the magnitude of autogenous shrinkage strain.

Effect of shrinkage on compressive strength

1. Compressive strength of air cured samples is on average 10% lower than those of moist cured.
2. Drying shrinkage does not significantly affect the concrete compressive strength.

Shrinkage predictive models assessment

1. None of the current models adopted by North American, European and Japanese standards are able to predict adequately the shrinkage strain for the early ages of concrete.

2. At 28 and 119 days, ACI – 209 and B3 predicts reasonably well the strains due to shrinkage.
3. The predictability of the assessed models from this study is ranked from best to worst as follows, B3, ACI – 209, CEB – FIP 1990, EHE, Eurocode 2, GL 2000 and JSCE 2002.
4. The developed regression models yield values that are significantly closer to the measured strain values at all the ages considered, i.e. 3 days, 7 days, 14 days, 28 days, 56 days, and 119 days.

6.2 Recommendations

Although many findings were uncovered during the course of this study, they also revealed that there are more studies are still needed in the study of concrete shrinkage strains, specifically,

1. Expand the experimental program to include mixtures with varying amount of mineral and chemical admixtures.
2. Predictive models need to be developed on the basis of more scientific knowledge and need to include the effects of mineral and chemical admixtures.
3. Develop standard test method for measuring autogenous shrinkage.
4. Develop best practice guide to mitigate chemical, autogenous, and drying shrinkage.
5. Extend the experimental program to include the interaction between shrinkage strains, crack width and durability.
6. Carry comprehensive study to study all of concrete early age properties, namely, shrinkage, creep and thermal.
7. Study the effect of the various restraints, such as steel reinforcement, aggregate, geometry, etc., on drying shrinkage strain and autogenous shrinkage strain.

References

- ACI Committee 209, *Modelling and Calculation of Shrinkage and Creep in Hardened Concrete*, American Concrete Institute, ACI 209.2R-08, 2008.
- Al-Manaseer A., and Ristanovic S., *Predicting Drying Shrinkage of Concrete*, Concrete International, 26(8), 79-83, 2004.
- Al-Manaseer A., and Lam, *Statistical Evaluation of Creep and Shrinkage Models*, ACI Materials Journal, 102(3), 170-176, 2005.
- Amen D. K. H., and AL-Rawi R. S., *Development of A Graphical and Statistical Model for The Ultimate Shrinkage of Concrete*, International Computers and Industrial Engineering Conference, Istanbul, Turkey, June 19-22, 2005.
- American Society for Testing and Materials, *Standard Specification for Air-Entraining Admixtures for Concrete*, ASTM, West Conshohocken, PA, ASTM C260-06, 2006a.

American Society for Testing and Materials, *Standard Practice for Length Change of Cast, Drilled, or Sawed Specimens of Hydraulic – Cement Mortar and Concrete*, ASTM, West Conshohocken, PA, ASTM C341/C 341M-06, 2006b.

American Society for Testing and Materials, *Standard Specification for Chemical Admixtures for Concrete*, ASTM, West Conshohocken, PA, ASTM C494/C 494M-08a, 2008.

Australia Standards, *Chemical Admixtures for Concrete*, Standards Australia Committee BD-033, AS 1478.1-2000, Sydney, Australia, 2000.

Azenha M., Faria R., and Figueiras J.A., *Thermo-Mechanical Analysis of Young Concrete*, Springer Netherlands, 91-97, 2006.

BASF The Chemical Company, *Micro Air – Air Entraining Agent*, BASF Admixtures for Improving Concrete, division 03, durability-enhancing admixture, 2007a.

BASF The Chemical Company, *Glenium 7500 – High Range Water Reducing Agent*, BASF Admixtures for Improving Concrete, division 03, water reducing admixture, 2007b.

BASF The Chemical Company, *Rheomac VMA 358 – Viscosity Modifying Admixture*, Admixtures for Improving Concrete, division 03, Speciality Products, 2007c.

BASF The Chemical Company, *Rheoplus 800S – Shrinkage Reducing Agent*, BASF Pozzolith, Tokyo, Japan, 2008.

Bažant and Baweja, *Creep and Shrinkage Prediction Model for Analysis and Design of Concrete Structures: Model B3*, American Concrete Institute Special Publication, 194(SP), 1-84, 2000.

Bažant Zdenek P., and Li Guang-Hua, *Comprehensive Database on Concrete Creep and Shrinkage*, ACI Materials Journal, 105(6), 635-637, 2008.

Bažant Zdenek P., and Li Guang-Hua, *Unbiased Statistical Comparison of Creep and Shrinkage Prediction Models*, ACI Materials Journal, 105(6), 610-621, 2008.

Bentz D. P., *A Review of Early-Age Properties of Cement – Based Materials*, Cement and Concrete Research, 38, 196–204, 2008.

Bentz D. P., and Jensen O.M., *Mitigation Strategies for Autogenous Shrinkage Cracking*, Cement & Concrete Composites, 26(6), 677-685, 2004.

Bentz D. P., and Weiss W. J., REACT: *Reducing Early-Age Cracking Today*, Concrete Plant International, 3, 56-61, 2008.

Byfors J., *Plain Concrete at Early Ages*, Swedish Cement and Concrete Research Institute, Report 3(80), 1980.

Cement and Concrete Association of Australia, *Drying Shrinkage of Cement and Concrete*, P6, July, 2002.

Chidiac S. E., *Civil Engineering Course CE732: Concrete Structures-Materials, Maintenance and Repair*, Department of Civil Engineering, McMaster University, Canada, 2009.

Canadian Standards Association, *Density of Aggregate: Concrete Materials and Methods of Concrete Construction – Methods of Tests for Concrete*, CSA, Mississauga, A23.2-10A, 2000.

Canadian Standards Association, *Relative Density and Absorption of Coarse Aggregate: Concrete Materials and Methods of Concrete Construction – Methods of Tests for Concrete*, CSA, Mississauga, Ontario, A23.2-12A, 2000.

Canadian Standards Association, *Sieve Analysis of Fine and Coarse Aggregate: Concrete Materials and Methods of Concrete Construction - Methods of Tests for Concrete*, CSA, Mississauga, Ontario, A23.2-2A, 2000.

Canadian Standards Association, *Air Content of Plastic Concrete by the Pressure Method: Concrete Materials and Methods of Concrete Construction – Methods of Tests for Concrete*, CSA, Mississauga, Ontario, A23.2-4C, 2000.

Canadian Standards Association, *Relative Density and Absorption of Fine Aggregate: Concrete Materials and Methods of Concrete Construction – Methods of Tests for Concrete*, CSA, Mississauga, Ontario, A23.2-6A, 2000.

Canadian Standards Association, *Compressive Strength of Cylindrical Concrete Specimens: Concrete Materials and Methods of Concrete Construction – Methods of Tests for Concrete*, CSA, Mississauga, Ontario, A23.2-9C, 2000.

Cusson D., and Hoogeveen T., *Preventing Autogenous Shrinkage of High-Performance Concrete Structures by Internal Curing*, S.P. Shah Symposium on Measuring, Monitoring and Modelling Concrete Properties, Alexandroupolis, Greece, July 3-7, 2006.

D'Ambrosia M. D., Lange D. A., and Grasley Z. C., *Measurement and Modeling of Concrete Tensile Creep and Shrinkage at Early Age*, American Concrete Institute Special Publication, 220(SP), 99-112, 2004.

Daoud O. I., *Correlating Concrete Mix Design to Rheological Properties of Fresh Concrete*, M.A.Sc. Thesis, Department of Civil Engineering, McMaster University, Canada, 2008.

Eguchia K., and Teranishib K., Prediction *Equation of Drying Shrinkage of Concrete Based on Composite Model*, Cement and Concrete Research, 35(3), 483–493, 2005.

Fernández-Gómez J., and Agranati Landsberger G., *Evaluation of Shrinkage Prediction Models for Self-Consolidating Concrete*, ACI Materials Journal, 104(5), 464-473, 2007.

Gardner, *Comparison of Prediction Provisions for Drying Shrinkage and Creep of Normal Strength Concretes*, Canadian Journal of Civil Engineering, 31(5), 767-775, 2004.

Geiker M.R., Bentz D.P., and Jensen O.M., *Mitigating Autogenous Shrinkage by Internal Curing*, American Concrete Institute Special Publication, 218(SP), 143-154, 2004.

Gilbert R.I., *Shrinkage, Cracking and Deflection - The Serviceability of Concrete Structures*, Electronic Journal of Structural Engineering, 1(1), 2-14, 2001.

Gribniak V., Kaklauskas G., and Bacinskas D., *Shrinkage in Reinforced Concrete Structures: A Computational Aspect*, Journal of Civil Engineering and Management, 14(1), 49-60, 2008.

Hammer T.A, *Test Methods For Linear Measurements of Autogenous Shrinkage Before Setting*, Autogenous Shrinkage of Concrete, 143-154, E & F Spon, London, 1999.

Haque M., *Strength development and drying shrinkage of high strength concretes*, Cement and Concrete Composites 18(5), 333–42, 1996.

Hedlund H., *Stresses in High Performance Concrete Due To Temperature and Moisture Variations at Early Ages*, Licentiate Thesis, Lulea University of Technology, Lulea, Sweden, 1996.

Heirman G., Vandewalle L., and Gemert D.J., *Influence of Mineral Additions and Chemical Admixtures on Setting and Volumetric Autogenous Shrinkage of SCC-Equivalent-Mortar*, Belgium, K.U. Leuven, 2007.

Holt E., *Contribution of Mixture Design to Chemical and Autogenous Shrinkage of Concrete at Early Ages*, Cement and Concrete Research, 35(3), 464–472, 2005.

Holt E., *Early Age Autogenous Shrinkage of Concrete*, Technical Research Center of Finland–ESPOO, VTT PUBLICATIONS, 446, 2001.

Houst Y.F., *Carbonation Shrinkage of Hydrate Cements Paste*, CANMET/ACI International Conference on Durability of Concrete, Ottawa, Canada, July 1, 1997.

Huo X. S., and Wong L., *Experimental Study of Early-Age Behaviour of High Performance Concrete Deck Slabs Under Different Curing Methods*, Construction and Buildings Materials, 20(10), 1049–1056, 2006.

Janz M., *Moisture Transport and Fixation in Porous Materials at High Moisture Levels*, PhD Thesis, Lund Institute of Technology, Lund, Sweden, 2000.

Jensen, O.M., and Hansen, P.F., *Water-entrained Cement-based Materials I. Principle and Theoretical Background*, Cement and Concrete Research, 31(4), 647-654, 2001.

Justnes H., Van Gemert A., Verboven F., and Sellevold E.J., *Total and External Chemical Shrinkage of Low W/C Ratio Cement Pastes*, Advances in Cement Research, 8(31), 121–126, 1996.

Kangvanpanich K., and Ouchi M., *Early Age Creep of Self-compacting Concrete Using Low Heat Cement at Different Stress/Strength Ratios*, Department of Infrastructure System Engineering, Kochi University of Technology, Kochi, Japan, 2002.

Khatri R.P., and Sirvivatnanon., *Effect of different supplementary cementitious materials on mechanical properties of high performance concrete*, Cement and Concrete Research, 25(1), 209-220, 1995.

Kiang K. H., *Development of Creep and Shrinkage Prediction Model for Malaysian Normal Strength Concrete*, Universiti Teknologi Malaysia, Malaysia, 2006.

Kronlöf A., Leivo M., and Sipari P., *Experimental Study on the Basic Phenomena of Shrinkage and Cracking of Fresh Mortar*, Cement and Concrete Research, 25(8), 1747-1754, 1995.

Lee K.M., Lee H.K., Lee S.H., and Kim G.Y., *Autogenous Shrinkage of Concrete Containing Granulated Blast-Furnace Slag*, Cement and Concrete Research, 36(7), 1279–1285, 2006.

Li H., Wee T. H., and Wong S. F., *Early-Age Creep and Shrinkage of Blended Cement Concrete*, ACI Materials Journal, 99(1), 3-10, 2002.

Li J., and Yao Y., *A study on creep and drying shrinkage of high performance concrete*, Cement and Concrete Research, 31(8), 1203-1206, 2001.

Lin F., and Meyer C., *Modelling Shrinkage of Portland Cement Paste*, ACI Materials Journal, 105(3), 302-311, 2008.

Lura P., Jensen O. M., and Van B. K., *Autogenous Shrinkage in High-Shrinkage Cement Paste: An evaluation of Basic Mechanisms*, Cement and Concrete Research, 33(2), 223– 232, 2003.

Mak S.L., Ritchie D., Taylor A., And Diggins R., *Temperature Effects on Early Age Autogenous Shrinkage in High Performance Concrete*, Autogenous Shrinkage of Concrete, 155-166, E & F Spon, London, 1999.

Mazloom M., Ramezanianpour A.A., Brooks J.J., *Effect of silica fume on mechanical properties of high-strength concrete*, Cement and Concrete Composites, 26(4), 347– 357, 2004.

McDonald D. B., and Roper H., *Accuracy of Prediction Models for Shrinkage of Concrete*, ACI Materials Journal, 90(3), 265-271, 1993.

Mehta P.K., and Meterio P.J., *Concrete Microstructure, Properties, and Materials*, Third Edition, New York, McGraw-Hill Companies, Inc, 2006.

Melo A., Cincotto A., and Wellington R., *Drying and Autogenous Shrinkage of Pastes and Mortars with Activated Slag Cement*, Cement and Concrete Research, 38(4), 565– 574, 2008.

Mokarem D. W., *Development of Concrete Shrinkage Performance Specifications*, Virginia, Faculty of the Virginia Polytechnic Institute and State University, Blacksburg, Virginia, 2002.

Montgomery D.C. and Runger G.C., *Applied Statistics and Probability for Engineers*, Third Edition, New York, John Wiley and Sons Inc., 2003.

Nawa T., and Horita T., *Autogenous Shrinkage of High – Performance Concrete*, Proceeding of the International Workshop on Microstructure and Durability to Predict Service Life of Concrete Structures, Sapporo, Japan, February, 2004.

Newman J., and Seng Choo B., *Advanced Concrete Technology*, 1st Edition, Oxford, Elsevier Ltd., 2003.

Omar W., Makhtar A.M., Lai T.P., Omar R., and Kwong N.M., *Creep, Shrinkage and Elastic Modulus of Malaysian Concrete*, Final Report–Project, No: LPIPM/CREAM/UPP 02–02–06–09–23, 2008.

Paillère A.M., Buil M., and Serrano J.J., *Effect of Fiber Addition on the Autogenous Shrinkage of Silica Fume Concrete*, ACI Materials Journal, 86(2), 139-134, 1989.

Paulini P., *Outlines of Hydraulic Hardening – an Energetic Approach*, Workshop NTNU/SINTEF – Trondheim, Norway, November 28-29, 1996.

Pease B.J., *The role of Shrinkage Reducing Admixtures on Shrinkage, Stress Development, and Cracking*, Purdue University, Indiana, 2005.

Powers T.C., *Absorption of Water by Portland Cement Paste during the hardening Process*, Industrial and Engineering Chemistry, 27(7), 1935.

Razaqpur G., *Civil Engineering Course CE704: Advanced Concrete Design*, Department of Civil Engineering, McMaster University, Canada, 2008.

Radocea A., *A study on the Mechanisms of Plastic Shrinkage of Cement-Based Materials*, PhD Thesis, CTH Goteborg, Sweden, 1992.

Sakata K., and Shimomura T., *Recent Progress on and Code Evaluation of Concrete Creep and Shrinkage in Japan*, Journal of Advanced Concrete Technology, 2(2), 113-140, 2004.

Smadi M.M., Slate F.O., and Nilson A.H., *Shrinkage and Creep of High-, Medium-, and Low- Strength Concretes, Including Overloads*, ACI Materials Journal, 84(3), 224-234, 1987.

Suzuki M., Maruyama I., and Sato R., *Properties of Expansive-Ultra High-Strength Concrete*, American Concrete Institute Special Publication, 228(SP), 1159-1174, 2005.

Tazawa E., and Miyazawa S., *Influence of Cement and Admixtures on Autogenous Shrinkage of Cement Paste*, Cement and Concrete Research, 25(2), 281-287, 1995.

Tazawa E., Miyazawa S., and Kasai T., *Chemical Shrinkage and Autogenous Shrinkage of Hydrating Cement Paste*, Cement and Concrete Research, 25(2), 288-292, 1995.

Tazawa E., *Autogenous Shrinkage of Concrete*, London, E. & FN Spon, 1999.

Uno P.J., *Plastic Shrinkage Cracking and Evaporation Formulas*, ACI Materials Journal, 95(4), 365-375, 1998.

Yang Y., Sato R., and Kawai K., *Autogenous Shrinkage of High-Strength Concrete Containing Silica Fume Under Drying at Early Ages*, Cement and Concrete Research, 35(3), 449–456, 2005.

Zhang M. H., Tam C.T., and Leow M.P., *Effect of Water-to-Cementitious Materials Ratio and Silica Fume on the Autogenous Shrinkage of Concrete*, Cement and Concrete Research, 33(10), 1687–1694, 2003.